BRIDGE DECK ASPHALT CONCRETE PAVEMENT ARMORING

Final Report

PROJECT SPR 815

Oregon Department of Transportation

BRIDGE DECK ASPHALT CONCRETE PAVEMENT ARMORING

Final Report

PROJECT SPR 815

by

Matthew Haynes, Graduate Research Assistant
Erdem Coleri, PhD, Assistant Professor, PI
Shashwath Sreedhar, Graduate Research Assistant
Ihsan Ali Obaid, Graduate Research Assistant

School of Civil and Construction Engineering
Oregon State University
101 Kearney Hall
Corvallis, OR 97331
Phone: 541-737-0944

for

Oregon Department of Transportation
Research Section
555 13th Street NE, Suite 1
Salem OR 97301

and

Federal Highway Administration
1200 New Jersey Ave SE
Washington, DC 20590-0003

March 2020

Technical Report Documentation Page

1. Report No. FHWA-OR-RD-20-04	2. Government Accession No.	3. Recipient's Catalog No.
4. Title and Subtitle BRIDGE DECK ASPHALT CONCRETE PAVEMENT ARMORING		5. Report Date March 2020 6. Performing Organization Code
7. Author(s) Matthew Haynes; 0000-0003-4361-8217 Erdem Coleri, PhD; 0000-0002-1904-878X Shashwath Sreedhar; 0000-0003-1786-6372 Ihsan Ali Obaid; 0000-0001-9048-8342		8. Performing Organization Report No.
9. Performing Organization Name and Address School of Civil and Construction Engineering Oregon State University 101 Kearney Hall, Corvallis, OR 97331		10. Work Unit No. (TRAIS) 11. Contract or Grant No.
12. Sponsoring Agency Name and Address Oregon Dept. of Transportation Research Section 555 13th Street NE, Suite 1 Salem, OR 97301 Federal Highway Admin. 1200 New Jersey Ave SE Washington, DC 20590-0003		13. Type of Report and Period Covered Final Report 14. Sponsoring Agency Code
15. Supplementary Notes		

16. Abstract:

Deterioration of the concrete bridge deck is one of the most significant problems affecting the service life of bridges in the United States. Moisture penetration into the asphalt overlay and standing water on the concrete bridge deck result in expansion and contraction at the interface on the bridge deck during freeze-thaw cycles. This causes debonding at the interface and results in an increased rate of deterioration for the asphalt concrete overlay. Additionally, the deicing salts permeate into the deck and cause corrosion of the steel reinforcement, weakening the structural integrity of the bridge. Waterproofing membranes with an asphalt overlay were developed as a strategy to protect concrete bridge decks.

The main goals of this study were to provide the industry and Oregon Department of Transportation (ODOT) with better insight on the failure mechanisms of asphalt overlays on concrete bridge decks and establish field and laboratory experiments to evaluate the performance of these overlays. The most effective deck waterproofing systems and overlay strategies (in terms of both cost and performance) were determined for concrete bridge decks in Oregon. By determining the most effective waterproofing methods and strategies, this research will serve to decrease repair and replacement costs, and increase the service life of asphalt overlays on concrete bridge decks in Oregon.

17. Key Words Bridge deck; asphalt; waterproofing membrane; debonding; impermeable asphalt; permeability; freeze-thaw.	18. Distribution Statement Copies available from NTIS, and online at http://www.oregon.gov/ODOT/TD/TP_RES/

19. Security Classification (of this report) Unclassified	20. Security Classification (of this page) Unclassified	21. No. of Pages 129	22. Price

SI* (MODERN METRIC) CONVERSION FACTORS

APPROXIMATE CONVERSIONS TO SI UNITS

Symbol	When You Know	Multiply By	To Find	Symbol
		LENGTH		
in	inches	25.4	millimeters	mm
ft	feet	0.305	meters	m
yd	yards	0.914	meters	m
mi	miles	1.61	kilometers	km
		AREA		
in^2	square inches	645.2	millimeters squared	mm^2
ft^2	square feet	0.093	meters squared	m^2
yd^2	square yards	0.836	meters squared	m^2
ac	acres	0.405	hectares	ha
mi^2	square miles	2.59	kilometers squared	km^2
		VOLUME		
fl oz	fluid ounces	29.57	milliliters	ml
gal	gallons	3.785	liters	L
ft^3	cubic feet	0.028	meters cubed	m^3
yd^3	cubic yards	0.765	meters cubed	m^3
~ NOTE: Volumes greater than 1000 L shall be shown in m^3.				
		MASS		
oz	ounces	28.35	grams	g
lb	pounds	0.454	kilograms	kg
T	short tons (2000 lb)	0.907	megagrams	Mg
		TEMPERATURE (exact)		
°F	Fahrenheit	(F-32)/1.8	Celsius	°C

APPROXIMATE CONVERSIONS FROM SI UNITS

Symbol	When You Know	Multiply By	To Find	Symbol
		LENGTH		
mm	millimeters	0.039	inches	in
m	meters	3.28	feet	ft
m	meters	1.09	yards	yd
km	kilometers	0.621	miles	mi
		AREA		
mm^2	millimeters squared	0.0016	square inches	in^2
m^2	meters squared	10.764	square feet	ft^2
m^2	meters squared	1.196	square yards	yd^2
ha	hectares	2.47	acres	ac
km^2	kilometers squared	0.386	square miles	mi^2
		VOLUME		
ml	milliliters	0.034	fluid ounces	fl oz
L	liters	0.264	gallons	gal
m^3	meters cubed	35.315	cubic feet	ft^3
m^3	meters cubed	1.308	cubic yards	yd^3
		MASS		
g	grams	0.035	ounces	oz
kg	kilograms	2.205	pounds	lb
Mg	megagrams	1.102	short tons (2000 lb)	T
		TEMPERATURE (exact)		
°C	Celsius	1.8C+32	Fahrenheit	°F

*SI is the symbol for the International System of Measurement

ACKNOWLEDGEMENTS

The authors would like to thank the Oregon Department of Transportation (ODOT) for providing funding for this research. The authors thank the members of the ODOT Project Technical Advisory Committee and ODOT research for their advice and assistance in the preparation of this report. In particular, Norris Shippen, Larry Ilg, William Bennett, Dean Chess, Travis Kenny, and Tim Rogers participated on the TAC. Authors would also like to thank our lab manager, Mr. James Batti, for providing support whenever needed in the laboratory. Authors would also like to thank Blaine Wruck and all undergrad research assistants for their ongoing assistance in the laboratory with sample preparation and testing. The authors also thank Mostafa Estaji for developing the finite element model given in Chapter 3 of this report. Jonnic Construction is also deserving of thanks. Jonnic Construction volunteered both time and materials to assist with the installation of membranes and overlays on the laboratory samples.

DISCLAIMER

TABLE OF CONTENTS

LIST OF FIGURES

LIST OF TABLES

1.0 INTRODUCTION

Bridges make up a vital component of the nation's infrastructure by connecting transportation networks and facilitating the movement of goods and people. In the United States, bridges are typically constructed of steel or concrete, with each material type presenting its own advantages and disadvantages. This study focuses on the evaluation of several strategies used to preserve the integrity of concrete bridges, namely through the use of waterproofing membranes and impermeable pavement overlays.

Concrete bridges are comprised of a series of piers or braces which support the concrete bridge deck. The bridge deck itself can be constructed of pre-cast concrete slabs or cast-in-place reinforced concrete. Concrete is naturally strong in compression and weak in tension, thus steel reinforcement is typically placed within the bridge deck to provide additional tensile strength to the structure (CRSI 2019). Most bridges will have drains or culverts along their span to remove rainfall from the roadway surface and reduce the risk of hydroplaning. In order to protect a concrete bridge deck from traffic loadings and environmental effects, an asphalt pavement overlay is commonly constructed on top of the concrete deck to act as a wearing surface (Russell 2012).

In the 1960s, many state transportation agencies were experiencing unexpected concrete bridge decks failures occurring long before reaching the design life. It was determined that moisture penetration into the bridge decks and expansion during freeze-thaw cycles was causing an increased rate of deterioration. Additionally, the deicing salts being used to prevent hazardous roadway surfaces in the winter were permeating into the deck and causing corrosion of the steel reinforcement, weakening the structural integrity of the bridge. This realization led many state DOTs to seek an additional means of protection for concrete bridge deck structures (Manning, 1995).

Waterproofing membranes were one strategy developed to protect bridge decks from moisture and temperature related damage. Although many types of waterproofing membranes exist, they all function by creating an impermeable layer on top of a concrete bridge deck which serves to prevent infiltration of water and chlorides into the deck. Although the advantages of a waterproofing membrane system have been proven significant, many state highway agencies are still hesitant to employ these systems. These agencies state poor performance on experimental installations, the inability to inspect the concrete deck surface below a membrane after installation, and early failure of asphalt pavement overlays as reasons to not use waterproofing membranes (Russell, 2012).

Impermeable asphalt overlays are another strategy used to prevent water and chloride infiltration on bridge decks. Impermeable asphalt waterproofing systems are generally constructed by applying a tack coat directly to the exposed concrete deck and paving over the deck using a specially modified asphalt mixture (Russell 2012). Unlike the waterproofing membranes described previously, impermeable asphalt concretes utilize a highly modified asphalt wearing

course which can support traffic loads while preventing water infiltration into the concrete bridge deck. Impermeable asphalt overlays eliminate the need for a waterproofing membrane, decreasing the time and cost associated with bridge deck waterproofing (Frosch et al. 2013). The impermeable asphalt concrete, however, utilizes a different mix design than the adjacent highway, meaning that the paver would need to be emptied and refilled with the modified mix immediately prior to paving over the bridge deck. Since it is difficult to produce two different mixes on the same day, another strategy is to grind out all of the bridge decks for a project and then pave them all at once at a later date using the impermeable asphalt mixture. The Bridge Deck Waterproofing Surface Course (BDWSC), described below, is one such impermeable asphalt waterproofing strategy evaluated in this study. Laboratory tests were conducted to determine its effectiveness in terms of permeability and resistance to high truck traffic.

The Bridge Deck Waterproofing Surface Course (BDWSC) is a highly modified asphalt pavement developed by the New Jersey DOT which creates an impermeable asphalt wearing course to prevent water infiltration into bridge decks (Bennert et al. 2011). The BDWSC achieves impermeability through high compaction and low air voids, which is made possible by a modified gradation and a modified asphalt binder (Bennert et al. 2011). The BDWSC is generally constructed using static rollers and a 1.5-inch to 2.5-inch (38.1 mm to 63.5 mm) lift thickness (McCarthy 2017). Asphalt pavement analyzer rut tests and flexural beam fatigue tests were suggested to be used to evaluate the performance of the BDWSC mix design (Bennert et al. 2011).

Today, waterproofing membranes with an asphalt overlay are a commonly used strategy on concrete bridge decks to prevent water on the roadway surface from permeating into the deck and reduce the damage to the bridge deck resulting from freeze-thaw cycles (Manning, 1995). Preformed and liquid applied waterproofing membranes are the most commonly used systems in the United States, however other waterproofing methods, such as impermeable asphalt pavements, have also been proven effective. Preformed and liquid applied membranes are generally constructed by applying a primer layer to an exposed concrete bridge deck. The waterproofing membrane is then applied on top of the primer layer. A tack coat is sprayed on top of the membrane and paved over using traditional paving methods. Impermeable asphalt waterproofing systems are generally constructed by applying a tack coat directly to the exposed concrete deck and paving over the deck using the specially modified asphalt mixture (Russell, 2012).

The early failure of asphalt pavement overlays on concrete bridge decks with spray-on waterproofing membranes has been recognized as a significant issue by the Oregon Department of Transportation. Potential reasons for the failure of the asphalt overlay were thought to be due to poor adhesion between the waterproofing membrane and the asphalt wearing course, and the material properties of the asphalt layer. By determining the most effective waterproofing methods and strategies, this research will serve to decrease repair and replacement costs, and increase the service life of asphalt overlays on concrete bridge decks in Oregon.

1.1 KEY OBJECTIVES OF THIS STUDY

The research study presented in this report seeks to provide the industry and ODOT with better insight on the failure mechanisms of asphalt overlays on concrete bridge decks and establish

field and laboratory experiments to evaluate the performance of these overlays. The most effective deck waterproofing systems and overlay strategies were determined for concrete bridge decks in Oregon. An ideal waterproofing system is one in which there is no early failure of the asphalt overlay, adequate bonding exists between the waterproofing membrane, asphalt and concrete layers, and one that is simple and cost effective to construct in the field.

1.2 ORGANIZATION OF THE REPORT

This report is organized as follows:

- This introductory chapter is followed by the literature review.
- The potential use of impermeable asphalt concrete layers to protect and seal concrete bridge decks are discussed in Chapter 3.0.
- Chapter 4.0 presents the results of the finite element models developed to determine the deformation levels on concrete bridge decks with different properties.
- Effectiveness of different waterproofing membrane strategies to protect and seal concrete bridge decks is discussed in Chapter 5.0.
- Chapter 6.0 compares the installation and equipment costs for the proposed membrane strategies.
- Finally, Chapter 7.0 presents the conclusions, summary of the work and recommendations.

2.0 LITERATURE REVIEW

2.1 BRIDGE DECK ASPHALT OVERLAY CONSTRUCTION PRACTICES AND SPECIFICATIONS

The construction of an asphalt pavement overlay on a concrete bridge deck is a common practice which poses many benefits to the maintenance and service life of the bridge deck, but also presents several drawbacks. Installation of an asphalt overlay can improve the ride quality experienced by users by reducing International Roughness Index (IRI), improve the continuity of the roadway by eliminating the need for butt joints at the bridge ends and prevent damage to the concrete deck from factors such as studded tires and freeze-thaw cycles. Additionally, maintenance and repair of the asphalt overlay is simple and cost effective, allowing the quality of the wearing surface to remain high throughout the service life of the bridge. The implementation of an asphalt overlay, however, limits the ability to inspect the concrete bridge deck for defects. As a result, problems which could have been easily repairable early on may be allowed to propagate, ultimately resulting in more expensive repairs. Water has also been known to pass through the asphalt concrete overlay and penetrate the concrete deck, allowing water and corrosive salts to access the steel reinforcement within the deck. To minimize the risk of reinforcement corrosion and concrete bridge deck damage, a waterproofing membrane must be installed between the concrete deck and asphalt overlay to act as a barrier against water and salt penetration into the deck (WSDOT, 2016).

The Oregon Department of Transportation (ODOT) constructs bridge deck asphalt overlays in the same manner as a typical highway asphalt overlay (ODOT, 2015). If an existing asphalt overlay is in place, it will be removed from the bridge deck using either a cold plane or rotomill grinding machine. The grinding machine must have a maximum tooth spacing of ¼ inches, weigh less than 35 tons, have a forward speed less than 2.5 feet per minute and operate at a drum speed of at least 120 rpm. Existing asphalt concrete is ground off of the roadway surface, exposing the concrete bridge deck beneath. If a waterproofing membrane is being used, it will be installed on top of the exposed concrete bridge deck. Once the existing asphalt has been removed, the asphalt overlay will be constructed using traditional paving methods over the waterproofing membrane or concrete deck. The asphalt mix design used for the bridge overlay will be the same as that of the adjacent highway, requiring no stopping of the paver and allowing for the construction of a continuous overlay. After being placed on the bridge deck, compaction by the breakdown and intermediate rollers should occur before the asphalt concrete drops below 180°F (82.2°C). There is no specified compaction density for an asphalt overlay being constructed on a concrete bridge deck, and the same roller pattern should be used as established for the rest of the highway, albeit without the use of vibration.

Although vibratory roller compaction is not traditionally used on concrete bridge decks in Oregon, there has been discussion regarding its use if a higher compaction density can be achieved. A higher density of the asphalt overlay will help to create an impermeable wearing course and protect the bridge structure from freeze-thaw and corrosion related damage.

Depending on the type of asphalt mix used, impermeable wearing courses can even eliminate the need for waterproof membranes and significantly reduce the material costs for bridge deck asphalt construction (Bennert, 2011). Today, vibratory compaction is widely accepted as a more efficient method of roadway compaction, with the majority of initial research regarding its efficiency being conducted in the 60's and 70's. One such study by the Kentucky Transportation Center compared the percent compaction of static rollers to that of several different vibratory rollers for two field construction projects. Compaction percentage was measured using a nuclear density gauge. It was determined that for both construction projects, vibratory rollers produced a higher compaction percentage with a fewer number of passes compared to conventional static rollers. For example, a roller with two vibratory drums achieved an average percent compaction of 98.0% after an average of five roller passes, whereas the conventional static roller achieved an average percent compaction of only 94.0% after an average of seven roller passes. While the number of passes varied, the same roller pattern was used for each type of roller. The study concluded that vibratory compaction could be used to achieve the asphalt pavement design density with fewer roller coverages, however the static roller was still capable of compacting to the design density with an increased number of passes (Newberry Jr., 1973).

2.2 WATERPROOFING MEMBRANE AND BOND FAILURE MECHANISMS

2.2.1 The effect of ambient and asphalt mix temperatures during construction on asphalt and membrane performance

Ambient and asphalt mix temperatures have a wide range of effects on bridge deck waterproofing systems. Many of the products used in liquid applied spray membranes are especially susceptible to ambient temperature variations. Colder ambient and deck surface temperatures can cause primer to set sooner, preventing it from adequately penetrating into the deck, and warmer ambient and deck surface temperatures can reduce the viscosity of the liquid membrane resulting in inconsistent thicknesses (Frosch et al. 2013). The Oregon DOT states that the spray membrane should be stored at a temperature between 55°F (12.8°C) and 95°F (35.0°C), and that manufacturer's recommendations for application temperatures should be followed while installing the membrane (ODOT, 2015).

The temperature of the hot-mix asphalt (HMA) wearing course during compaction is one of the most critical concerns throughout the construction. Excessively high HMA temperatures can soften the membrane, causing it to become less viscous and flow during compaction of the asphalt pavement, resulting in an uneven membrane distribution (Frosch et al. 2013). ODOT currently has no specification detailing the required temperature of the HMA overlay being placed over a waterproof membrane, however membrane manufacturers often specify this information in the installation procedure for their product.

Zhou et al. (2008) conducted a study regarding the interface adhesion of waterproofing membranes under critical factors, one of which being the construction temperature. Three types of waterproofing membranes were tested- a polymer modified liquid asphalt coat, an atactic polypropylene (APP) modified asphalt roll sheet and a self-adhesive roll sheet membrane. For each membrane type, samples were prepared by installing the membrane over a concrete slab,

then using a roller compactor to construct an asphalt wearing course layer with dimensions of 30x300x50mm (1.2x11.8x2.0in) over the waterproofing membrane. To evaluate the influence of construction temperature on interface adhesion strength, the asphalt overlays were constructed at temperatures of 100, 130, 160 and 190°C (212, 266, 320 and 374°F). Pull-off and peel adhesion tests conducted at various temperatures were the main metrics used to evaluate adhesion strengths of the waterproofing membranes (Zhou et al. 2008). From the results in Figure 2.1, it can be observed that the compaction temperature of the asphalt concrete overlay played a significant and varying role in controlling the bonding strength for each waterproofing membrane strategy. It should be noted that a styrene-butadiene-styrene (SBS) modified asphalt layer was used as a subcoat for the APP modified-asphalt roll sheet membrane to improve adhesion between the membrane and the concrete deck. This is the reason for the significantly higher bond strengths exhibited by the APP roll sheet membrane, when compared with the self-adhesive roll sheet membrane and the polymer modified liquid asphalt coat.

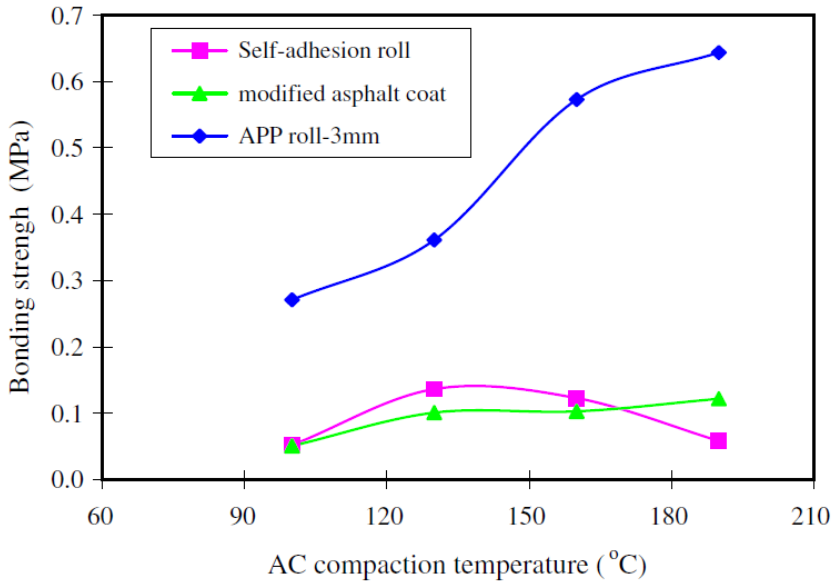

Figure 2.1: Measured pull-off strengths for three waterproofing membranes types and different asphalt compaction temperatures (Zhou et al. 2008)

The authors recommended that an asphalt concrete compaction temperature greater than 130°C (266°F) would ensure adequate bonding between the waterproofing layer and the asphalt wearing course, however for some strategies, a compaction temperature above 170°C (338°F) could introduce aging of the asphalt or result in damage to the membrane, decreasing the interface adhesion strength.

2.2.2 Factors controlling bond failure

The adhesive layer in a roadway is critical to providing adequate shear strength between pavement layers, allowing them to act as a monolithic structure. Poor bonding between pavement layers will provide lower resistance to the shear forces caused by vehicle loading, and will result in cracking and rutting of a pavement (Coleri et al. 2016). Many factors, such as

temperature, adhesive type and surface roughness will affect the shear strength between pavement layers.

A 2005 NCAT report (West et al. 2005) conducted shear tests using the NCAT bond strength device and a universal testing machine (UTM) to test tack coat shear performance of samples constructed from two asphalt layers adhered using one of three different tack coats. These samples simulated two typical lifts of an asphalt pavement, with no waterproofing membrane present. Tests were carried out at three different temperatures and it was determined that bond shear strength decreased as temperature increased for each of the three tack coats tested (West et al. 2005).

Covey et al. (2017) conducted similar tests on a series of six tack coat types. The rheological properties of the tack coats were determined and the tack coats were evaluated based on interlayer shear strength (ISS). The impacts of surface texture, tire tracking, tack coat type, traffic/environmental loading and tack coat spray rate on ISS were also considered. Direct shear tests were used to quantify the ISS. Results from the study showed that positive correlations existed between rheological test results and ISS of the field cores sampled. A positive correlation was also established between pavement surface texture and ISS, with higher surface textures producing generally larger interlayer shear strengths. Traffic and environmental factors were correlated to significant losses in ISS between pavement layers.

These results were consistent with the findings of another study (Liu et al. 2014) which utilized a skew-shear test with a UTM to determine the shear strength of four different waterproofing adhesive layers (WALs) being used to bond an asphalt pavement to a concrete substrate. The four different WALs consisted of SBS modified asphalt, SBS modified emulsified asphalt, rubberized asphalt and FYT-1 Bridge waterproofing coating (a polymer modified asphalt). The WALs were sprayed onto a concrete slab, then asphalt was compacted on top of the WAL to make the samples representative of waterproofing membranes which had been applied to concrete bridge decks in the field. The four sample types were tested using a shear rate of 50mm/min (2.0in/min) at temperatures of 3°C, 27°C and 40°C (37°F, 81°F and 104°F). As can be seen in Table 2.1, for all tested waterproofing adhesive types, increasing temperature decreases the shear strengths (Liu et al. 2014). Thus, temperature was concluded to be a significant factor controlling bond strength and performance.

Table 2.1: Temperature and Shear Strength of Waterproofing Adhesive Layers (Lie et al. 2014)

Temperature (C)	SBS Modified Asphalt (MPa)	Rubber Asphalt (MPa)	FYT Waterproof Coating (MPa)	SBS Modified Emulsified Asphalt (MPa)
3	3.78	3.82	1.90	0.65
27	0.68	0.72	0.41	0.14
40	0.35	0.37	0.11	0.08

Aside from temperature effects, Lie et al. (2014) also investigated the effect of various adhesive spraying quantities and concrete surface roughness on the shear strength of waterproofing adhesive layers. To test the effect of waterproofing adhesive quantity on shear performance, a

styrene-butadiene-styrene (SBS) modified asphalt waterproofing adhesive was used to bond the asphalt and concrete layers, and was tested using the skew-shear test method previously described. Tests were carried out at a constant 27°C (81°F) with adhesive application quantities of 0.8, 1.0, 1.3, 1.5 and 1.7 L/m^2 (0.18, 0.22, 0.29, 0.33 and 0.38 gal/yd^2). Results showed that an optimal adhesive spray quantity of approximately 1.3 L/m^2 (0.29 gal/yd^2) would provide the greatest shear strength (Liu et al. 2014).

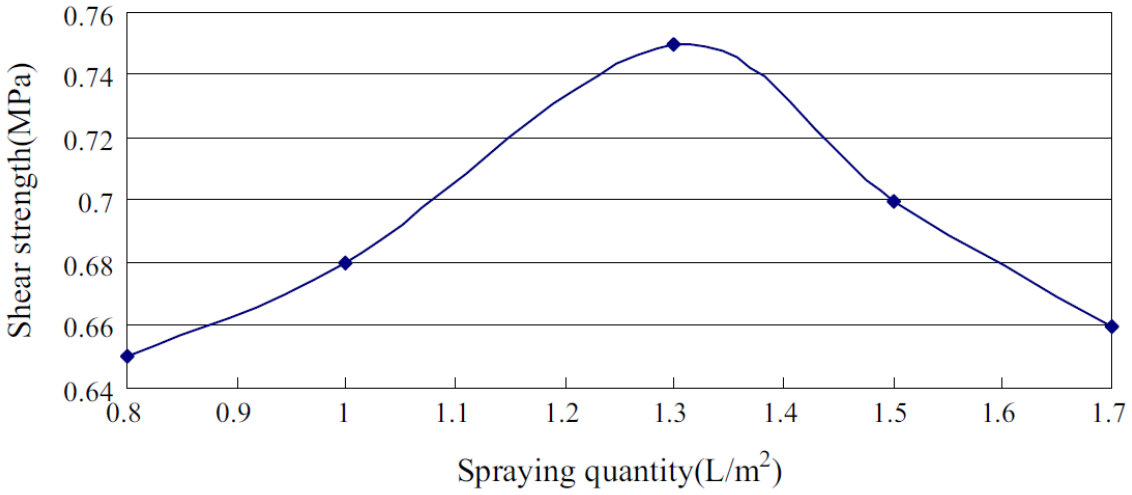

Figure 2.2: Effect of spray quantity on shear strength of waterproofing adhesive layer (Liu et al. 2014)

To examine the effect of concrete surface roughness on the shear performance of waterproofing adhesive layers, SBS modified asphalt was again used with an optimal spray quantity of 1.3 L/m^2 (0.29 gal/yd^2) and a constant temperature of 27°C (81°F). The skew-shear test was used to evaluate shear strength. Three surface roughness tests were carried out with metrics of "no roughening," "transversal or longitudinal roughening" which is comprised of artificial surface roughening in one direction and "transversal and longitudinal roughening," which is comprised of artificial surface roughening in two perpendicular directions. "Transverse or longitudinal roughening" of the concrete surface proved to provide the greatest shear strength. Liu et al. (2014) theorized that this roughness profile allowed for improved aggregate interlock without being so rough as to prevent the waterproofing adhesive from penetrating into the deeper grooves (thus reducing the contact surface area and shear strength). In a study by Covey et al. (2017), roughening was again found to be an important factor in the evaluation of interlayer shear strength. Based on the results from a field study, it was found that samples with a milled surface texture exhibited a higher average bond strength than samples with an overlaid surface texture. Additionally, a positive correlation was determined between the mean texture depth of the milled samples and the interlayer shear strength of those samples.

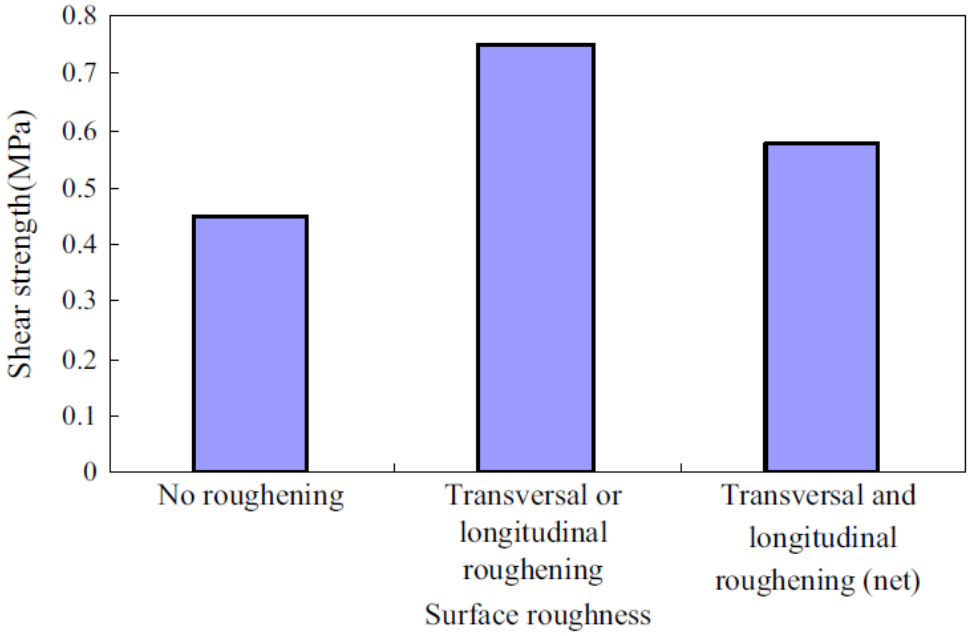

Figure 2.3: Effect of concrete surface roughness on shear strength of waterproofing adhesive layers (Liu et al. 2014)

2.2.3 Freeze-thaw cycles

A large benefit of using waterproofing membranes on concrete bridge decks is to protect the deck from deterioration due to repeated freeze-thaw cycles (Manning, 1995). While the membranes have generally been effective at protecting concrete bridge decks from freeze-thaw damage, problems have been experienced with the failure of asphalt wearing courses constructed on top of waterproofing membranes. When water permeates through the asphalt wearing course, it has been reported to become trapped between the waterproof membrane and asphalt layer, resulting in the spalling of the asphalt with subsequent freeze-thaw cycles. Once the asphalt wearing course has failed, the waterproofing membrane and concrete deck deteriorate at a faster rate (Russell, 2012). Limited research has been done to investigate the freeze-thaw cycle susceptibility of asphalt wearing courses on concrete bridge decks with a waterproofing membrane.

Özgan et al. (2013) investigated the effects of various durations of freeze-thaw cycle exposure on laboratory-produced asphalt concrete samples. A total of 15 samples with binder contents of 5.8% were prepared using a Marshall Compactor to simulate the asphalt concrete wearing course. The samples were split into five groups with one group acting as the control group while the other four groups were subjected to freeze-thaw cycles for either 6, 12, 18, or 24 days. The mechanical properties being tested and compared between sample groups were the Marshall stability (kg), flow (mm), change in voids volume (%), voids ratio filled with asphalt (%) and voids ratio inside mineral aggregate (%). Results of the study concluded that freeze thaw cycles had a negative effect on the mechanical properties of asphalt concrete. One of the more significant changes occurred in the Marshall Stability property, the value of which saw a 77.4% reduction between the control group and the test group exposed to freeze-thaw cycles for 24

days. While this study describes the response of asphalt to freeze-thaw cycles, it does not investigate the effect of freeze-thaw at an interface, such as the asphalt-concrete interface of a bridge deck.

A study by Sakulich et al. (2012) looked at increasing the service life of bridge decks by reducing the number of freeze-thaw cycles using phase change materials (PCMs). Bridge deck exposure to freeze-thaw cycles promotes cracking through the expansion of water in the concrete pores, allowing salts to penetrate the deck and corrode the steel reinforcement. By changing the chemical properties of the bridge deck using PCMs, the number of freeze-thaw cycles within the deck will be reduced, thus mitigating cracks and slowing bridge deterioration. In this study, the effectiveness of 12 different PCMs were modelled in 237 different locations which experienced a variety of freeze-thaw cycle durations and frequencies. Results from models of the 25 locations with the shortest and longest freezing events indicated that in less than half of cases, PCMs were effective at increasing the service life of the bridge deck. Increases in service life ranged from 1.2 to 4.8 years. The authors also explain that a negative aspect of PCMs are that they reduce the compressive strength of bridge decks due to foreign materials being introduced to the mix design, and that more work should be done to prevent mechanical property reduction in the bridge deck and improve the overall reliability of PCMs. These shortcomings highlight the advantages of a waterproofing membrane system, which creates a physical barrier to keep water out of the concrete deck to prevent freeze-thaw damage, as well as prevents corrosion due to the penetration of chlorides into the deck. Additionally, waterproofing membranes have no effect on the mechanical properties of the concrete bridge deck.

While freeze-thaw cycles have been shown to have a detrimental effect on the bond between aggregate and binder (Ozgan et al. 2013), no information could be found regarding the effect of freeze-thaw cycles on the tack coat bond between asphalt layers. Additionally, little research has been conducted regarding the direct influence of freeze-thaw cycles on the deterioration of asphalt overlays for concrete bridge decks employing waterproofing membranes. It is hypothesized that freeze-thaw cycles may have a detrimental impact on the tack coat bond between the waterproofing membrane and asphalt overlay layers. This study seeks to fill in gaps in knowledge by conducting experiments using samples previously exposed to freeze-thaw cycles, for various bridge deck waterproofing membrane systems. These samples will be compared to a control group not exposed to freeze-thaw cycles to draw conclusions regarding the effect of freeze-thaw conditions on the mechanical properties of bridge deck waterproofing systems with an asphalt overlay.

2.3 FIELD AND LABORATORY TESTS FOR BOND AND ASPHALT MIXTURE PERFORMANCE EVALUATION

2.3.1 Chain dragging and hammer sounding

Due to their simple and efficient nature, chain dragging and hammer sounding are the two most common field test methods for bond performance evaluation used by DOT's throughout the United States (Gucunski et al. 2013). The chain dragging test is performed by dragging chains across a bridge deck and listening to the sound made by the chains. Gucunski et al. (2013) describes a clear ringing sound as an indicator of a properly bonded deck, whereas a dull, hollow sound indicates an area of delamination. Once a general area of delamination has been

established using chain dragging, an inspector can then use a hammer to tap on the bridge deck and determine the precise borders of the delaminated area. ASTM D4580/D4580M-Procedure B outlines the standard practice for measuring bridge deck delamination using the chain dragging and hammer sounding methods (ASTM Standard D4580/D4580M, 2012).

Areas of moderate to severe delamination can quickly be identified and mapped using this method, and the conductor of the tests requires little training. Chain dragging and hammer sounding are limited, however, by their inability to detect the onset of delamination or accurately determine its severity. These tests also require an individual to be on the bridge, which may necessitate the use of traffic control. Nosie from traffic can also impede one's ability to correctly identify areas of delamination (Gucunski et al. 2013).

2.3.2 Ground Penetrating Radar (GPR)

Ground penetrating radar (GPR) is a non-destructive field test which utilizes electromagnetic waves to identify abnormal subsurface features on a roadway or bridge deck. It works by transmitting electromagnetic waves into a deck. When the waves reach a point of interference, such as a crack in the bridge deck, they are reflected back up to the GPR antenna. With respect to bridge decks, GPR is often used to measure deck thickness, measure concrete cover of rebar, identify and map out subsurface delamination (when possible), and identify corrosive environments. Though it have been used successfully in many situations, there are some limitations to the use of GPR. Since the electromagnetic waves travel easily through air without interference, GPR can only be used to detect subsurface delamination when the delamination is filled with water or another foreign material. Additionally, factors like extreme cold, frozen moisture within the pavement and deicing salts can alter the GPR results (Gucunski et al. 2013).

A study by Dong et al. (2016) investigated the potential of a vehicle-mounted ground penetrating radar system. The goal of the study was to produce a reliable method for the determination of asphalt surface layer thickness and develop theoretical methods for detection of the degree of compaction and delamination at a pavement layer interface. The degree of compaction was estimated by developing a model which correlated it to density- a parameter indirectly measured by the GPR. A method for identifying delamination was developed by analyzing the distinctions in GPR measurements caused by thin air gaps in the delamination and comparing these to GPR results of sound pavements. A comparison of GPR simulation results can be seen in Figure 2.4. From the simulation, it can be seen that detection of different thin air gaps was possible, however further research should be conducted to validate these results.

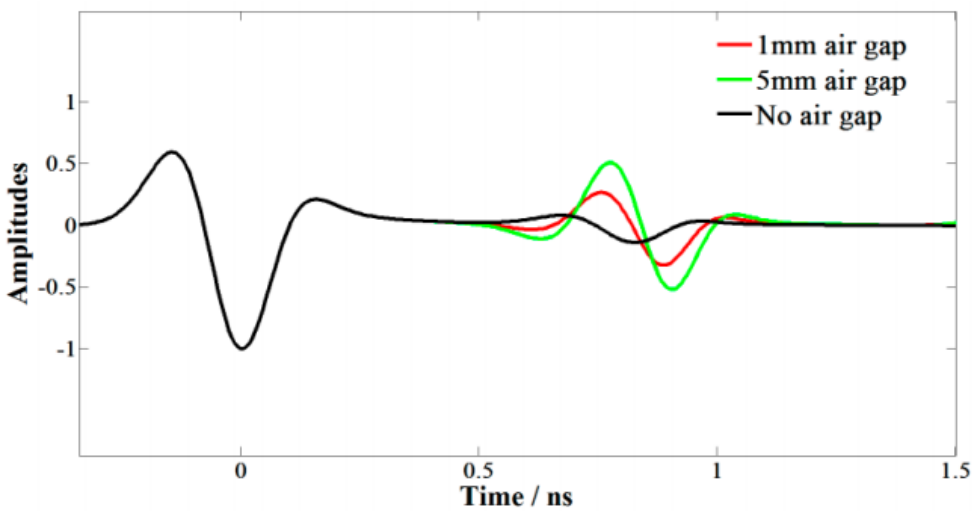

Figure 2.4: The simulated GPR signals of models with three different air gaps (Dong et al. 2016)

2.3.3 Infrared thermography

Infrared thermography is another non-destructive field test used to identify subsurface defects in a concrete roadway or bridge structure. Cracks, delamination, voids and material changes can all be identified due to variations in the density, thermal conductivity and specific heat capacity of these defects (Gucunski et al. 2013). Advantages of using infrared thermography to identify roadway defects include ease of use, high accuracy of measurements and the ability to collect data from a safe location (i.e. from the roadway shoulder). Since changes in environmental conditions can alter the image results, infrared thermography generally cannot be used to compare the progression of a subsurface defect over time (Clark et al. 2003).

In the past, infrared thermography has been limited by the thermal camera systems inability to detect smaller changes in temperature, but technological advancements have made it possible to detect much more subtle temperature changes (Clark et al. 2003). ASTM D4788-03 specifies that thermal imaging systems used for detecting delamination in bridge decks must be able to detect a 0.5°C (0.9°F) minimum temperature differential between acceptable concrete and a defect on a bridge deck (ASTM Standard D4788-03 2013).

A study conducted by NEXCO-West USA, Inc. compared three types of FLIR thermal imaging cameras, the FLIR T420, the FLIR T640 and the FLIR SC5600, and evaluated their ability to accurately detect delamination on concrete bridge decks. Each camera was tested on a concrete bridge section with known areas of delamination previously determined using conventional ground penetrating radar methods (NEXCO, 2014). Infrared outputs from each camera were analyzed using IrBAS- a specialized infrared analyzation software developed by NEXCO. Tests were carried out in the evening from a vehicle travelling at 30 mph (48 km/hr) when the sub-surface temperature difference between acceptable concrete and sub-surface defects was 0.2°C (0.36°F) and the same tests were repeated at night once the sub-surface temperature difference had lowered to 0.1°C (0.18°F). Results showed that the FLIR SC5600 was successful at detecting all known delaminations for both the 0.2°C (0.36°F) and 0.1°C (0.18°F) temperature

differentials. The FLIR T420 and FLIR T640 faired much worse, detecting only one out of seven and two out of seven known delaminations, respectively, for both the 0.2°C (0.36°F) and 0.1°C (0.18°F) temperature differentials (NEXCO, 2014).

2.3.4 Pull-off tension test

The pull-off tension test is a commonly used method of evaluating the tensile strength and adhesion performance of coatings being applied to the surface of a bridge or roadway. ODOT utilizes these tests in accordance with ASTM D4541, Method E (2017) to determine whether a waterproofing membrane is properly bonded to the concrete bridge deck. The waterproofing membrane must have a tensile bond strength of at least 175 psi (1.21 MPa) for it to be considered adequately bonded to the concrete substrate (ODOT, 2015).

Pull-off testing can also be implemented in a laboratory setting. A study from Hohai University produced samples consisting of concrete and asphalt layers, which were bonded together using four different waterproofing adhesive layers. Samples were prepared by first heating the waterproofing adhesive layer and adhering it to the concrete slab. Asphalt mixture was then heated and compacted on top of the waterproofing adhesive layer using a roller compactor, and cylindrical samples were cut from the prepared slab. A pull-off tension tester was used to compare the differences in tensile strength between the four waterproofing layers. Tests of the four samples were conducted at 3°C, 27°C and 40°C (37°F, 81°F and 104°F) and pulled using a drawing rate of 100-200 N/s (22.5-45.0 lbf/s). For each of the four strategies tested, the tensile strength decreased as the testing temperature increased (Liu et al. 2014).

A study by Tarefder et al. (2012) utilized a pull-off test to investigate the effect of moisture damage on asphalt. The stress-strain response from the pull-off test was compared to results from direct tension and direct shear tests to determine which test is most ideal for evaluating moisture damage. Samples were constructed by compacting asphalt mix on top of a matrix. Prior to testing, half of the pull-off test samples were submerged in water for 24 hours, where they were subjected to a 50 kPa (7.3 psi) vacuum pressure to eliminate air within the sample and simulate moisture damage. Results for the pull-off tests for wet and dry samples can be seen in Figure 2.5. While the shapes of the curves were similar in nature, the ultimate strength of the wet sample was much lower than that of the dry sample. These results indicated that moisture within the sample has a significant effect on the tensile strength of the interface between asphalt and matrix.

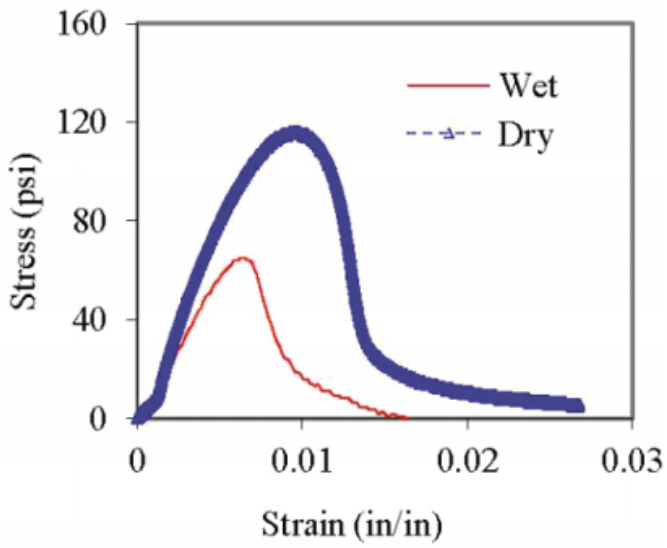

Figure 2.5: Pull-off test for wet and dry samples (Tarefder et al. 2012)

2.3.5 Oregon field torque tester (OFTT)

The Oregon Field Torque Tester (OFTT) was developed by Coleri et al. (2017) as a low cost, practical and less destructive field test device used to evaluate the long-term post-construction tack coat performance of pavement sections. The OFTT is used in conjunction with 2.5-inch (6.35-cm) cores as opposed to traditional 6-inch (15.24-cm) cores, thereby causing less damage to the pavement structure. Platens are glued to the 2.5-inch (6.35-cm)cores using a fast setting epoxy to provide a means for the OFTT to apply a torque to the core sample (Mahmoud et al., 2017).

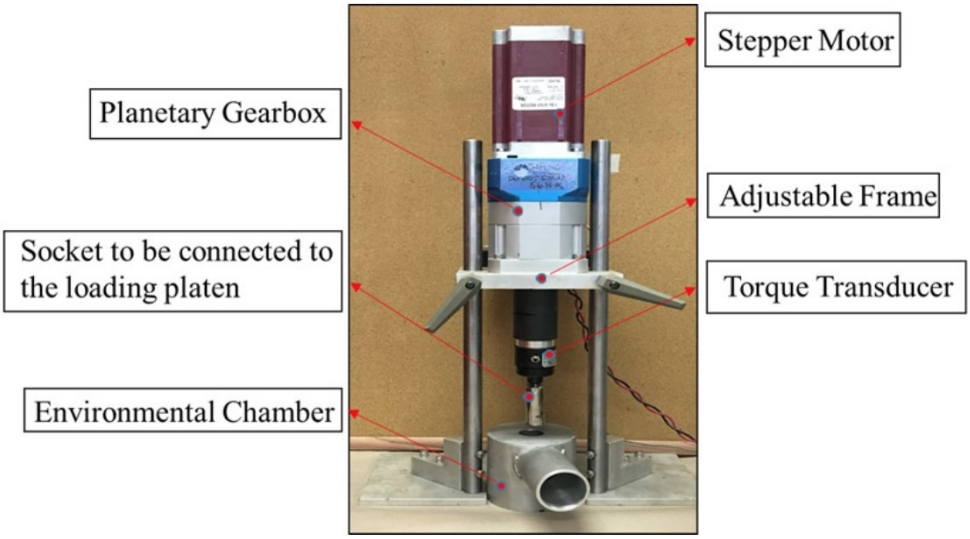

Figure 2.6: OFTT test device (Coleri et al. 2017).

Torsional shear at the tack coat interface is measured in real-time as the tests are conducted. After conducting a test and obtaining the peak torque strength for a core, the measured torque strength (Nm) will be converted to OFTT shear strength (kPa) using Equation (2-1) below (Muslich, 2009).

$$\tau = \frac{12M \times 10^6}{\pi D^3} \quad \textbf{(2-1)}$$

Where:

τ	=	Interlayer shear strength (OFTT shear strength) (kPa),
M	=	Peak torque at failure (Nm),
D	=	Diameter of the core (mm).

Coleri et al. (2017) compared the in-situ results of the Oregon Field Torque Tester to results obtained through laboratory shear tests on 6-inch (15.24-cm) cores conducted in accordance with the AASHTO TP114 (2015) specification. To prevent variability between samples, the 2.5-inch (6.35-cm) cores tested using the OFTT were taken within one foot of the 6-inch (15.24-cm) cores used in the laboratory shear tests. Figure 2.7 compares the shear strengths from laboratory prepared samples with those of equivalent field samples tested using the OFTT. It can be observed that the correlation between the OFTT test results and the laboratory shear strength results is statistically significant with a coefficient of determination (R^2 value) of 0.6544.

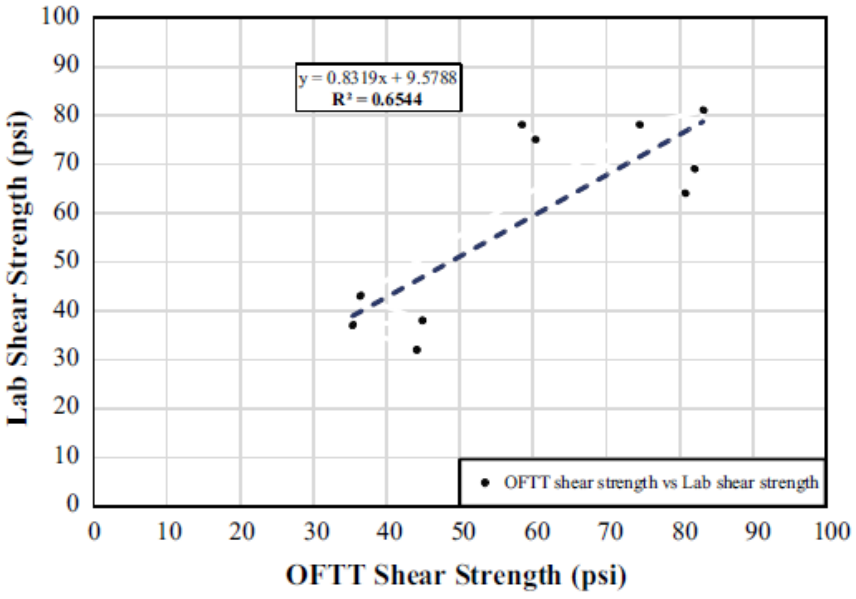

Figure 2.7: Correlation between OFTT shear strength (psi) and lab shear strength (psi) (Coleri et al. 2017)

Figure 2.8 shows the mean OFTT and laboratory shear strengths for cores tested in each of the three test locations.

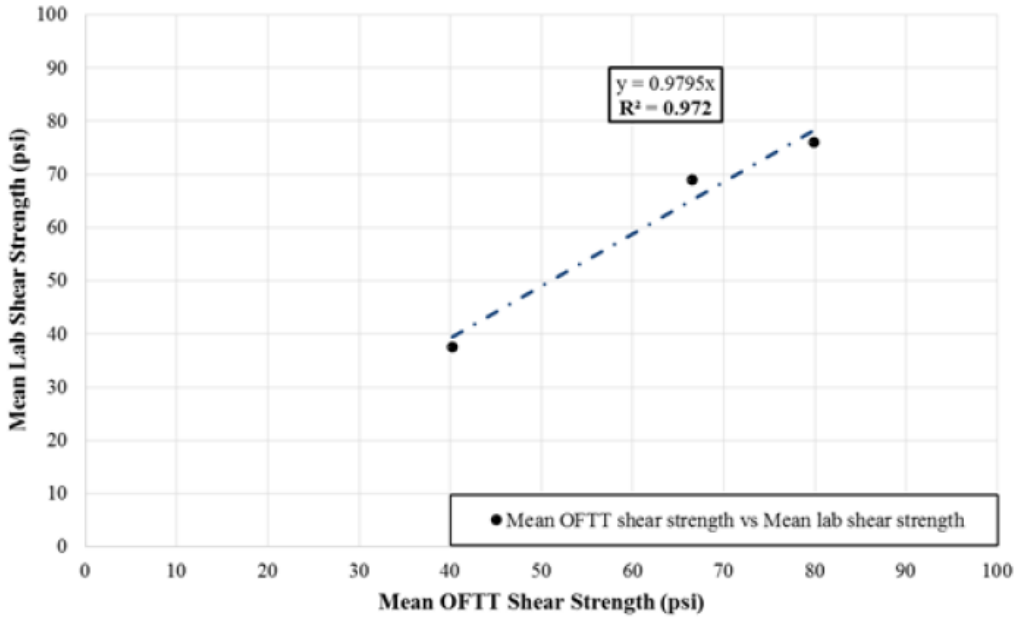

Figure 2.8: Correlation between mean OFTT shear strength (psi) vs mean laboratory shear strength (psi) (Coleri et al. 2017)

The shear strength results from the OFTT were highly correlated to those obtained through laboratory shear testing. This correlation suggests that the OFTT is an effective, low cost, less destructive alternative to typical laboratory shear tests for monitoring long-term in-situ bond strength. It was noted that factors such as stiffness above and below the interface, layer thickness, climate, traffic loading and non-uniform application of the tack coat could contribute to variability within the results. Additionally, more replicate tests in the field could reduce the test result variability. Though no work has been conducted on the matter, the OFTT could be a useful tool to evaluate the interface bond strength of a waterproofing membrane on a concrete bridge deck while minimizing damage to the deck and asphalt overlay.

2.3.6 Direct shear

Due to its relative simplicity and reliability, direct shear testing is one of the most common methods of evaluating the shear bond strength between asphalt layers. Many different test apparatuses have been developed to measure shear strength for both field and laboratory samples. AASHTO Standard TP114-15 (2015) outlines the standard procedure for determining interlayer shear strength between asphalt pavement layers. The standard gives detail on test procedures for both 150mm (5.9 in) and 100mm (3.9 in) diameter core samples.

The Florida direct shear test (or FDOT shear tester) was developed by Florida Department of Transportation (Sholar et al. 2004) to measure the interface bond strength by applying a shear load in the vertical direction (Figure 2.9). Two-layered specimens with a diameter of 6 in. (152.4 mm) were tested in shear by moving one of the loading collars (loading frame) in the vertical

direction. The gap between the loading frame and the reaction frame was specified to be 4.8 mm. A loading rate of two inches per minute (50.8mm/min.) was used.

Field cores with RS-1 emulsion were tested at 25°C (77°F). Residual application rates were 0.00, 0.02, 0.05, and 0.08 gal/yd^2 (0.00, 0.09, 0.23 and 0.36 L/m^2). The emulsion was applied on wet and dry surfaces to investigate the effect of water on bond strength. The major conclusions of the study were:

- Water reduced bond strengths. Wet sections with a 0.08 gal/yd^2 application rate have significantly higher bond strengths than the wet sections with lower application rates.
- Tack coats applied on milled surfaces had higher bond strengths.
- The standard deviation of the measured interface bond strengths was determined to be 9.6 psi.
- The interface bond strength difference between the sections with no tack coat (0.00 gal/yd^2) and 0.02 gal/yd^2 application rate was measured to be minimal. However, increasing the application rate to 0.05 gal/yd^2 created a significant increase in measured bond strengths.

Figure 2.9: Florida direct shear test device (Sholar et al. 2004)

Mohammad et al. (2012) developed the Louisiana Interlayer Shear Strength Tester (LISST) for the characterization of interface shear strength. The LISST apparatus (Figure 2.10) consists of a two-part frame which houses a cylindrical core sample, with the interface of the core sample lying between the two frame halves. One part of the frame moves to create a shear force on the sample while the other part holds the sample in place. The LISST was developed to be compatible with any Universal Testing Machine. Direct shear tests were performed using the LISST to evaluate the effects of temperature, tack coat type, pavement surface type, wet conditions and dusty conditions on the interface shear strength. Notable results of the LISST testing concluded that increased temperature decreased bond strength, trackless tack coat

produced the highest bond strength, rougher pavement surfaces increased bond strength and water had little effect on bond strength.

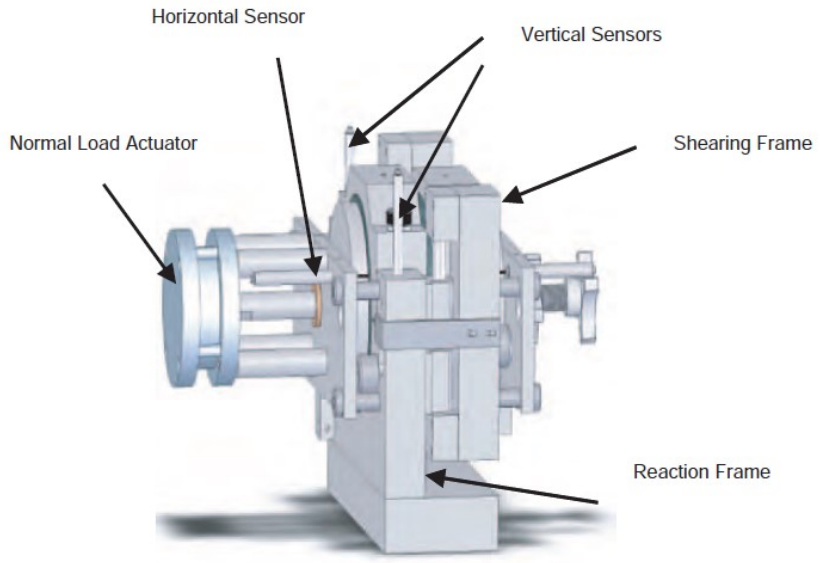

Figure 2.10: Louisiana interlayer shear strength tester (LISST) (Mohammad et al. 2012)

West et al. (2005) used the NCAT bond strength device to evaluate shear strength of a cylindrical asphalt sample interface. Similar to the LISST, the NCAT bond strength device (Figure 2.11) can be loaded using a universal testing machine and a two-part housing holds the core sample. The NCAT differs, however, in that it has the ability to apply a horizontal load via a screw assembly (simpler than the pneumatic normal load actuator used by LISST) to act as a normal pressure on the samples. It was hypothesized that the normal pressure was needed to properly evaluate the effects of surface friction on bond strength. In this experiment, tests were carried out using various tack coat types, application rates, temperatures and normal pressures. The interlayer bond strength was calculated using Equation 2.2 below (West et al. 2005).

$$S_B = \frac{P_{MAX}}{A} \tag{2-2}$$

Where:

S_B = Bond strength (psi),

P_{MAX} = Maximum load applied to specimen (lbf),

A = Cross-sectional area of test specimen (in^2).

With regards to the effects of normal pressure on bond strength, the NCAT bond strength tests concluded that at high temperatures, bond strength increased with an increase in normal pressure,

however at medium and low temperatures, bond strength was not affected by variations in normal pressure.

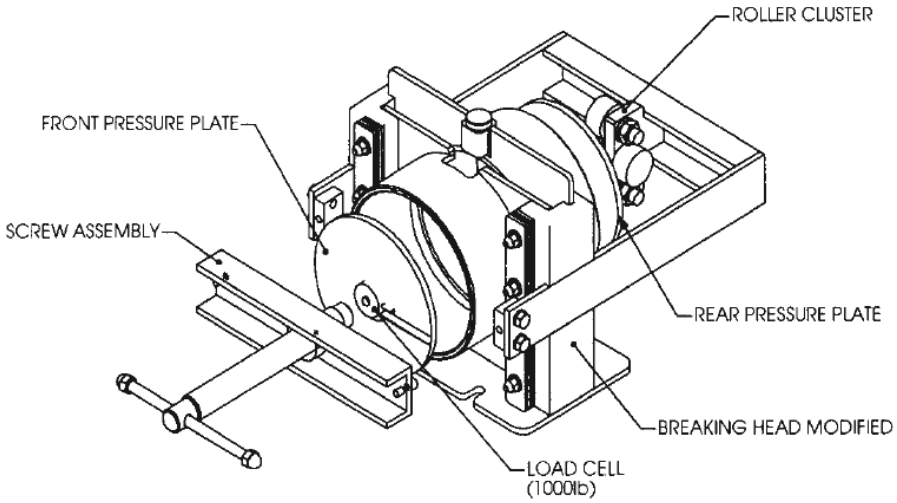

Figure 2.11: NCAT bond strength device (West et al. 2005)

Coleri et al. (2017) used a hybrid variation of the LISST and NCAT devices in laboratory testing of their samples. The jig itself is similar to that of the NCAT device, however the operational procedure follows that of the LISST. Like the LISST, this device employs a confining pressure actuator. However, the confining pressure load in this actuator is driven by a spring, whereas the LISST is a pneumatically operated. The device used by Coleri et al. (2017) is shown below in Figure 2.12.

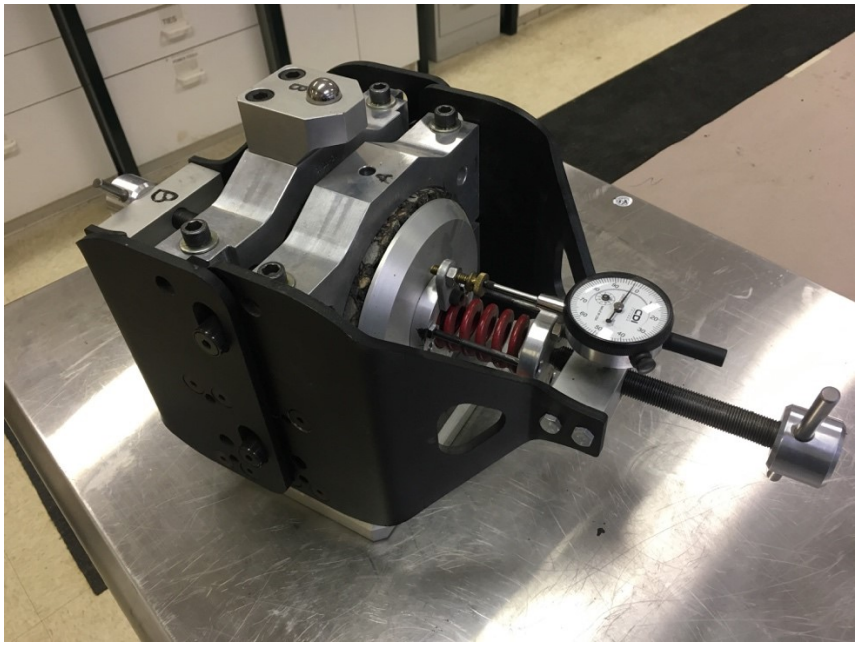

Figure 2.12: Shear test device used by Coleri et al. (2017)

2.3.7 Bending beam fatigue (BBF)

The four-point bending beam fatigue test is a simple flexural test used to simulate fatigue damage on a rectangular asphalt concrete specimen using a servo hydraulic or computer controlled pneumatic loading system. Simple flexural tests are favored over other fatigue damage tests, as simple flexural tests simulate fatigue damage at the bottom of the sample as it would occur in the field. Four-point bending tests are favored over other simple flexural tests, such as the three-point bending test, since the four-point test allows cracking to initiate in an area of uniform stress between the centers of two loading points (Hartman et al. 2004). The AASHTO T321-14 (2014) standard outlines the procedure for determining the fatigue life of HMA samples subjected to repeat flexural bending. The standard specifies that the failure point corresponds to the number of cycles at which the sample reaches 50% of its initial stiffness.

Hartman et al. (2004) used a four-point bending test to evaluate the dynamic mechanical properties within rectangular asphalt beam samples, and compare the results to those obtained through indirect tensile fatigue testing. The testing apparatus for the four-point bending test employed a closed loop servo hydraulic feedback system and constant clamping system. Test samples consisted of rectangular Hot Rolled Asphalt beams with dimensions of 305x45x50mm (12.0x1.8x2.0 in). Samples were tested at a temperature of 20°C (68°F) and loads applied at a frequency of 4Hz. Deflections were measured with an external linear variable differential transformer (LVDT) sensor mounted at the center of the beam sample. Equation 2.3 shows the general relationship used to evaluate the flexural strength of the samples (Applied Research Associates Inc., 2004).

$$N_f = Ck_1\left(\frac{1}{\varepsilon_t}\right)^{k_2}\left(\frac{1}{E}\right)^{k_3} \quad \textbf{(2-3)}$$

Where:

N_f	=	Number of repetitions to fatigue cracking,
$\mathcal{E}_T$	=	Tensile strain at the critical location,
k_1, k_2, k_3	=	Laboratory regression coefficients,
E	=	Stiffness of the material,
C	=	Laboratory to field adjustment factor

The fatigue life predictions from the four-point bending test results were compared with those from an indirect tensile fatigue test conducted at a frequency of 0.67 Hz, and it was found that the four-point bending fatigue tests predicted a fatigue life that was 48 times greater than the fatigue life predicted by the indirect tension tests. The authors attributed this with differences in the loading mode, load waveform, test frequency and method of load application (Hartman et al. 2004).

Coleri et al. (2017) tested both laboratory and field samples using a four-point bending test to evaluate the fatigue life of pavement layers by simulating repeated traffic loading. Asphalt beam samples were cut to dimensions of 380x50x63mm (15.0x2.0x2.5 in) and tested at 20°C (68°F) using 400 microstrain and a loading frequency of 10Hz. Field samples were cut from four separate Oregon State Highway sections (Coleri et al. 2017).

Though no information could be found regarding the use of the four-point bending test in conjunction with layered beam samples, the results from the test may be beneficial for this study. Conducting four-point bending tests with samples consisting of asphalt and concrete layers with a waterproofing membrane will provide information as to how different waterproofing strategies affect the fatigue life of bridge deck pavement structures- specifically at the bond interface between the concrete bridge deck, waterproofing membrane and asphalt overlay.

2.3.8 Semi-Circular Bend (SCB) test

Wu et al. (2005) developed the semi-circular bend (SCB) test (Figure 2.13) to determine the fracture resistance characteristics of asphalt concrete. This test works on the principle of elastoplastic fracture mechanics and uses notched semi-circular specimens to determine the critical energy strain rate of mixtures. Various advantages of this test are: (1) different notch depths can easily be introduced into the samples which makes the evaluation of true fracture properties of asphalt mixtures with regards to the crack propagation much easier; (2) the test setup and procedure is relatively simple; (3) the SCB specimens can be prepared by taking cores from Superpave gyratory compacted specimens; and (4) multiple specimens can be obtained from the same Superpave gyratory compacted specimen thus reducing the error caused by heterogeneities of different samples. In this test, the semi-circular specimen was loaded monotonically until failure under a constant cross-head deformation rate of 0.5 mm/min (0.02 in/min) at a test temperature of 25 ± 1ºC (77°F). The load and vertical deformation were measured continuously and load-displacement curve was plotted.

A total of 117 SCB tests were conducted at 25ºC (77°F), resulted from 13 Superpave mixtures × 3 notch depths × 3 replicates for each mixtures. The notch depths that were used in this study were 25.4, 31.8, and 38.0 mm (1.0, 1.25, and 1.5 in). It is required to have at least two notch depths in the experimental design to be able to calculate the strain energy release rate (Jc). The major conclusions of this study were:

- For a single notch depth, the fracture resistance based on average strain energy was found to be consistent with that from average vertical displacement, but different from that based on the peak load.
- Mixtures with higher tensile strengths could be more brittle and less fracture resistant than those with lower tensile strengths.
- Superpave mixtures with larger NMAS were found to have better fracture resistance.
- Superpave mixtures with softer asphalt binders were found to have more fracture resistance.

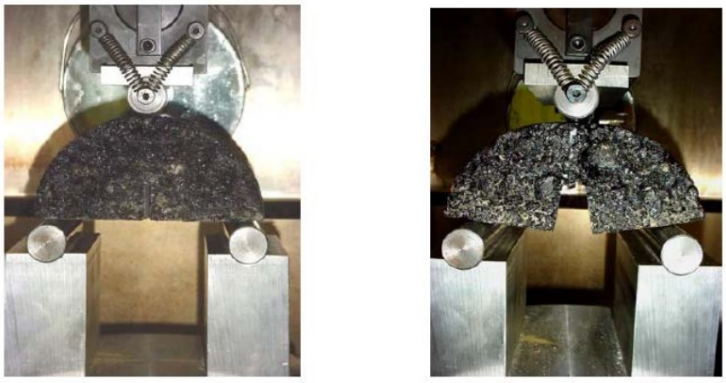

Figure 2.13: Semi-circular bend (SCB) test apparatus (Wu et al. 2005)

Coleri et al. (2017) utilized the SCB test to investigate cracking resistance on a series of samples possessing different binder types, binder contents and air void contents. The flexibility index parameter was used to evaluate the fatigue response of the samples. This parameter is the ratio of the fracture energy (Gf) to the slope of the line at the post-peak inflection point of a load-displacement curve such as the one generated through SCB tests. Several SCB tests were conducted on samples with varying properties, and flexibility indexes were determined for each. This allowed one to evaluate the impacts of several mixture properties on cracking resistance. Figure 2.14 shows the results of the SCB tests, with higher flexibility indexes corresponding to better cracking resistance. It was concluded that mixtures using an ER binder (Mix 1 and Mix 2) had a higher flexibility index and thus superior cracking resistance. Additionally, it was found that a 0.7% increase in binder content increases the flexibility index by 2 to 3 times.

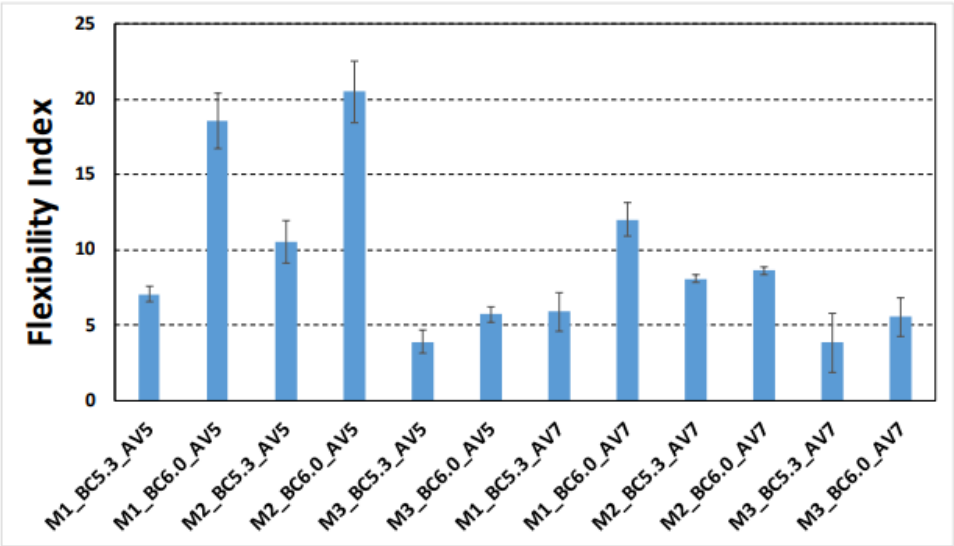

Figure 2.14: SCB results for the mixtures with different binder contents (5.3% and 6%), and air void contents (5% and 7%) (Coleri et al. 2017)

Note: M1: Mix 1-PG70-22ER-Fine gradation; M2: Mix 2-PG70-22ER-Coarse gradation
M3: Mix 3-PG70-22-Coarse gradation; BC: Binder Content; AV: Air Void Content

2.3.9 Flow number

The flow number (FN) test is a type of repeated load permanent deformation laboratory test used to evaluate the rutting characteristics of an asphalt sample (Bonaquist et al. 2003). The flow number parameter itself represents the onset of tertiary flow which indicates shear deformation in asphalt concrete mixtures (Biligiri et al. 2007). Repeated load permanent deformation tests apply thousands of load repetitions while recording the cumulative permanent deformation of the test sample, the results of which are then related to the cumulative permanent strain. The permanent strain response curve is categorized into three main sections, which can be seen in Figure 2.15. Permanent deformation is accrued rapidly in the primary zone before lowering to a constant rate in the secondary zone and finally resuming a rapid deformation increase in the tertiary zone. The flow number is the cycle which marks the transition between the secondary and tertiary zones.

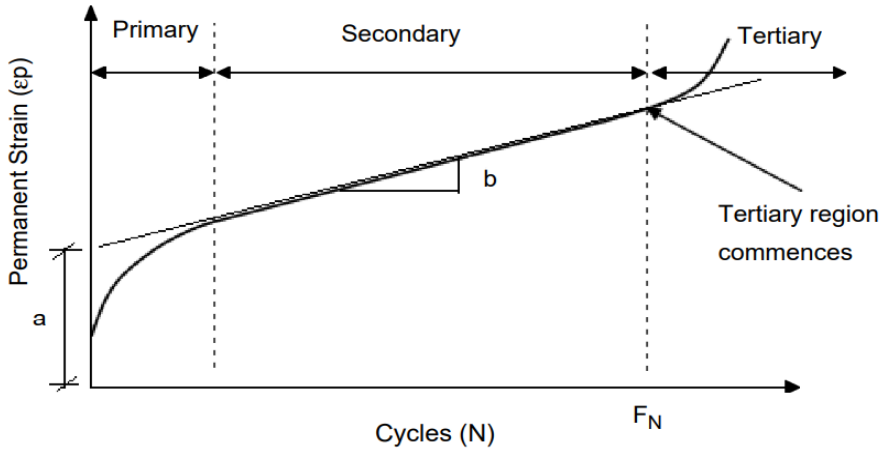

Figure 2.15: Relationship between permanent strain and load repetitions in the FN test (Biligiri, 2007)

A study conducted by Biligiri et al. (2007) evaluated commonly used permanent deformation models to determine which model best fit the permanent deformation data and provided the most accurate estimation of the flow number parameter. The authors determined that the Francken model provided the most comprehensive fit of the FN test data. The basis of the Francken model is defined in Equation (**2-4** as follows (Francken, 1977).

$$\epsilon_P(N) = AN^B + C(e^{DN} - 1) \quad \textbf{(2-4)}$$

Where:

ϵ_P	=	Permanent deformation or permanent strain from FN test,
N	=	Number of loading cycles,
A, B, C, D	=	Regression constants.

Taking the derivative of Equation (**2-4** yields the strain rate of change. Because the strain rate of change is constant throughout the secondary zone, the flow number is ultimately calculated by taking the derivative of the strain rate of change (i.e. the second derivative of Equation (**2-4**). The second derivative of the Francken model is represented in Equation 2-5, and the flow number corresponds to the inflection point, or number of cycles at which this equation is equal to zero (Biligiri et al. 2007).

$$\frac{\partial^2 \epsilon(p)}{\partial N^2} = A * B * (B-1) * N^{(B-2)} + (C * D^2 * e^{D*N}) \quad \textbf{(2-5)}$$

Although the flow number test has not been used to evaluate the structural resistance of a system with an asphalt overlay and concrete bridge deck with a waterproofing membrane, this study will use the test look at whether different waterproofing strategies have an impact on structural resistance. Additionally, the flow number test will be used to evaluate the rutting characteristics of impermeable pavement overlays for concrete bridge decks, which may be more susceptible to rutting due to a softer binder and increased binder content.

2.3.10 Hamburg wheel tracking test

The Hamburg Wheel-Tracking Device (HWTD) (Figure 2.16) was developed to measure rutting and moisture damage (stripping) susceptibility of an asphalt concrete sample. Tests are conducted by immersing the asphalt concrete sample in a hot water bath (40 or 50°C) and rolling a steel wheel across the surface of the sample to simulate vehicle loading.

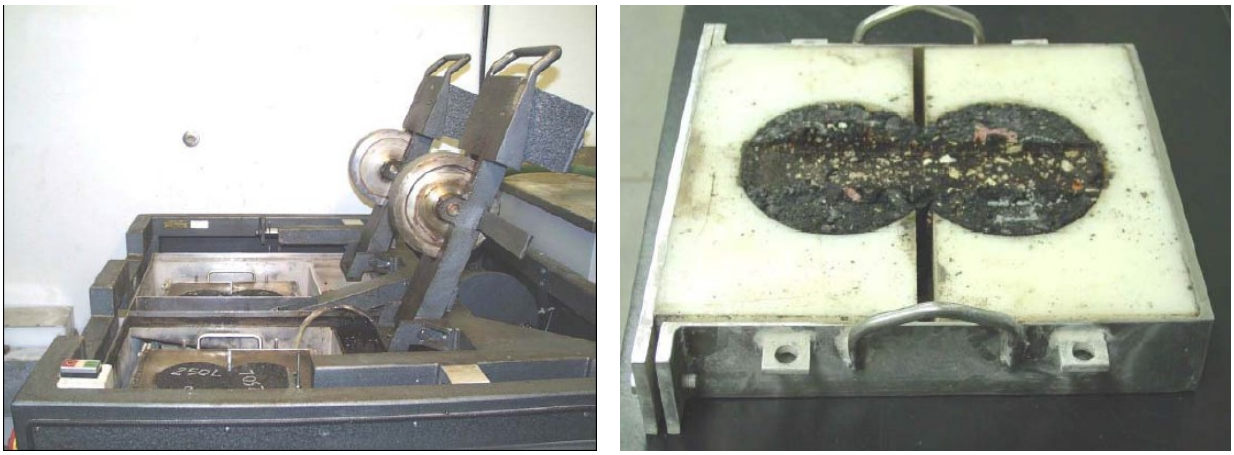

(a) **(b)**

Figure 2.16: (a) HWTD (b) Rutted samples following HWTD test (Yildirim et al. 2007)

Approximately 20,000 wheel passes are commonly used to evaluate the rutting and stripping resistance of a sample. Figure 2.17 shows an example of typical results obtained from the HWTD test. The test provides information related to the total rut depth, post-compaction, creep slope, stripping inflection point and stripping slope of the asphalt concrete sample (Yildirim et al. 2007).

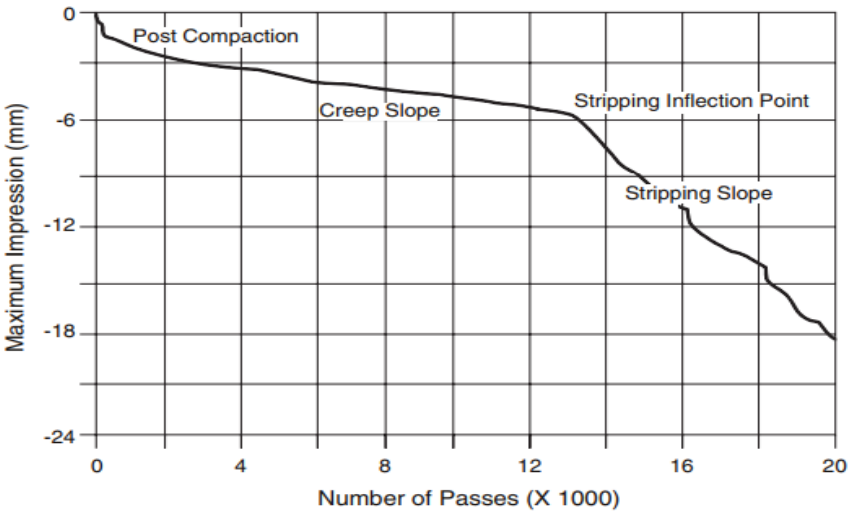

Figure 2.17: Typical HWTD test results (Yildirim et al. 2007)

The deformation after the first 1,000 wheel passes is the post-compaction consolidation, and is thought to occur rapidly because the applied load is densifying the asphalt mixture. Creep slope measures the accumulated permanent deformation after post-compaction and prior to the onset of stripping, and is an indicator of rutting susceptibility. Creep slope deformation is generally due to a mechanism other than moisture damage. The number of passes at which the creep slope transitions to the stripping slope is the stripping inflection point. The stripping slope measures the accumulated permanent deformation resulting from moisture, and is an indicator of the asphalt mixture's resistance to moisture-induced damage (Yildirim et al. 2007).

Yildirim et al. (2007) conducted an investigation to determine significant factors affecting HWTD test results. The Texas Department of Transportation (TxDOT) Hamburg database, consisting of 840 HWTD tests, was utilized for the investigation. The authors explained that the TxDOT uses the HWTD tests on a pass/fail basis. If a sample of a certain mixture produces a rut depth less than 12.5 mm (0.5 in) after 20,000 wheel passes, the mixture is considered to have acceptable rutting resistance. Results of the investigation found that temperature has a large effect on HWTD test results. Higher temperatures resulted in larger rut depths, and the authors suggested that samples should be tested at the temperature closest to that which will be experienced in the field. The effect of three commonly used binder types, PG64-22, PG70-22 and PG76-22 were also considered. As would be expected, the results of the HWTD tests showed that stiffer binders improved rutting resistance. Aggregate type and mix type were also investigated but were not found to significantly affect HWTD test results.

The use of the HWTD has become more common throughout DOTs in recent years for evaluating moisture sensitivity in HMA samples. A study by Tsai et al. (2016) sought to provide recommendations for obtaining more consistent and representative results for this test as described in AASHTO T 324 – Hamburg Wheel-Track Testing of Compacted Hot Mix Asphalt (HMA). A micromechanical finite element model was used to evaluate the effects of gap/bonding and specimen shape used on the tests, and whether consistent HWTD results could be obtained. Results from this study concluded that:

- Slab specimens can provide more reliable test results due to larger size and uniform geometry.

- Two cylindrical specimens (cores) should be glued together to prevent localized failure due to larger peak maximum principal strains when there is no bonding.

- Measurements of average rut depth should be collected from stations near the centers of cylindrical specimens to keep the specimen shape effects to the lowest possible level.

- An agency should not allow both specimen setups to be used interchangeably in the HWTD specifications.

The HWTD test is one option to characterize the structural resistance of various waterproofing bridge deck strategies. It could be particularly useful when the waterproofing strategy being tested is an impermeable pavement. Impermeable pavements generally employ a high-density asphalt mixture which is achieved by using a softer asphalt binder or higher binder content. These factors make the asphalt pavement more susceptible to rutting from repeated vehicle loading. Since the HWTD test simulates vehicle tire loading, it could be ideal for evaluating susceptibility of impermeable asphalt pavement mixtures on concrete bridge decks.

2.4 STRATEGIES TO REDUCE ASPHALT OVERLAY FAILURE ON BRIDGE DECKS WITH A WATERPROOFING MEMBRANE

2.4.1 Deck preparation

The bond between the waterproof membrane, the concrete bridge deck and the asphalt overlay is the most critical part of the waterproofing system. Any dirt or debris present on the deck at the time of the primer application will prevent the primer from adequately bonding to the deck (Frosch et al. 2013). Most waterproofing strategies stress the importance of preparing and cleaning the bridge deck prior to a membrane installation, regardless of the type of membrane. ODOT specifies that a concrete bridge deck should be shot blasted according to standard SSPC SP13/NACE 6, and that the surface roughness of the bridge must have a surface texture depth profile of at least 1/16 inch (1.6 mm), as determined by a Sand Patch Test (ASTM E965). Prior to installation of the primer, the shot blasted deck should be cleaned using compressed air (ODOT, 2015).

2.4.2 Primer layer

The majority of waterproofing strategies utilize a primer or adhesive layer which is applied to the bare concrete bridge deck. This primer layer penetrates into the bridge deck, sealing pores and creating a uniform surface upon which the waterproofing membrane can be applied. The primer layer is also specially formulated to bond with the waterproofing layer and improve the overall adhesion between the waterproofing system and the concrete substrate (Russell, 2012). A pull-test is commonly conducted to ensure adequate bond strength between the primer and the concrete bridge deck. The Oregon DOT conducts a pull test in accordance with ASTM D4541,

Method E, using a Type V tester and steel dollies to evaluate primer bond strength to the substrate (ODOT, 2015).

Table 2.2 outlines positive and negative attributes of generic primers and adhesives commonly used in waterproofing systems. It should be noted that this table extends only to generic materials, and that extensive variation can exist between specific products within the generic primer and adhesive classes shown.

Table 2.2: Performance of Generic Primers and Adhesives (Manning, 1995)

Type of Material	Positive Attributes	Negative Attributes
Bituminous primers	Workable over ambient temperatures range although some unmodified solvented types increased viscosity at low temperatures.	Drying time was temperature and moisture dependent and took from 1 to 48 hours, depending on composition; limited waterproofing ability and poor long term adhesion
Resinous primers	Workable over ambient temperature range; moderate waterproofing ability and good resistance to chloride penetration.	Pot life limited at high temperatures.
Oxidized bitumen adhesives	Effective barrier to water and chloride transmission when fully bonded and free from blow holes; minimal water absorption.	Significant increase in stiffness at low temperatures; prone to embrittlement and debonding; generally poor long term bond.
Latex adhesives		Very poor adhesion to concrete; ineffective barrier to water or chloride transmission.
Self-adhesive backing to sheet membranes	Bond generally effective when applied at above 10 degrees Celsius.	Below 10 degrees Celsius, bond progressively weaker and almost non-existent below 5 degrees Celsius; poor bond if laitance or contamination of concrete; prone to debonding in the long term.

2.5 MOST EFFECTIVE STRATEGIES FOR BRIDGE DECK ASPHALT CONSTRUCTION

There are multiple strategies for installing a waterproofing bridge deck system. Liquid applied and preformed waterproofing systems are the two most common waterproofing strategies. Each

of these strategies have distinct advantages and disadvantages which are summarized in **Error! Reference source not found.**Table 2.3. These strategies, both of which are implemented by the ODOT, utilize a thin waterproofing layer placed on top of an exposed bridge deck or on top of a primer layer, which is then paved over with asphalt concrete. Membrane types and installation techniques vary from state to state, with no clear consensus regarding the most successful installation practices. Some states avoid the use of waterproofing membranes altogether and others have developed alternate solutions to prevent water infiltration on concrete bridge decks such as impermeable pavements (Russell, 2012). Several waterproofing strategies that have been proven effective are described below.

Table 2.3: Comparison of Preformed and Liquid Applied Membranes (Frosch et al. 2013)

Liquid Applied Membranes	Performed Membranes
Easy to install on skewed or otherwise irregularly shaped bridge decks	Difficult to install on skewed or otherwise irregularly shaped bridge decks
On largely sloped bridge decks, the liquid might flow upon placement	Sheet systems are not sensitive to varying slopes
It is difficult to install a liquid membrane layer of constant thickness	All sheets are the same thickness
A seamless layer or membrane product can be installed	Sheets come in predetermined size, laps are necessary
Liquid materials can release harmful fumes in the air	Sheet systems do not pose the threat of releasing harmful fumes
Often mixed on site providing potential for inconsistencies in the product	Production of the product is factory controlled

2.5.1 Liquid membranes

Liquid waterproofing membranes are either poured or sprayed onto an exposed concrete deck. These membranes create a seamless impermeable barrier against water penetration, and can be easily applied to decks of an irregular shape. The installation of liquid membranes, however, is more difficult than that of other strategies and cost is often greater (Frosch et al. 2013). An outline of liquid waterproofing membrane types can be seen in Figure 2.18, and several liquid waterproofing strategies are described below.

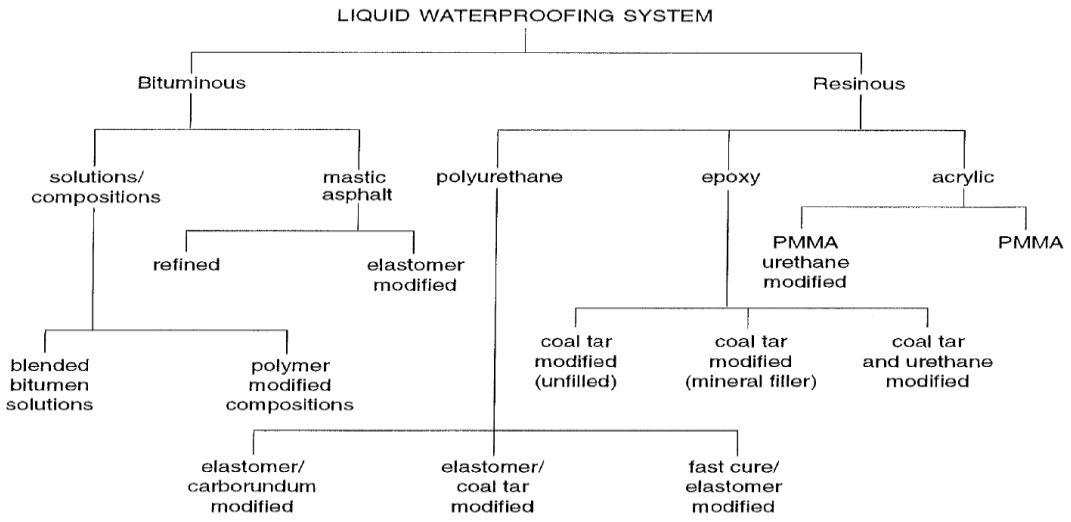

Figure 2.18: Liquid waterproofing systems (Manning, 1995)

2.5.1.1 Spray membrane

A spray membrane is a liquid applied membrane which can be applied to a multitude of bridge deck shapes, and can easily coat the sides of drainage curbs to prevent water penetration from the bridge deck perimeter. While spray membranes are more challenging to install than roll-on membranes, careful mixing and application practices can result in a seamless impermeable layer. ODOT utilizes a two-component polyurea waterproofing membrane which is sprayed over the top of a primer layer on a shot blasted concrete bridge deck. The membrane is evenly sprayed to obtain a coverage of 0.45 gallons/yd^2 (2.0 L/m^2). ODOT recommends that the membrane should be paved over using a minimum of 3 inches (7.6 cm) of asphalt concrete with a PG64-22 binder (ODOT, 2015).

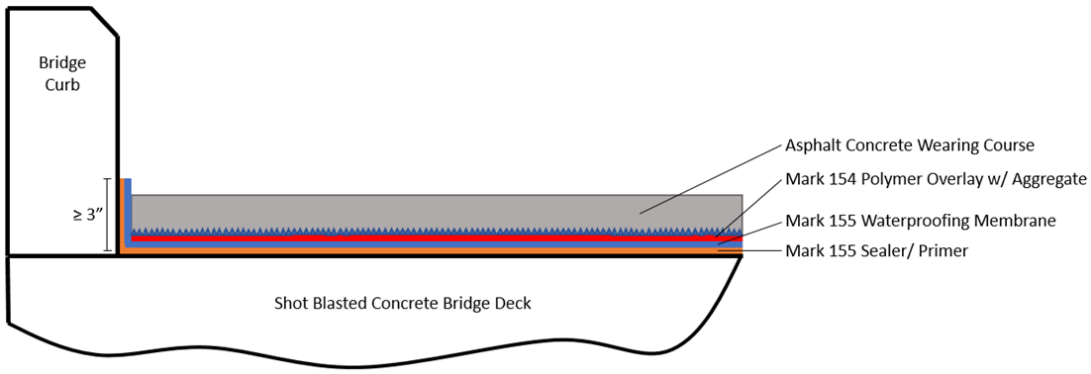

Figure 2.19: Waterproofing spray membrane – Oregon DOT

2.5.1.2 Polymer membrane

ODOT also utilizes a poured polymer membrane as an acceptable bridge deck waterproofing strategy. In this process, existing asphalt is first ground off the bridge

deck, leaving the exposed concrete deck. The deck is then swept and shot blasted according to SSPC SP13/NACE No. 6 until a 1/16-inch (1.6 mm) surface texture depth profile has been achieved. A primer coat is poured and spread over the bridge deck according to the manufacturer's recommendations and the primer layer is allowed to penetrate into the concrete deck for a minimum of 15 minutes. The epoxy polymer waterproofing membrane resin is then poured over the primer layer, covering a maximum area of 0.18 gallons/yd^2 (0.82 L/m^2) and achieving a minimum membrane thickness of 3/16 inches (4.8 mm). Aggregate is broadcast over the resin to complete coverage. Pull tests are conducted to check for a minimum bond strength of 175 psi (1.21 MPa), and chain dragging and coring are used to check for delamination and bond failure. Traffic is allowed on the membrane for 7 days before the bridge deck must be paved using conventional paving methods (ODOT, 2015).

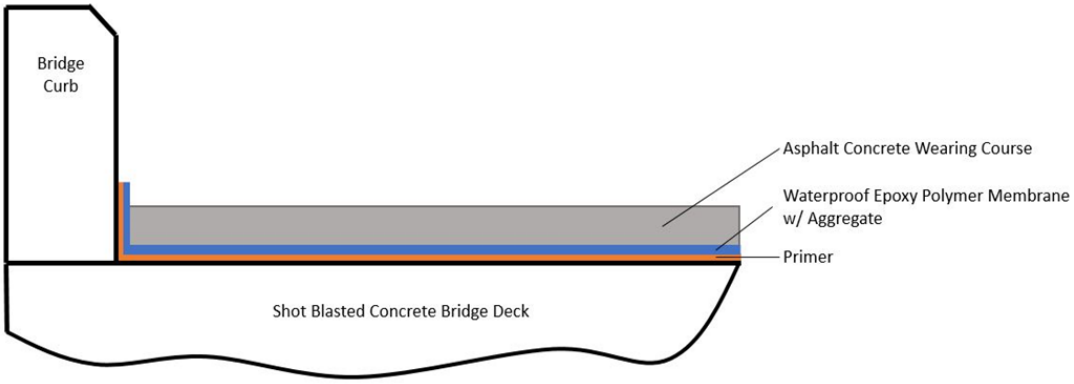

Figure 2.20: Waterproofing polymer membrane - Oregon DOT

2.5.1.3 Mastic asphalt layer on glass fiber net

Sweden has been successfully using a mastic asphalt layer on top of a glass fiber net as an effective bridge deck waterproofing strategy. The glass fiber net acts as a ventilating layer and is adhered to a shot blasted bridge deck using a primer layer. A 10mm (0.39 in) thick mastic asphalt layer is then poured over the glass fiber net. The mastic asphalt layer serves to waterproof the bridge deck and consists of polymer modified bitumen, limestone filler and sand. Dense asphalt concrete, mastic asphalt or concrete is placed over the mastic asphalt waterproofing layer to act as a protective surface layer (EAPA, 2013).

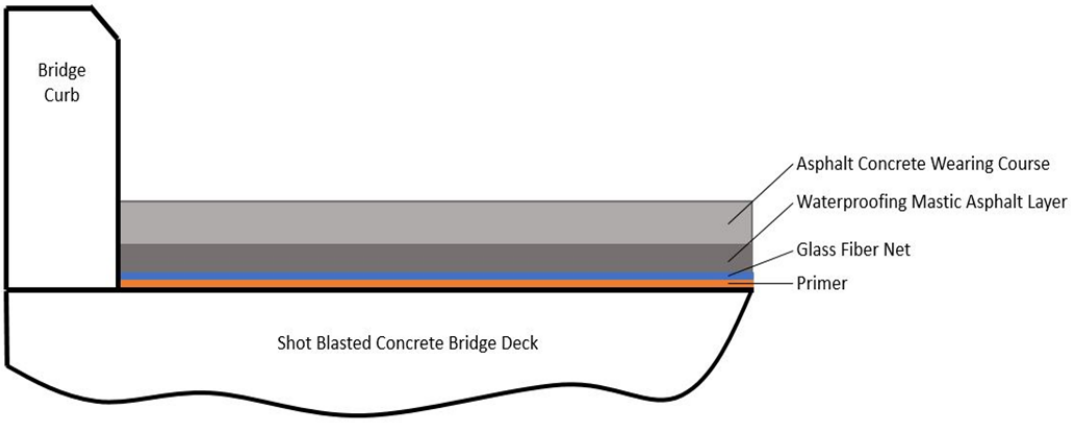

Figure 2.21: Mastic asphalt on glass fiber net - EAPA (Sweden)

2.5.1.4 Texas Bridge Deck Protection System

The Texas Protection System (TPS) is a series of three separate waterproofing strategies employing the use of bridge deck surface treatments and an asphalt overlay (Sherman et al. 1993). The first strategy is a 2inch (50.8 mm) overlay which utilizes two courses of asphalt surface treatment followed by an asphaltic concrete overlay. The second strategy is a 1-1/2-inch (38.1 mm) overlay which implements one course of a latex asphalt, followed by a lightweight surface treatment and a latex asphaltic concrete overlay. The third strategy is a 1-inch (25.4 mm) overlay which uses three courses of asphaltic surface treatment. The Texas Protection System is not commonly used due to a variety of problems encountered. It was found that water which penetrated the asphalt overlay was trapped next to the surface treatment, causing it to deteriorate and enter the concrete deck. Since the asphalt surface treatment concealed the underlying concrete, minor issues which could have been easily repaired were hidden and allowed to develop into larger problems. Additionally, many problems were encountered with cracking, rutting and shoving of the asphalt overlays (Sherman et al. 1993).

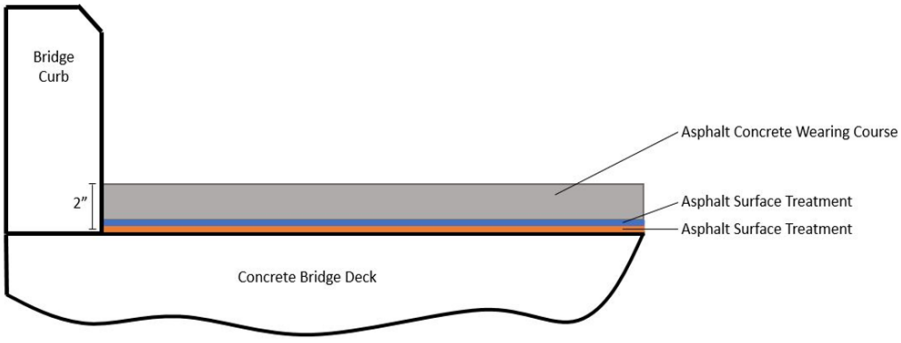

Figure 2.22: Texas bridge deck protection system (1) - Texas DOT

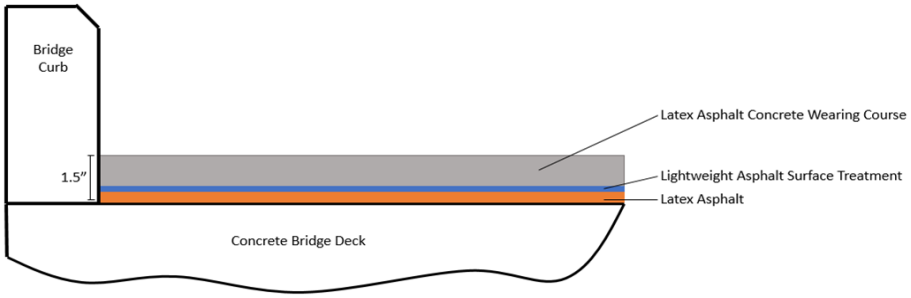

Figure 2.23: Texas bridge deck protection system (2) - Texas DOT

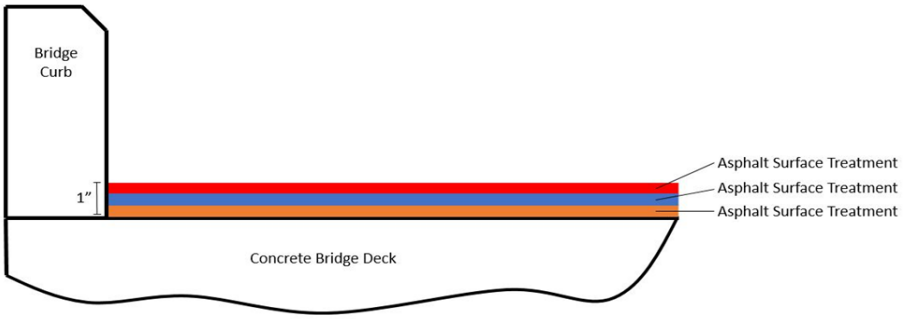

Figure 2.24: Texas bridge deck protection system (3) - Texas DOT

2.5.1.5 Linseed Oil

The use of linseed oil applied directly to a concrete bridge deck is a commonly used method of sealing and waterproofing the bridge deck. As of 2007, linseed oil was the only viable concrete sealer presented in the Missouri DOT's standard specifications (Wenzlick, 2007). The use of linseed oil as a sealer is also common practice in Texas, which has moved away from their Texas Bridge Deck Protective System in favor of the cheaper and easier-to-use oil and is implemented by the Texas DOT in areas exposed to coastal saltwater, deicing salts, and areas where freeze-thaw cycling occurs (Lee, 2017). Problems associated with the placement of linseed oil include poor penetration into the bridge deck, excessive curing time and loss of skid resistance (Sherman et al. 1993).

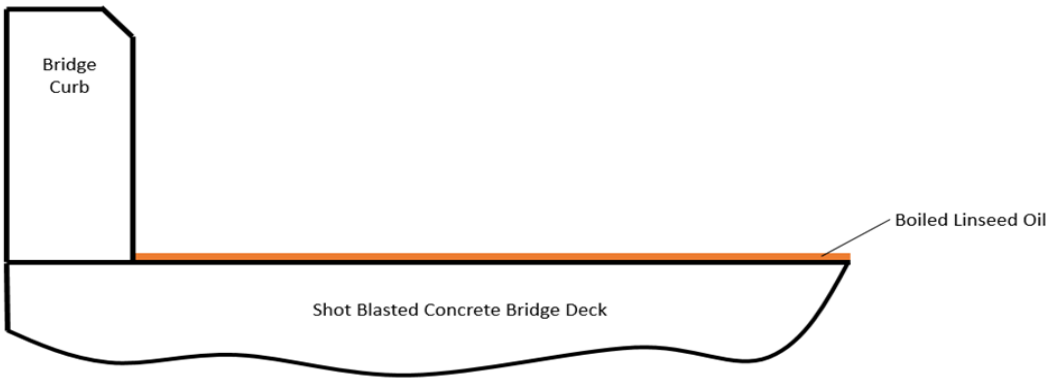

Figure 2.25: Linseed oil - Texas DOT & Missouri DOT

2.5.2 Preformed membranes

Preformed waterproofing membranes often come in sheets which can then be directly placed on top of the concrete bridge deck. The preformed sheets are produced in a factory, reducing the risk of inconsistencies between sheets. They come in uniform thicknesses and installation is straight-forward. Sheets placed side by side, however, create seams in the waterproofing membrane through which water can penetrate if the sheets are not properly adhered to one another (Frosch et al. 2013). These seams can be seen in Figure 2.26. With the large number of joints, it is easy to see how proper adhesion between sheets is a critical factor.

Figure 2.26: Waterproofing roll-on sheet membrane seams (Russell, 2012)

An outline of preformed waterproofing membrane types can be seen in Figure 2.27, and several preformed waterproofing strategies are described below.

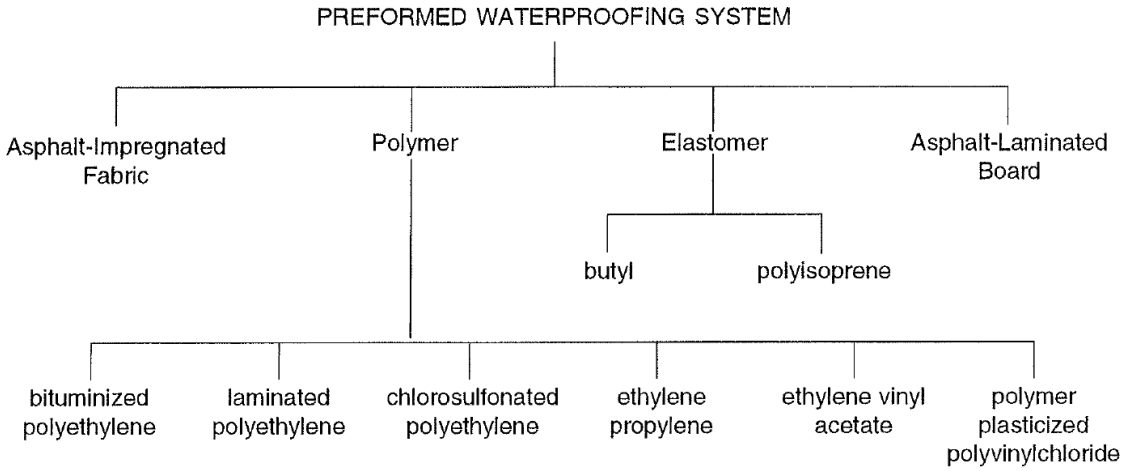

Figure 2.27: Preformed waterproofing systems (Manning, 1995)

2.5.2.1 Roll-on membrane

Roll-on membranes consist of a preformed waterproof sheet which is usually applied longitudinally onto a concrete bridge deck surface. These sheets come in rolls ranging in size from 3 to 5 feet (0.9 to 1.5 m) wide and 30 to 50 feet (9.1 to 15.2 m) long (Manning, 1995). Membrane sheets are bonded to the concrete deck in a variety of ways. Adhesive backings, which are either directly applied or first heated with a blow torch to activate the adhesive, are the most common application method. Another strategy is to pour hot oxidized bitumen onto the concrete deck in front of the membrane as it is being rolled out (Manning, 1995). Some membranes, such as the Soprema Flam membranes require a primer layer to be put down prior to membrane installation. Once in place, the membranes are paved over using traditional paving methods (Russell, 2012).

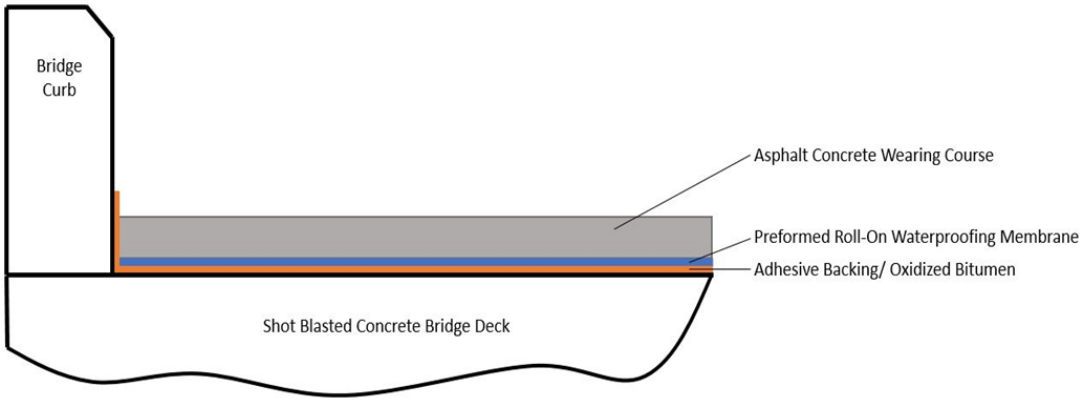

Figure 2.28: Roll-on sheet membrane - NHCRP (Widespread use in USA & Europe)

2.5.2.2 Dual asphalt layer with bitumen sheet

According to a 2013 report published by the European Asphalt Pavement Association (EAPA), Germany employs a concrete bridge deck waterproofing system consisting of a waterproofing bitumen sheet underneath two layers of asphalt. The concrete deck is first cleaned by shot blasting. An epoxy resin primer gritted with 300-500 g/m^2 (8.85 – 14.75 oz/yd^2) quartz sand is spread over the deck to penetrate and seal the concrete pores. A bitumen sheet waterproofing layer (4.5-5.5mm thickness) (0.18 – 0.22 in) is then rolled onto the deck over the primer and a mastic asphalt layer is poured onto the deck at a thickness of 35-40mm (1.38-1.58 in) to act as a protective layer for the bitumen sheets. Finally, a surface layer is constructed which acts as a suitable wearing course for vehicles. This surface course has a thickness of 35-40mm (1.38-1.58 in) and can be constructed of mastic asphalt, stone mastic asphalt, porous asphalt or traditional asphalt concrete (EAPA, 2013).

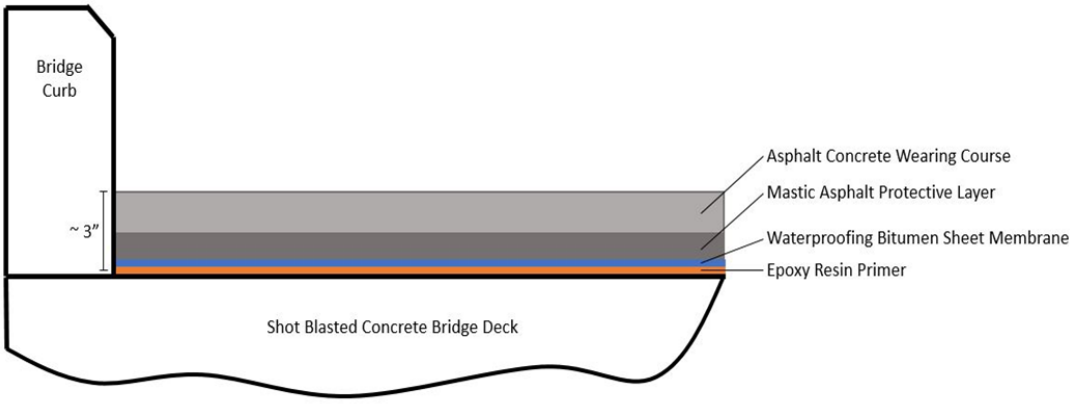

Figure 2.29: Dual asphalt layer w/ bitumen sheet - EAPA (Germany)

2.5.3 Impermeable asphalt concretes

Unlike the waterproofing membranes described previously, impermeable asphalt concretes utilize a highly modified asphalt wearing course which can support traffic loads while preventing water infiltration into the concrete bridge deck. Impermeable asphalt concretes eliminate the need for a waterproofing membrane, decreasing the time and cost associated with bridge deck waterproofing (Frosch et al. 2013). The impermeable asphalt concrete, however, utilizes a different mix design than the adjacent highway, meaning that the paver would need to be emptied and refilled with the modified mix immediately prior to paving over the bridge deck. Since it is difficult to produce two different mixes on the same day, another strategy is to grind out all of the bridge decks for a project, then pave them all at once at a later date using the impermeable asphalt mixture. Several impermeable asphalt waterproofing strategies are described below.

2.5.3.1 Bridge deck waterproofing surface course

The Bridge Deck Waterproofing Surface Course (BDWSC) is a highly modified asphalt pavement developed by the New Jersey DOT which creates an impermeable asphalt wearing course to prevent water infiltration into bridge decks (Bennert, 2011). The BDWSC achieves impermeability through high compaction and low air voids, which is made possible by a modified gradation and a polymer-modified PG76-28 or PG82-34 asphalt binder (AAPT, 2011). The BDWSC is generally constructed using static rollers and a 1.5-inch to 2.5-inch (38.1 mm to 63.5 mm) lift thickness (McCarthy, 2017). Asphalt pavement analyzer rut tests and flexural beam fatigue tests are used to evaluate the performance of the BDWSC mix design (Bennert, 2011).

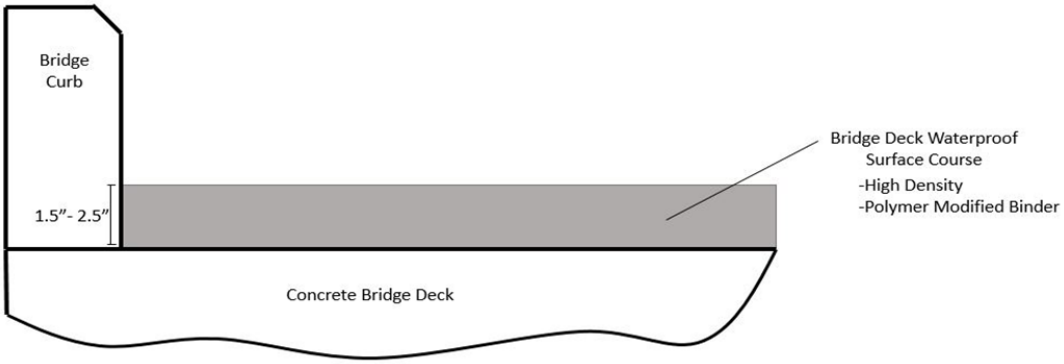

Figure 2.30: Bridge deck waterproofing surface course - New Jersey DOT

2.5.3.2 Polymer modified asphaltic concrete

Polymer modified asphaltic concrete overlays are produced by mixing a polymer material with the binder during the mixing process, allowing the asphalt overlay to act as both a wearing course and a waterproofing layer. These polymer modified asphalt overlays are constructed using traditional paving methods, allowing for a faster and simpler installation process than many other waterproofing membranes. The polymer modifier was determined to increase cracking resistance in the asphalt concrete.

In a study by Coleri et al. (2017), two asphalt mixtures with polymer modified binder and one mixture with traditional binder were evaluated using several test methods to investigate the potential cracking and rutting resistance benefits of using polymer modified binders. Results from this study found that polymer modification did not create a significant change in the mixture stiffness, however the polymer modification serves to impart ductility to the mix, thereby significantly increasing its cracking resistance as compared to the non-polymer modified mixture.

As of 2013, the product Rosphalt by Royston Laboratories was the only commonly used polymer modified asphalt concrete specifically designed for waterproofing purposes. This product consists of a polymeric additive which is directly added to the asphalt binder at the asphalt plant (Frosch et al. 2013). The Maine DOT conducted a study in 2009 on Rosphalt overlays installed on three separate bridge decks, concluding that each overlay was still performing well after five years. The Wisconsin DOT and Kentucky Transportation Cabinet have also found Rosphalt to be very effective as a waterproofing overlay on high volume roads and bridges (Frosch et al. 2013).

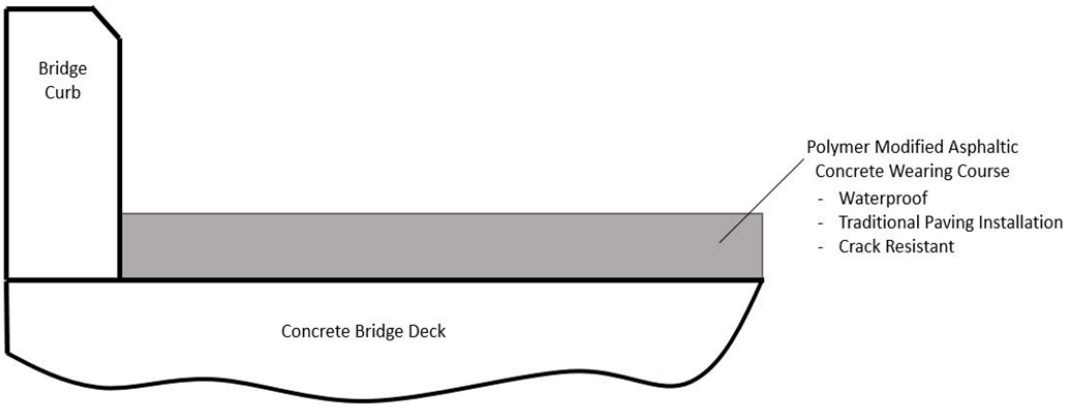

Figure 2.31: Polymer modified asphalt concrete - Maine DOT & Wisconsin DOT

2.5.4 Selected bridge deck waterproofing strategies

Based on comments and recommendations from the technical advisory committee (TAC), five of the nine bridge deck waterproofing strategies described above were selected for further investigation in this study. The spray membrane, polymer membrane, roll-on membrane, dual asphalt layer with bitumen sheet and bridge deck waterproofing surface course will be tested to evaluate their viability as effective waterproofing strategies. The Oregon Department of Transportation has experience implementing the spray membrane, polymer membrane and roll-on membrane strategies. The bridge deck waterproofing surface course has been proven effective in the state of New Jersey and the dual asphalt layer with bitumen sheet has been successfully implemented in Europe (Bennert 2011, EAPA 2013).

2.6 SUMMARY

A review of the literature indicated that the construction of an asphalt overlay on concrete bridge decks is common practice to extend the service life of the bridge. An overlay helps prevent damage to the deck from factors such as studded tires, de-icing chemicals and freeze-thaw cycles. In some cases, water has been known to pass through the asphalt overlay and penetrate the concrete deck, allowing corrosive materials to access the steel reinforcement within the deck. This necessitates that a waterproofing membrane be installed between the concrete bridge deck and asphalt overlay to prevent water penetration into the deck (WSDOT, 2016). Additional problems have been observed regarding bonding at the interface between the waterproofing membrane, asphalt overlay and concrete bridge deck (Zhou et al. 2008, Mohammad et al. 2012). ODOT constructs bridge deck asphalt overlays in the same manner as a typical highway asphalt overlay. The asphalt overlay is constructed using traditional paving methods, directly over the top of any waterproofing membrane that has been installed, allowing for a seamless and continuous wearing course over the bridge deck (ODOT, 2015).

Three main failure mechanisms were investigated and found to contribute to waterproofing membrane and bond adhesion failure. Construction temperature effects, namely temperatures of the asphalt concrete overlay at its time of placement, were one of the most significant failure mechanisms for waterproofing membrane installation. Excessively high HMA temperatures

were capable of softening the waterproofing membrane and causing it to flow during compaction of the asphalt overlay, thereby creating a nonuniform impermeable layer (Frosch et al. 2013). Zhou et al. (2008) investigated the interface adhesion strength of waterproofing membranes under different compaction temperatures, concluding that there is an optimal temperature range between 130°C and 170°C (266°F - 338°F) to provide the highest interface pull-off strength. Shear forces exerted on waterproofing membranes were also found to be a significant failure mechanism. Liu et al. (2014) examined the factors affecting shear strength between samples which used a waterproofing adhesive layer to bond an asphalt pavement to a concrete substrate. Shear testing on the samples determined that increased external temperatures decreased shear strength, an adhesive spraying quantity of 1.3 L/m^2 (0.29 gal/yd^2) produced the optimal shear strength and a concrete surface that had undergone transversal or longitudinal roughening produced the highest shear strength results. Freeze-thaw cycles were another failure mechanism which had a large impact on waterproofing membrane effectiveness. It was found that when water permeates through the asphalt wearing course, it can become trapped between the waterproofing membrane and asphalt layer, resulting in spalling of the asphalt with subsequent freeze-thaw cycles (Russell, 2012). Limited research has been conducted which focuses on the freeze-thaw susceptibility of asphalt wearing courses on concrete bridge decks with a waterproofing membrane.

Several field and laboratory tests are commonly used to evaluate the bond performance on concrete bridge decks with a waterproofing membrane and asphalt overlay. Chain dragging and hammer sounding are field tests that can be used to identify areas of delamination. These tests are simple, but also time consuming and provide limited information (Gucunski et al. 2013). Infrared thermography is another non-destructive field test which can be used to quickly identify roadway defects under an asphalt overlay. The thermal images produced by the cameras can be difficult to interpret, and the cameras themselves have a varying degree of reliability (Clark et al. 2003). The pull-off tension test can be implemented in the field or laboratory and is an effective method of evaluating the bond strength between a waterproofing membrane and concrete bridge deck (Liu et al. 2014). Taking cores on a concrete bridge deck is often avoided due to the damage caused to the bridge structure. The Oregon Field Torque Tester (OFTT) is a less destructive field test device used to evaluate the long-term tack coat performance of pavement sections. This device could be used to evaluate the interface bond on concrete bridge decks with a waterproofing membrane and asphalt overlay without causing extensive damage to the bridge structure (Coleri et al. 2017). The four-point bending beam fatigue test is a simple flexural test that can be performed in the laboratory to simulate fatigue damage and determine the fatigue life of a sample (Hartman et al. 2004). Layered samples which include a waterproofing membrane can be produced with a roller compactor and used with the four-point BBF device. Direct shear laboratory tests can be used to evaluate the shear bond strength at the waterproofing membrane interface between asphalt and concrete layers. Many similar direct shear devices exist, most of which evaluate shear strength based on the maximum applied shear load divided by the cross-sectional area of a sample (Mohammad et al. 2012, West et al. 2005).

Flow number tests are a type of repeated load permeant deformation laboratory test used to evaluate the rutting characteristics of a sample. The flow number parameter represents the onset of tertiary flow which indicates shear deformation within an asphalt concrete sample (Biligiri et al. 2007). The Hamburg wheel tracking test is another test for determining the structural resistance of a sample and is conducted by rolling a steel wheel over a sample immersed in a hot

water bath to simulate vehicle tire loadings (Yildirim et al. 2007). Both the flow number and Hamburg wheel tracking tests can be used to determine the impact of waterproofing membrane strategies on the structural resistance of an asphalt overlay on a concrete bridge deck structure. These tests may be particularly useful in evaluating the performance of impermeable asphalt pavement overlay strategies (see section 2.5.3) which achieve a higher density through a softer binder and increased binder content.

Various strategies have been introduced to reduce the issue of asphalt overlay failure on bridge decks with a waterproofing membrane. Frosch et al. (2013) explains that any dirt or debris present on the deck during application of the primer for a waterproofing system will prevent the primer from adequately bonding to the deck. The Oregon Department of Transportation (ODOT) specifies that a concrete bridge deck must be shot blasted and cleaned using compressed air prior to the application of primer for a waterproofing system (ODOT, 2015). Membrane level sub-surface drainage has also been shown to prevent failure of the asphalt overlay. Without sub-surface drainage, water that penetrates the asphalt overlay can become entrained and pool on top of the waterproofing membrane. This will cause extensive damage to the asphalt overlay when that water expands during freeze-thaw cycles (Moser et al. 2017). Proper construction of the primer layer is critical to the bond between the concrete bridge deck, waterproofing membrane and asphalt overlay. The primer layer is specially formulated to bond with the waterproofing membrane, increasing the overall adhesion between layers (Russell, 2012). Allowing adequate setting time for the primer and conducting pull tests are two methods of ensuring an adequate bond between the primer and bridge deck (ODOT, 2015). Poor adhesion of the primer layer can result in the separation of the asphalt overlay and waterproofing membrane from the concrete bridge deck.

Three types of bridge waterproofing systems were deemed most effective through a review of the literature. Liquid membranes, which are either poured or sprayed onto the concrete deck create a seamless barrier against water penetration, but these systems are costly and difficult to install. Preformed membranes are often produced in large sheets and rolled over the concrete deck. Installation of these sheets is simple, however, sheets placed side-by-side create seams in the membrane through which water can penetrate if the sheets are not properly adhered to one another. Impermeable asphalt concretes utilize a highly modified mix design to produce an impermeable asphalt wearing course. These systems eliminate the need for a waterproofing membrane, but also require a modified asphalt mixture to install on a bridge deck (Frosch et al. 2013). Based on recommendations from the technical advisory committee (TAC), five of the nine bridge deck waterproofing strategies described previously will be investigated in this study. The five selected strategies are the sprayed waterproofing membrane, poured waterproofing membrane, roll-on waterproofing membrane, bridge deck waterproofing surface course and dual asphalt layer with bitumen sheet.

3.0 IMPERMEABLE ASPHALT CONCRETE LAYER TO PROTECT AND SEAL CONCRETE BRIDGE DECKS

3.1 INTRODUCTION

Impermeable asphalt overlays are one strategy used to prevent water and chloride infiltration on bridge decks. Impermeable asphalt waterproofing systems are generally constructed by applying a tack coat directly to the exposed concrete deck and paving over the deck using a specially modified asphalt mixture (Russell 2012). Unlike the waterproofing membranes described previously, impermeable asphalt concretes utilize a highly modified asphalt wearing course which can support traffic loads while preventing water infiltration into the concrete bridge deck. Impermeable asphalt overlays eliminate the need for a waterproofing membrane, decreasing the time and cost associated with bridge deck waterproofing (Frosch et al. 2013). The impermeable asphalt concrete, however, utilizes a different mix design than the adjacent highway, meaning that the paver would need to be emptied and refilled with the modified mix immediately prior to paving over the bridge deck. Since it is difficult to produce two different mixes on the same day, another strategy is to grind out all of the bridge decks for a project and then pave them all at once at a later date using the impermeable asphalt mixture. The Bridge Deck Waterproofing Surface Course (BDWSC), described below, is one such impermeable asphalt waterproofing strategy evaluated in this study. Laboratory tests were conducted to determine its effectiveness in terms of permeability and resistance to high truck traffic.

The Bridge Deck Waterproofing Surface Course (BDWSC) is a highly modified asphalt pavement developed by the New Jersey DOT which creates an impermeable asphalt wearing course to prevent water infiltration into bridge decks (Bennert et al. 2011). The BDWSC achieves impermeability through high compaction and low air voids, which is made possible by a modified gradation and a modified asphalt binder (Bennert et al. 2011). The BDWSC is generally constructed using static rollers and a 1.5-inch to 2.5-inch (38.1 mm to 63.5 mm) lift thickness (McCarthy 2017). Asphalt pavement analyzer rut tests and flexural beam fatigue tests were suggested to be used to evaluate the performance of the BDWSC mix design (Bennert et al. 2011).

The main goal of this part of the study is to develop and test an impermeable asphalt mixture produced using the BDWSC method that can seal and protect the concrete bridge deck by preventing water and deicing salts from penetrating into the deck. Permeability of different asphalt mixture types were quantified by permeability testing and moisture sensor measurements (first use of moisture sensors for permeability evaluation of BDWSC strategies). Rutting and cracking resistance of the developed impermeable asphalt mixture strategies were also evaluated by conducting flow number (FN) and semi-circular bend (SCB) tests in the laboratory, respectively.

3.2 OBJECTIVES

The major outcomes of this study are to:

- Develop an impermeable asphalt mixture using the BDWSC design method,
- Identify the required gradation and binder content needed to achieve a 1% air void mixture,
- Develop an experiment to test the impermeability of designed mixtures under realistic rainfall conditions over an extended period,
- Develop a moisture sensor and software setup capable of continually logging moisture infiltration data over an extended period,
- Evaluate the rutting resistance of specially designed impermeable asphalt mixes,
- Evaluate the cracking resistance of specially designed impermeable asphalt mixes,
- Identify how variations in binder content impact the cracking and rutting resistance of specially designed asphalt mixes,
- Conduct surface texture investigations to evaluate potential skid resistance issues with high binder content mixes, and
- Provide perspective on how impermeable asphalt mixes can be used to protect and seal concrete bridge decks in Oregon.

3.3 MATERIALS AND METHODS

3.3.1 Experimental design

To investigate the feasibility of using specialized mix designs to create an impermeable asphalt overlay, three different binder contents were chosen to produce samples based on the BDWSC design method. The specifications for the BDWSC mix design stated that an air void content of 1.0% that can be reached with 50 gyrations in a Superpave Gyratory Compactor (SGC) was used to create an impermeable asphalt. In the asphalt mix design, this low air void content was achieved by applying 50 gyrations to an asphalt mixture with a modified PG76-22 binder type at a binder content of 8.5%. In addition to mix design, this study sought to investigate whether lower binder contents and higher air void contents could also be used to achieve impermeability while maintaining structural capacity of the pavement. Laboratory tests were conducted on samples with binder contents of 7.5%, 8.0% and 8.5%. The air void contents for the 7.5%, 8.0% and 8.5% binder content samples after applying 50 gyrations were 4.9%, 3.2% and 1.0%, respectively. The high binder contents were expected to produce samples that were resistant to cracking, thus the primary areas of concern were rutting resistance and impermeability when evaluating the performance of each sample for the three binder contents. Tests conducted on each sample type included semi-circular bending (SCB), dynamic modulus (DM), flow number (FN), Oregon Field Torque Tests (OFTT), permeability and rainfall simulation tests.

An additional mix design was conducted using a PG70-22ER asphalt binder. Designing a mixture with this binder grade and a binder content of 8.5% achieved an air void content of 3.17% which was significantly higher than that of a mixture designed with a PG76-22 binder and the same binder content. The lowest air void content achieved with the PG70-22ER binder was a 2% air void content when using a 9.5% binder content. At this high of a binder content, there would be issues with constructability in the field. Aside from the mix design, no further testing was conducted with the PG70-22ER binder grade and it is not recommended for use in an impermeable asphalt mixture.

A comprehensive experimental factorial for rutting, cracking and bond strength tests is shown below in Table 3.1. All cracking and rutting tests were conducted on asphalt samples with three different binder contents (7.5%, 8.0%, and 8.5%). Bond strength tests were conducted on samples with 8.0% and 8.5% binder contents. Three replicate samples of each binder content were prepared for the DM and FN tests, and four replicate samples were prepared for the SCB tests. All samples were prepared using a PG76-22 binder grade, a 20% RAP content and a fine gradation developed from the BDWSC design method (Bennert et al. 2011).

Table 3.1: Experimental Design for Rutting, Cracking and Bond Strength Tests

Test type	Binder content	Binder grade	Temp.[2]	Air-void content	Repl.[3]	Total tests
SCB	7.5%		25ºC (77°F)	4.9% (7.5% BC)	4	12
	8.0%	PG 76-22		3.2% (8.0% BC)		
	8.5%			1.0% (8.5% BC)		
Dynamic Modulus	7.5%		4°C (39.2°F) [1]	4.9% (7.5% BC)	3	27
	8.0%	PG 76-22	20°C (68°F)	3.2% (8.0% BC)		
	8.5%		40°C (104°F)	1.0% (8.5% BC)		
Flow Number	7.5%		54.7ºC (130.5°F)	4.9% (7.5% BC)	3	9
	8.0%	PG 76-22		3.2% (8.0% BC)		
	8.5%			1.0% (8.5% BC)		
	8.0%			3.2% (8.0% BC)		
OFTT	8.5%	PG76-22	25ºC (77°F)	1.0% (8.5% BC)	6	12

Note: [1]All DM samples were tested at temperatures of 4°C, 20°C and 40°C (39.2°F, 68°F and 104°F) and the loading frequencies of 0.1, 0.5, 1, 5 and 10 Hz. A loading frequency of 0.01 Hz was also used for 40°C (104°F) tests.

[2]Temp. = Temperature

[3]Repl. = Replicate

A full experimental plan for permeability tests is shown below in Table 3.2. All permeability tests were conducted on samples of three different binder contents (7.5%, 8.0%, and 8.5%). Two replicate samples of each binder content were prepared for the rainfall simulation and infiltration tests. All experimental samples were prepared using a PG76-22 binder grade, a 20% RAP content and a fine gradation from the BDWSC design method (Bennert et al. 2011). Two traditional production mix samples with air void contents of 7.0% were also prepared and tested to act as a control.

Table 3.2: Experimental Plan for Permeability Tests

Test type	Binder content	Binder grade	Test duration	Air-void content	Replicate	Total tests
Infiltration	Prod. Mix 7.5%		4 hrs	7.0% (Prod. Mix) 4.9% (7.5% BC)	2	8
	8.0%	PG 76-22		3.2% (8.0% BC)		
	8.5%			1.0% (8.5% BC)		
Rainfall Simulation	Prod. Mix 7.5%		5 days	7.0% (Prod. Mix) 4.9% (7.5% BC)	2	8
	8.0%	PG 76-22		3.2% (8.0% BC)		
	8.5%			1.0% (8.5% BC)		

3.3.2 Materials and asphalt mixture gradation

This section provides information about virgin binders, virgin aggregates and RAP material used in this study. All the materials were obtained from local sources.

3.3.2.1 Aggregates

Virgin aggregates were obtained from a local quarry in Salem, Oregon. The virgin aggregates were delivered in three gradations, namely coarse (1/2" to #4), medium (#4 to #8), and fine (#8 to zero). To determine the gradation of each stockpiled aggregate, wet-sieve and dry-sieve analyses were performed on multiple samples of each stockpile following AASHTO T 27-11 (2011).

3.3.2.2 Recycled Asphalt Pavement (RAP) and Recycled Asphalt Shingles (RAS)

RAP materials were sampled from a plant in Salem, Oregon. Gradation, binder content and theoretical maximum specific gravity (G_{mm}) of RAP materials were provided by the plant. AASHTO T 308-10 (2010) was followed for binder extraction and RAP binder content measurements. The quantity of binder in RAP materials was determined as 6.22%. AASHTO T 30-10 (2010) was followed to determine the gradation of extracted RAP aggregates.

3.3.2.3 Binders

A local producer in Oregon provided the virgin modified PG76-22 and PG70-22ER binder for this study. The binder was modified with polymers, allowing for the use of higher binder contents while maintaining enough stiffness to allow for adequate rutting resistance. Temperature curves, mixing temperatures and compaction temperatures were provided by the producer as well. Laboratory mixing and compaction temperatures were estimated by using the viscosity-temperature lines following the procedure described in Asphalt Institute guidelines (2016) and AASHTO T 316-11 (2011).

Asphalt mixtures in this study were prepared with three binder contents (7.5%, 8.0% and 8.5%). These binder contents are the percentage of the total binder by the weight of the mix, which includes the recycled binder from RAP materials. In this study, it was

assumed that all the RAP binder was completely blended with the virgin binder (100% blending).

3.3.2.4 Target gradations

Target gradation was obtained from the BDWSC impermeable asphalt mix design (Bennert et al. 2011). All mixes were designed to reach the target gradation and consisted of stockpile percentages of 0% coarse aggregates, 44% medium aggregates, 36% fine aggregates and 20% RAP. Target gradation and the gradations of virgin aggregates and extracted RAP aggregates are presented in Figure 3.1.

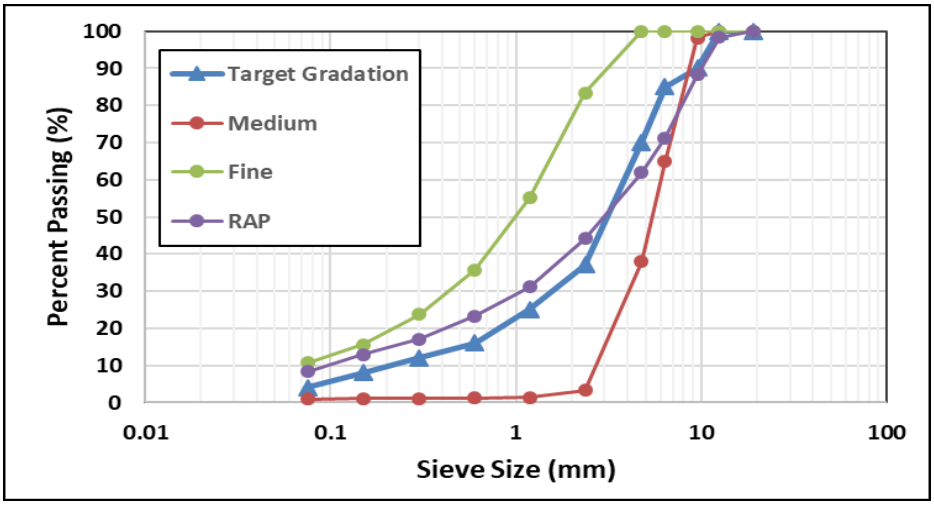

Figure 3.1: Target, extracted RAP, and stockpiled aggregate gradations (1 mm = 0.04 in)

As can be seen in Figure 3.2 the gradation for the BDWSC mix design for impermeable asphalt is significantly finer than that of a typical dense gradation.

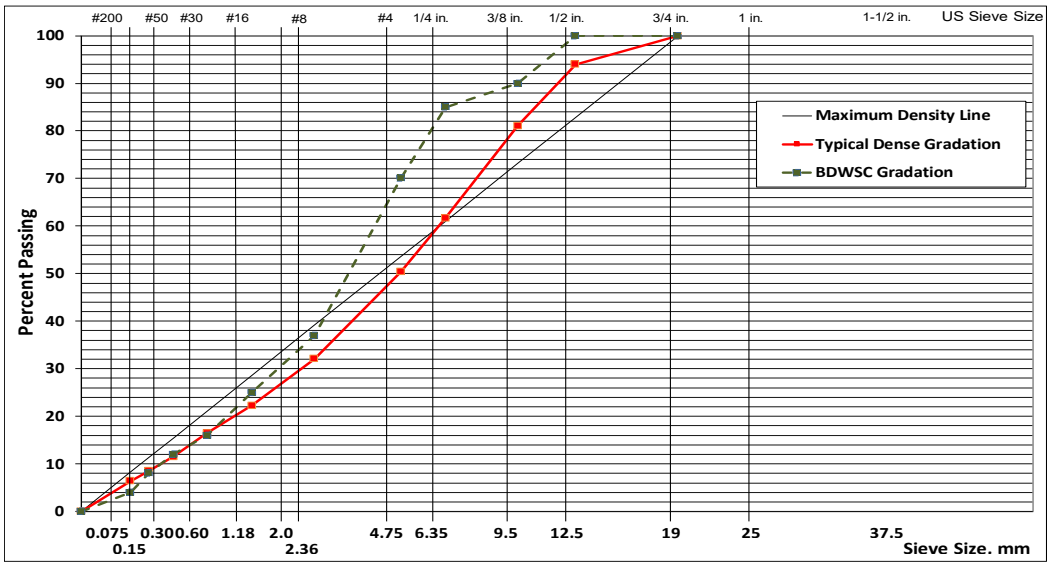

Figure 3.2: Gradation plot of BDWSC mix design

3.4 TEST METHODS AND SAMPLE PREPARATION

3.4.1 Batching, mixing, and compaction

For sample preparation, aggregates and RAP were batched to meet the final gradation obtained from the BDWSC design method (Newcomb et al. 2015). Then, batched samples were mixed and compacted according to the AASHTO T 312-12 (2012) procedure. Before mixing, aggregates were kept in the oven at 10 ºC higher than the mixing temperature, RAP materials were kept at 110 ºC (McDaniel and Anderson 2001), and binder was kept at the mixing temperature for 2 hours. After mixing, prepared loose mixtures were kept in the oven for 4 hours at 135 ºC (AASHTO R 30-10 2010) to simulate short-term aging. The goal of short-term aging is to simulate the aging and binder absorption that occurs during mixing phase of the production process. Then the aged loose asphalt mixtures were kept in the oven for 2 more hours at the compaction temperature prior to compaction. Compaction of cylindrical samples for the cracking and rutting tests was performed using a Superpave gyratory compactor. A roller compactor was used to compact block samples for permeability testing.

3.4.2 Sample preparation for rutting and cracking testing

Samples for the semi-circular bending (SCB), flow number (FN) and dynamic modulus (DM) tests were prepared using a laboratory Superpave Gyratory Compactor (SGC) in accordance with AASHTO T 312-12 (2012). Gradations were developed for the samples using the BDWSC mix design method (Bennert et al. 2011). A PG76-22 binder was used and binder contents of 7.5%, 8.0% and 8.5% were tested.

For the SCB tests, samples were compacted to a height of 130 mm (5.1 in). Two samples with a thickness of 57 ± 2 mm (2.2 ± 0.1 in) were then cut from each compacted sample using a high-accuracy saw. The circular samples were then cut into two identical halves. Based on methodology from past research, a 15 mm ± 0.5 mm (0.6 ± 0.02 in) notch was cut along the axis of symmetry using a table saw and a customized cutting jig developed at Oregon State University (OSU) (Coleri et al. 2017, Sreehar et al. 2018).

For the DM and FN tests, samples were compacted to a height of 170 mm (6.7 in). The samples were then cored, and the tops and bottoms were cut off to produce a cylindrical core sample with a height of 150 mm (5.9 in) and a diameter of 100 mm (3.9 in).

3.4.3 Semi-Circular Bend (SCB) test

SCB tests were conducted in this study to determine cracking performance of asphalt mixtures. The test method for evaluating cracking performance of asphalt concrete at intermediate temperatures developed by Wu et al. (2005) was followed.

Tests were conducted at 25ºC (77ºF) with a displacement rate of 0.5 mm/min (0.02 in/min). Samples were kept in the chamber at the testing temperature for conditioning the day before being tested. The flat side of semi-circular samples was placed on two rollers. As vertical load with constant displacement rate was applied on the samples, applied load was measured (AASHTO 2013). The test stopped when the load dropped below 0.5 kN (112.4 lbf). Flexibility

Index (FI) was the testing parameters obtained from the SCB test results (displacement vs. load curves). A MATLAB code and a stand-alone software were developed to take the raw SCB test data and calculate the FI parameter used for cracking performance evaluation in this study (MATLAB 2016).

FI is the ratio of the fracture energy (G_f) to the slope of the line at the post-peak inflection point of the load-displacement curve. FI correlates with brittleness, and it was developed for asphalt materials by Ozer et al. (2016). Lower FI values show that the asphalt mixtures are more brittle with higher crack growth rate (Ozer et al. 2016). G_f is obtained by dividing the work of fracture (W_f) by the ligament area (A_{lig} in Equation **Error! Reference source not found.**). Work of fracture is the area under load versus displacement (P-u) curve. The remainder of the curve is extrapolated by using a power function with a coefficient of -2 to estimate the area under the tail part of the P-u curve (AASHTO 2013). Coleri et al. (2017) determined that FI for high performance polymer-modified Oregon asphalt mixtures is 9. W_f is the sum of the area under the curve obtained from the test (W) and the extrapolated tail part (W_{tail}).

$$\mathbf{FI = A * \frac{G_f}{abs(m)}} \tag{3-1}$$

$$\mathbf{G_f = \frac{W_f}{A_{lig}}} \tag{3-2}$$

$$\mathbf{W_f = \int P\ du} \tag{3-3}$$

$$\mathbf{A_{lig} = (r-a) * t} \tag{3-4}$$

Where:

G_f = fracture energy (kJ/m^2) (ft-lbf/ft^2),

abs(m) = absolute value of the slope at inflection point of post-peak load-displacement curve,

A = unit conversion factor and scaling coefficient,

W_f = work of fracture (kJ) (ft-lbf),

P = applied load (kN) (lbf),

u = load line displacement (m) (ft),

A_{lig} = ligament area (m^2) (ft^2),

r = sample radius (m),

a = notch length (m), and

t = sample thickness (m).

3.4.4 Flow Number (FN) test

The flow number (FN) test is a performance test for evaluating rutting resistance of asphalt concrete mixtures (Bonaquist et al. 2003). In this test, while constant deviator stress is applied at each load cycle on the test sample, permanent strain at each cycle is measured. Permanent deformation of asphalt pavement has three stages: 1) primary or initial consolidation, 2) secondary and 3) tertiary or shear deformation (Biligiri et al. 2001). FN is the loading cycle at which the tertiary stage starts after the secondary stage.

In this study, testing conditions and criteria for FN testing described in AASHTO TP 79-13 (2013) for unconfined tests were followed. The recommended test temperature, determined by LTPPBind Version 3.1 software, is the average design high pavement temperature at 50% reliability for cities in Oregon with high populations and at a depth of 20 mm (0.79 in) for surface courses (Rodezno et al. 2015). Tests were conducted at a temperature of 54.7oC (130.5oF) with average deviator stress of 600 kPa (87.0 psi) and minimum (contact) axial stress of 30 kPa (4.4 psi). For conditioning, samples were kept in a conditioning chamber at the testing temperature a day prior to being tested. To calculate FN in this study, the Francken model was used (Francken 1977).

Recommended minimum FN values by AASHTO TP 79-13 (2013) for traffic levels of 3 to 10, 10 to 30, and higher than 30 million ESALs are 50, 190, and 740, respectively (Rodezno et al. 2015). In this study, mixes were evaluated based on the 30 million ESAL traffic levels. Thus, samples with a flow number greater than 740 were considered to have acceptable performance.

3.4.5 Dynamic Modulus (DM) test

The dynamic modulus test is a strong indicator of an asphalt mixture's response to loading speeds and temperatures. Dynamic modulus and phase angle are two performance variables obtained from DM tests. Dynamic modulus shows how stiff an asphalt mixture is, with higher dynamic modulus values representing a higher stiffness. The time delay between the time point at which peak stress is applied and the time point at which peak strain is observed are used to calculate phase angle. The phase angle represents viscoelastic characteristics of asphalt mixtures. A higher phase angle indicates that the samples are less viscous, more susceptible to rutting and more resistant to cracking (Darnell et al. 2015).

In this study, DM tests were carried out in accordance with the AASHTO TP 79-13 (2013) specification. Using the sample preparation method previously described, gauge points were

glued onto the samples to allow for the attachment of LVDT sensors. Samples were then allowed to condition in the environmental chamber overnight. Tests were carried out at 4°C (39.2°F), 20°C (68°F and 40ºC (104°F) temperatures and 0.1 Hz, 0.5 Hz, 1 Hz, 5 Hz and 10 Hz frequencies. For the 40ºC (104°F) case, a frequency of 0.01 Hz was also used. From the tests, master curves were developed for the dynamic modulus and phase angle parameters by following the AASHTO PP61-13 (2013) specification.

3.4.6 Sample preparation for permeability and bond strength tests

Samples for the infiltration, rainfall simulation and bond strength tests were composed of a 50 mm (2.0 in) thick concrete slab with a 50 mm (2.0 in) thick asphalt overlay. The prepared block samples had dimensions of 400 x 260 x 100 mm (15.8 x 10.2 x 2.0 in). Concrete slabs were cast using a high strength concrete mix and a grinder was then used to create texture on the concrete slab representative of a milled surface. The surface was ground to a mean texture depth (MTD) of 1.6 mm (0.0625 in) (ODOT 2015). The MTD of each concrete slab was determined using a sand patch test in accordance with ASTM E965-15 (2015).

Asphalt was then compacted over the concrete slab using a laboratory hydraulic roller compactor. Two hours prior to compaction, a high-performance tack coat was uniformly applied to the concrete slab using an application rate of 0.36 L/m^2 (0.08 gal/yd^2). This application rate was determined as an optimal application rate through studies by Coleri et al. (2017) and Covey et al. (2017). Immediately prior to compaction, two 100 mm (3.9 in) long metal rods were placed at each end of the concrete slab. After compaction, these rods were removed, creating openings in the sample through which the moisture sensor could then be inserted for rainfall simulation testing (Figure 3.3). Asphalt gradations were developed for the samples using the BDWSC mix design method. A PG76-22 binder was used and samples with 7.5%, 8.0% and 8.5% air-void contents were prepared. Additionally, control samples were produced using a production mix sampled from a drum plant in Oregon and compacted to an air void content of 7.0%, which corresponds to the asphalt layer density requirement for highway construction in Oregon (93% density level). For Oregon Field Torque Test (OFTT) bond strength tests, half of the samples tested were first subjected to a series of 15 freeze-thaw cycles. For freeze-thaw cycling, samples were first placed under the rainfall simulator and underwent a simulated rainfall event for a period of 48 hours. Samples were then placed in a freezer set at -20 ºC (-4 ºF) for 14 hours. The frozen samples were removed from the freezer to thaw for 10 hours at 20 ºC (68 ºF). This process was repeated for 15 days to simulate 15 freeze-thaw cycles.

3.4.7 Infiltration test method

Infiltration tests were conducted using a modified version of the ASTM C1701 (2017) testing procedure. This test method specifies the use of a 300 mm (12.0 in) hollow cylinder to be used as a testing apparatus. The laboratory produced blocks being tested, however, had a width of only 260 mm (10.2 in) thus a hollow cylinder with a diameter of 152.4 mm (6.0 in) was used for the tests. Due to the low air void contents of the samples being tested, a total of 0.15 kg (0.3 lbs) of water was used as opposed to the 3.6 kg (8.0 lbs) of water outlined in the standard.

To conduct the test, marks were made inside the hollow cylinder at heights of 10 and 15 mm (0.4 and 0.6 in) to allow a constant pressure head to be maintained as water is added. The cylinder

was then adhered to the center of the block sample using a waterproof silicone rubber to prevent water leaking from the bottom of the cylinder. Prewetting was conducted to fill surface voids and check for leaks by adding 50 g (0.1 lbs) of water to the cylinder and letting sit for 5 minutes. After the prewetting stage, 0.15 kg (0.3 lbs) of water was measured out and poured into the cylinder until filled to the 15 mm (0.6 in) mark. The start time was recorded and water was continually added to the cylinder to maintain a head between the marked lines. The test was stopped and the time recorded once all water poured into the cylinder had infiltrated through the asphalt surface. Tests were also stopped if no water had infiltrated after a span of four hours. The infiltration rate for each sample was calculated as follows:

$$\mathbf{I}=\frac{\mathbf{KM}}{(\boldsymbol{D^2}*\boldsymbol{t})} \qquad \textbf{(3-5)}$$

Where:

I = infiltration rate (mm/hr),

M = mass of infiltrated water (kg),

D = inside diameter of infiltration ring (mm),

t = time required for measured water to infiltrate (s),

K = 4,583,666,000 (mm^3*s)/(kg*h)

3.4.8 Moisture sensor and rainfall simulation test method

Rainfall simulation experiments were conducted using a rainfall simulator developed at OSU which simulated a natural rainfall pattern to continually saturate the sample over the course of a five-day span. A customized moisture sensor was used for the test and consisted of two main components. The sensor component consisted of a CS655 Water Content Reflectometer produced by Campbell Scientific, Inc. The CS655 possesses two 30 cm (11.8 in) nodes and is capable of measuring volumetric water content, bulk electrical conductivity and temperature. The data logger component, capable of running up to four SDI-12 sensors (such as the CS655) simultaneously, was developed. The SDI-12 data logger runs on an open source Python script and can collect continuous data for months at a time (Liu 2017).

For these laboratory experiments, the CS655 sensor was imbedded in the asphalt-concrete interface of the block samples, and fine sand was used to fill remaining voids around the sensor nodes and provide a medium through which any infiltrated water could reach the nodes. The moisture sensor was then sealed using a silicone gel to prevent water from reaching the sensor from the exterior, as opposed to reaching the sensor by permeating through the asphalt overlay (Figure 3.3b). The sensor was wrapped in plastic wrap, and protective covers were placed over the edges of the block to further ensure that no moisture reached the sensor from the sides of the sample or from the insertion point of the sensor nodes (Figure 3.3c). The complete moisture sensor setup is depicted in Figure 3.3 below.

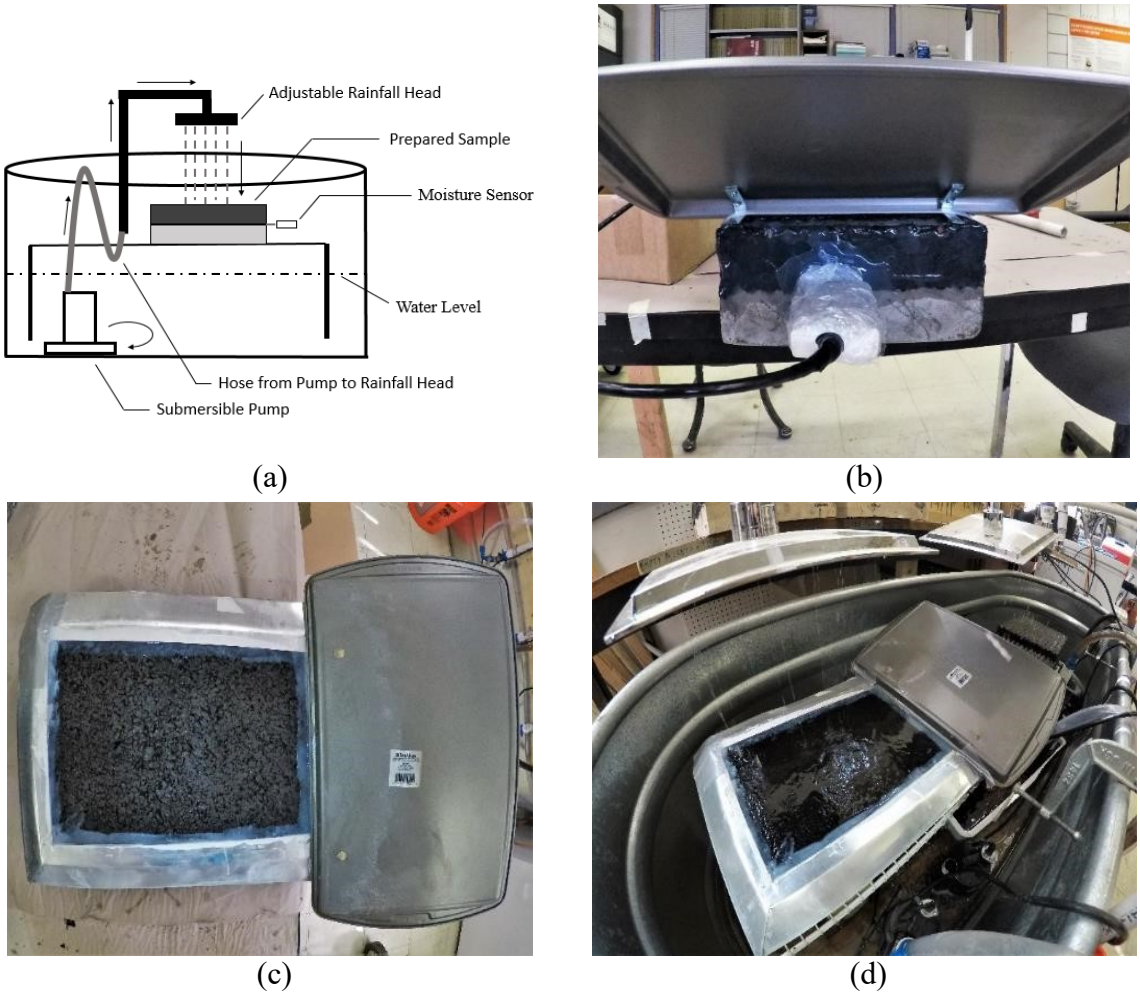

Figure 3.3: Sample with moisture sensor setup (a) Diagram of rainfall simulation setup (b) Sensor inserted in sample, sealed with silicone gel and wrapped in plastic wrap. Protective cover placed over sensor (c) Complete sample setup with side covers (d) Sample being tested in rainfall simulator

The moisture sensor used for the tests was calibrated to take moisture readings every 10 seconds and export the readings to a spreadsheet. Moisture readings were directly measured by reading the dielectric permittivity within a sample, then converting the reading to a volumetric water content (m3/m3). From the output, the amount of water present at the asphalt-concrete interface could be tracked over time, allowing one to determine at what point water had fully infiltrated the sample (Liu 2017).

3.4.9 Oregon Field Torque Test (OFTT) method

The OFTT in-situ torque tester, developed by Coleri et al. (2017), is used to characterize the interlayer shear strength of a multi-layer sample. In this study, the bonds being investigated were those between the concrete slab and the impermeable asphalt overlay. The hardware of the OFTT device consists of an automatic step motor, planetary gearbox, transducers, torque sensor and

amplifier, data acquisition and control systems, and an adjustable frame (Figure 3.4a). A software was developed to control the loading and rotation speed of the system.

To prepare samples for OFTT testing, block slabs were cored using a 2" core drill to a depth of a few millimeters below the base of the impermeable asphalt layer (i.e. a few millimeters into the concrete slab). This allowed the platen for the OFTT test to be adhered to an isolated area of the waterproofing overlay system for testing and allowed failures to occur at the interface between the asphalt and concrete layers. Six OFTT tests were conducted on a single block for each waterproofing strategy. After coring of OFTT blocks, platens were glues to the top of the cores using a fast-setting epoxy (Figure 3.4b).

To conduct the test, the OFTT test system was placed on the platens and the torque frame was adjusted to match the platens (Figure 3.4c). Using the control software, the torque transducer was rotated at 2^{o} per second until the interlayer bond within a sample was completely broken. The OFTT recorded the peak torque stress (strength) at the interface between pavement layers (Figure 3.4d). Using the rotation angle versus applied torque, torque strength was determined. After obtaining the peak torque strength for each sample, the measured torque strength (Nm) was converted to OFTT shear strength (kPa) using the equation given below (Muslich 2009):

$$\boldsymbol{\tau = \frac{12M \times 10^{6}}{\pi D^{3}}} \qquad \textbf{(3-6)}$$

Where;

τ is the interlayer shear strength (OFTT shear strength) (kPa);

M is the peak torque at failure (N.m), and

D is the diameter of the core (mm).

The OFTT testing setup can be observed in Figure 3.4.

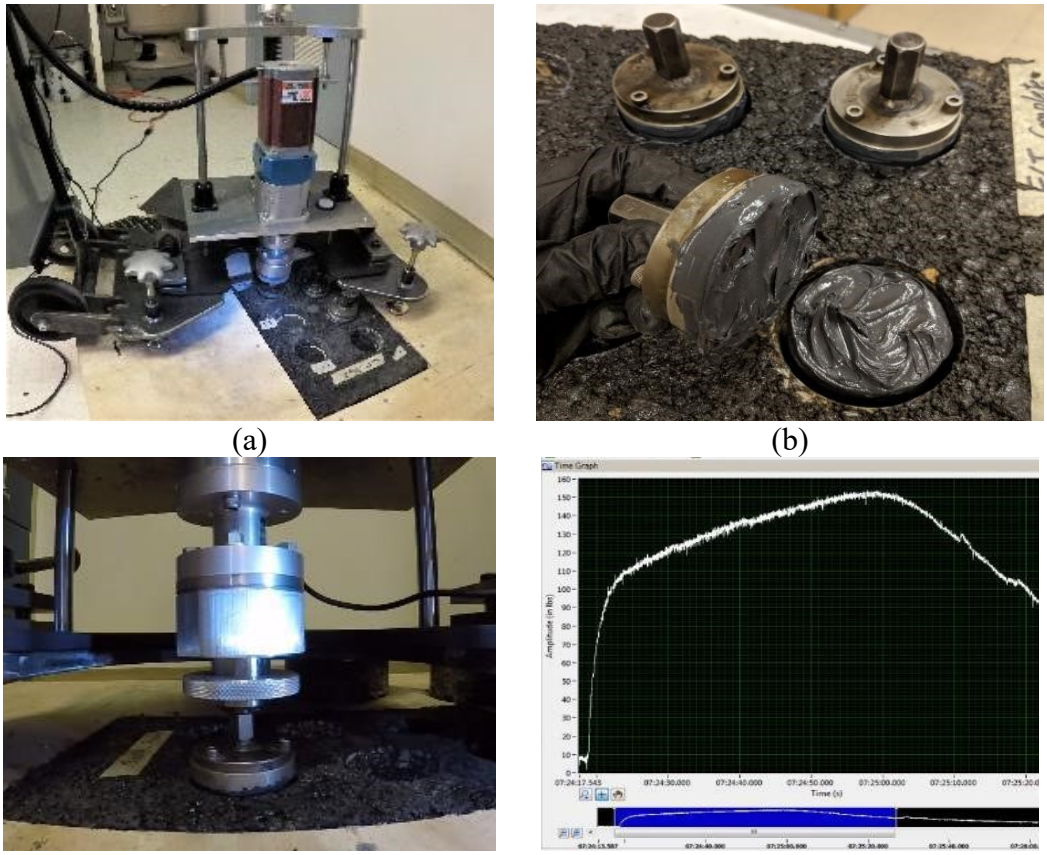

Figure 3.4: (a) Oregon Field Torque Test (OFTT) in-situ torque tester (b) Samples cored to 10mm below asphalt-concrete interface and platens glued to top of cores (c) OFTT transducer lowered onto platen (d) Torsional load is applied and amplitude is recorded

3.5 RESULTS AND DISCUSSION

3.5.1 Cracking resistance of high-density asphalt mixtures

3.5.1.1 Semi-Circular Bend (SCB) test results

Results from the SCB tests are presented in Figure 3.5. It was observed that samples with an 8.5% binder content, which were expected to be the least brittle, had a flexibility index which was significantly higher than the samples with 7.5% and 8.0% binder contents. Between samples with 7.5% and 8.0% binder contents, an increase in binder content of 0.5% resulted in approximately a 25% increase in the flexibility index. When considering samples with 8.0% and 8.5% binder contents, an increase in binder content of 0.5% resulted in approximately a 95% increase in the flexibility index. According to Coleri et al. (2017), a flexibility index of 8 is expected to provide high in-situ cracking resistance with a performance close to the performance of high quality polymer-modified asphalt mixtures used in Oregon.

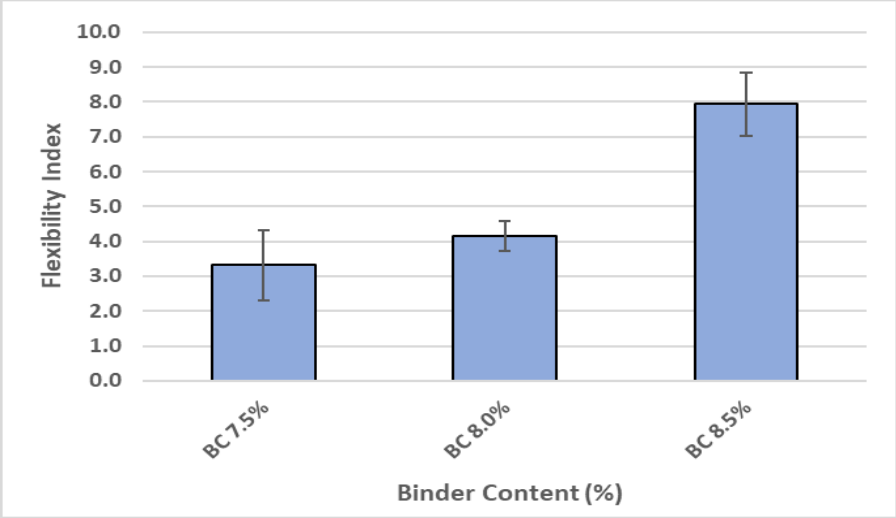

Figure 3.5: Flexibility index for 7.5%, 8.0% and 8.5% binder contents

3.5.1.2 Dynamic Modulus (DM) test results

Dynamic modulus master curves were developed for the 7.5%, 8.0% and 8.5% binder content mix designs (Figure 3.6). The average of test results for three replicate mixtures were used to develop each master curve. To allow for the direct comparison of all tests, a reference temperature of 20°C (68°F) was used, and the curves for 4°C (39.2°F) and 40°C (104°F) tests were shifted to match the reference temperature. As was expected, the 8.5% binder content samples, being the most flexible, possessed the lowest dynamic modulus. At the lowest reduced frequencies 8.0% binder content samples displayed the highest dynamic modulus, however the majority of results for the 7.5% and 8.0% binder content cases were nearly identical, and indicating this increase in binder had little impact on the asphalt mixture stiffness.

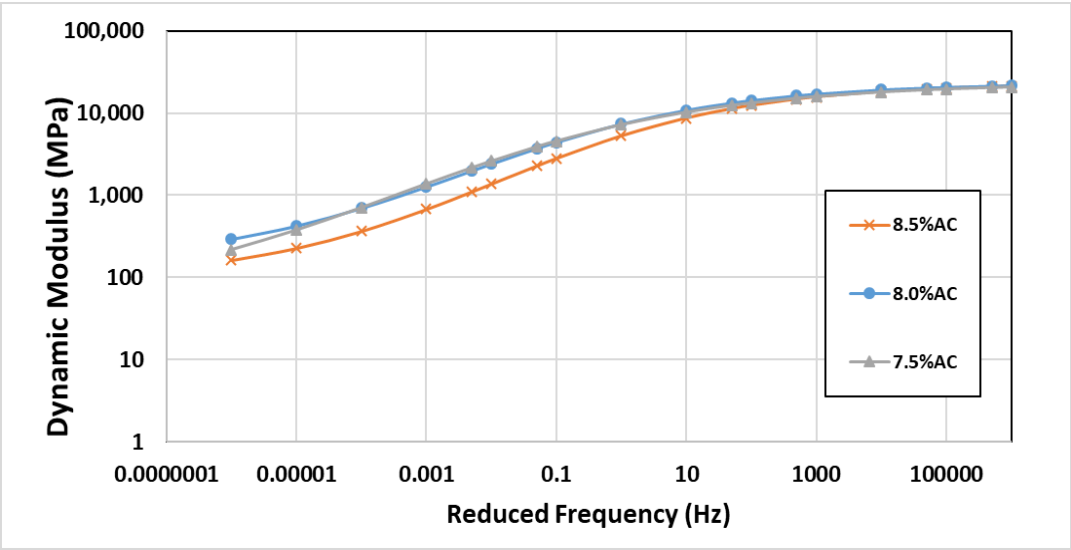

Figure 3.6: DM master curves for 7.5%, 8.0% and 8.5% binder contents (1 MPa = 145 psi). Note: AC= Binder Content

Phase angle master curves were also developed for the 7.5% 8.0% and 8.5% binder content mix designs (Figure 3.7). The same shift factor values, which were calculated and used for developing the master curves for DM tests, were used to develop the master curves for phase angles. Results from the phase angle master curves were in agreement with the dynamic modulus values, with the 8.5% binder content mixture having the highest phase angle and the 8.0% and 7.5% binder content mixtures sharing very similar phase angles. In general, it appears that decreasing binder content reduces measured phase angles. This result suggests that mixtures with higher binder contents will have higher cracking resistance, which supports the previous results obtained through SCB testing.

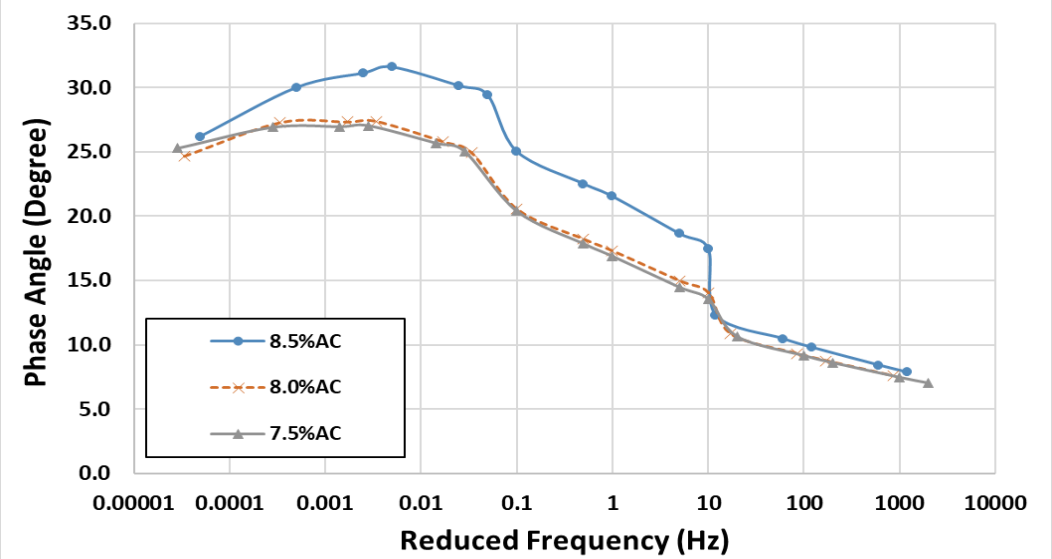

Figure 3.7: Phase angle master curve for 7.5%, 8.0% and 8.5% binder contents. Note: AC= Binder Content

3.5.2 Rutting resistance of high-density asphalt mixtures-flow number test results

Minimum required flow numbers (FN) suggested by AASHTO TP 79-13 (2013) for roadways with ESALs more than 30 million were specified as 740. The solid red line in Figure 3.8 shows the recommended FN for the traffic levels of ≥30 million ESALs. All three of the binder contents tested (7.5%, 8.0% and 8.5%) had FN values greater than 740. Average FN values for 7.5% and 8.0% binder contents were 5,736 and 5,208, respectively. While the average FN value for the 8.5% binder content case was significantly lower at 1,262, this result was still larger than the specified AASHTO TP 79-13 (2013) criteria value for ≥30 million ESALs (740). These results suggest that high-density mixtures with a PG76-22 binder and the specialized gradation previously described are not expected to experience rutting failures in the field.

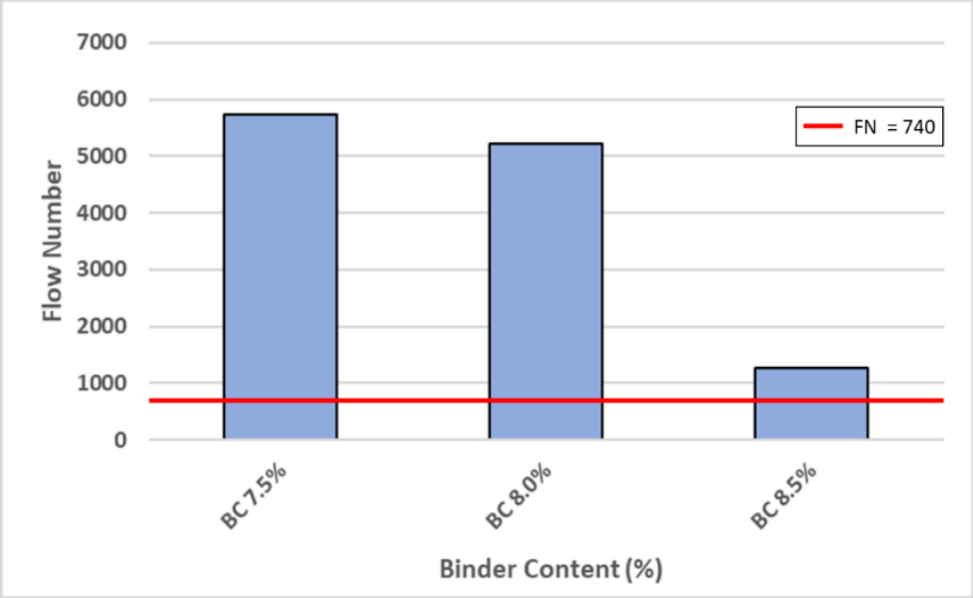

Figure 3.8: Flow number for 7.5%, 8.0% and 8.5% binder contents

3.5.3 Permeability of high-density asphalt mixtures

3.5.3.1 Tests conducted with moisture sensors and rainfall simulation

Rainfall simulation testing with an embedded moisture sensor was able to effectively capture changes in volumetric water content within samples over an extended period of time. Common trends were observed for both production mix samples tested. Both production mix sample blocks saw no initial infiltration followed by a rapid increase in volumetric water content as the infiltrated water began to reach the moisture sensor nodes. After the fine sand surrounding the sensor became saturated, the volumetric water content readings leveled off, becoming constant and indicating a 100% saturation level. At the end of the five-day analysis period, initial infiltration was observed in both 7.5% binder content samples. One sample saw 100% moisture infiltration, however testing was ceased prior to the other reaching a 100% saturation level . Both the 8.0% and 8.5% binder content samples experienced no infiltration over the analysis period. These trends can be observed in Figure 3.9 below. These results suggested that disconnected air-void channel networks within the asphalt microstructure for the mixes with 8.0% and 8.5% binder contents created an impermeable asphalt mixture.

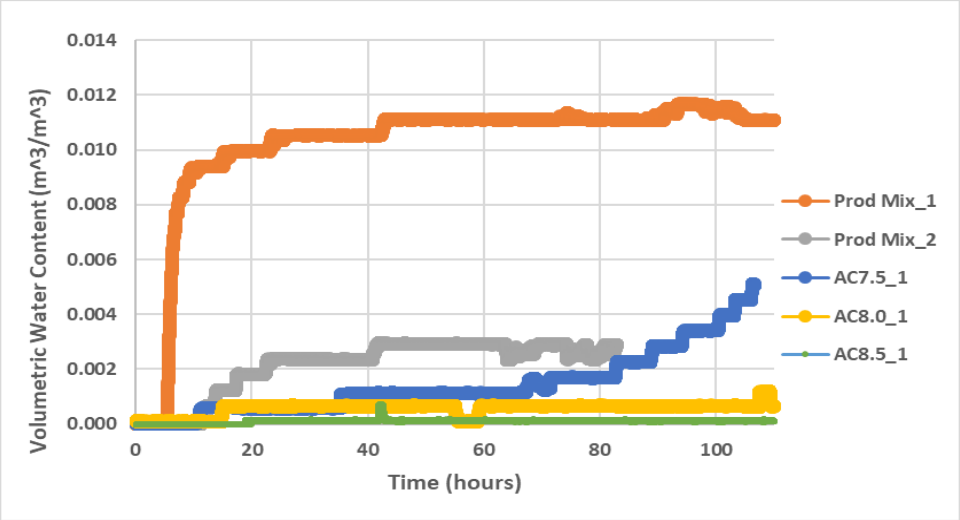

Figure 3.9: Moisture infiltration of high-density asphalt mixtures from rainfall simulation testing (1 m3 = 35.3 ft3)
Note: AC= Binder Content
Prod Mix= Production Mix Sample (7.0% Air Void Content)

To better observe the trends associated with infiltration times of each sample, bar charts were developed displaying the duration of testing to reach initial infiltration, 50% total volumetric water content (i.e. 50% saturation) and 95% total volumetric water content. Figure 3.10 outlines the times required for the moisture sensor to initially detect moisture at the asphalt-concrete interface of the sample. It was observed that production mix samples experienced moisture infiltration between five and ten hours after the initiation of the test. On average, the 7.5% binder content samples required approximately 34 hours to reach initial infiltration and the 8.0% and 8.5% binder content samples saw no infiltration over the test duration.

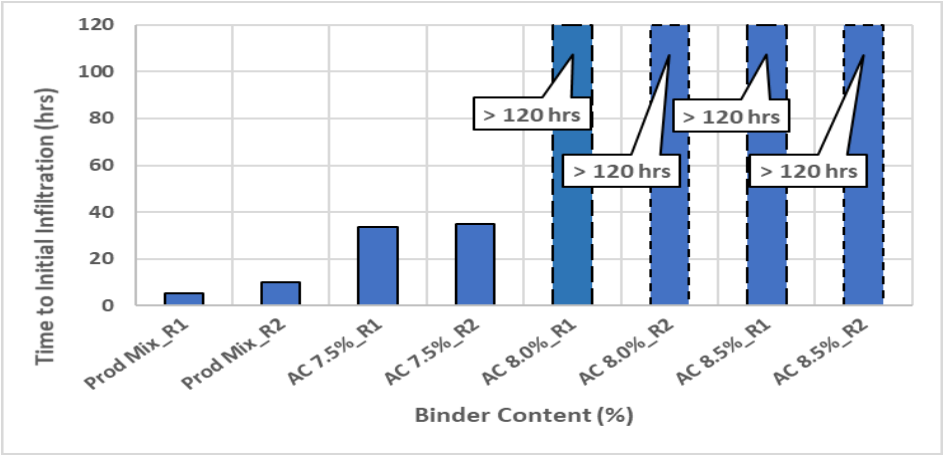

Figure 3.10: Time to reach initial water infiltration for rainfall samples
Note: AC= Binder Content
Prod Mix= Production Mix Sample (7.0% Air Void Content)

Figure 3.11 outlines the times required to reach 50% of the total volumetric water content. The production mix samples took approximately six and fourteen hours to reach 50% saturation, respectively, whereas the 7.5% binder content sample became saturated at a much slower rate after initial infiltration, with one sample taking 39 hours and the other taking 107 hours to reach a 50% saturation level.

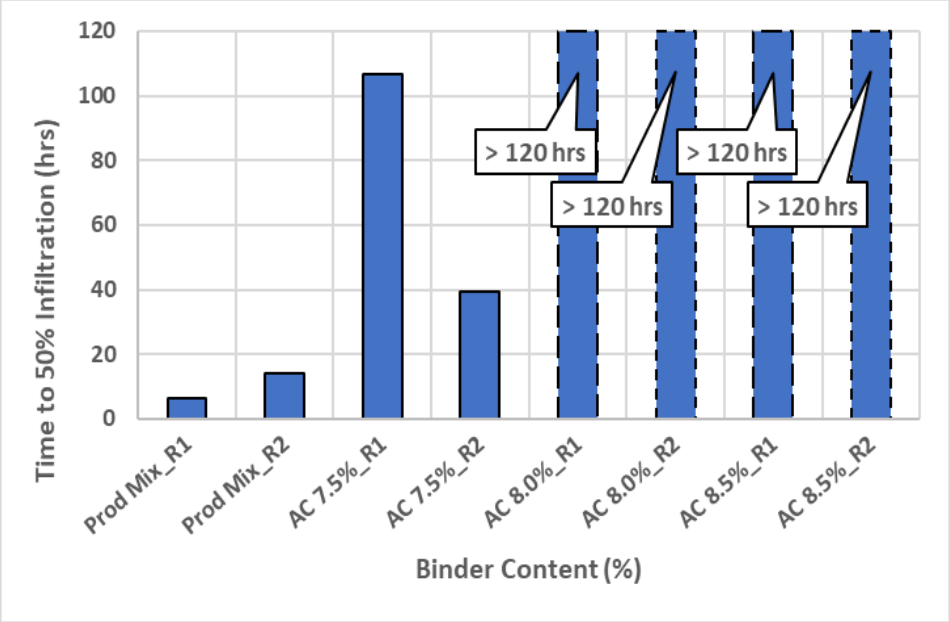

Figure 3.11: Time to reach 50% of total volumetric water content for rainfall samples
Note: AC= Binder Content
Prod Mix= Production Mix Sample (7.0% Air Void Content)

Figure 3.12 outlines the times required to reach 95% of the observed total volumetric water content. The production mix samples took approximately twenty-four and forty-two hours, respectively, to reach 95% saturation. One of the 7.5% binder content samples took approximately 57 hours to become 95% saturated whereas the other did not become fully saturated during the analysis period. None of the 8.0% or 8.5% binder content samples reached 95% of the total volumetric water content within the five-day testing period.

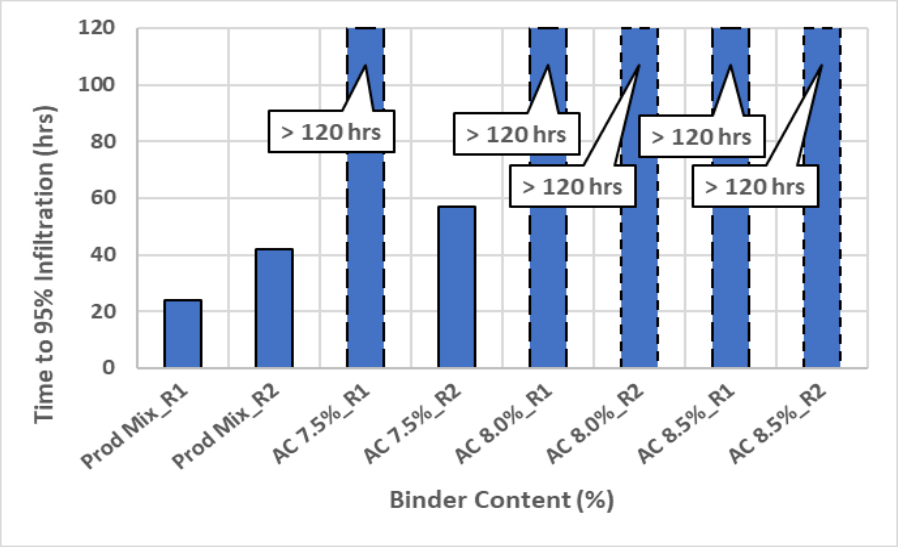

Figure 3.12: Time to reach 95% of total volumetric water content for rainfall samples
Note: AC= Binder Content
Prod Mix= Production Mix Sample (7.0% Air Void Content)

3.5.3.2 ASTM infiltration test results

Infiltration tests were conducted over a four-hour span. At the conclusion of the four-hour period, none of the tests conducted saw a significant amount of water infiltration, with only the production mix sample (7.0% air void content) registering a measurable amount of infiltration. Production mix replicates 1 and 2 experienced infiltration rates of 0.25 mm/hr (0.010 in/hr) and 0.19 mm/hr (0.006 in/hr), respectively. All high-density asphalt mixtures (7.5%, 8.0% and 8.5% binder contents) saw negligible infiltration over the analysis period. The results of this test indicate that the ASTM C1701 standard is not an effective method for measuring permeability in high-density asphalt mixtures, and should be reserved only for use with permeable pavements

3.5.4 Bond strength of high-density asphalt mixture – Oregon Field Torque Test results

Oregon Field Torque Test (OFTT) tests were conducted on samples produced using the 8.0% and 8.5% binder content impermeable asphalt mixtures. For both mixtures, one set of tests was conducted on blocks that had not been subjected to freeze-thaw cycles, and another set of tests was conducted on blocks which had been subjected to freeze-thaw cycles. Because these samples were deemed to be impermeable, no rainfall should be infiltrating the samples when placed under the rainfall simulator prior to freeze-thaw cycling. Since the samples were not saturated, effects from the freeze-thaw cycles were expected to be insignificant.

From the OFTT tests, the average interlayer shear strengths at the asphalt-concrete interface were determined for each sample. These results can be seen in Figure 3.13. From the results, it could be seen that very little variation existed between samples which had and had not been subjected to freeze-thaw cycles. When comparing 8.0% binder content samples, the average interlayer

shear strength was higher for the sample subjected to freeze-thaw cycles. While unexpected, this can likely be explained by the unavoidable variation in the grinding process of the concrete blocks prior to compaction of the asphalt overlays. Average interlayer shear strengths for 8.5% binder content samples were nearly identical for the freeze-thaw and non-freeze-thaw cases.

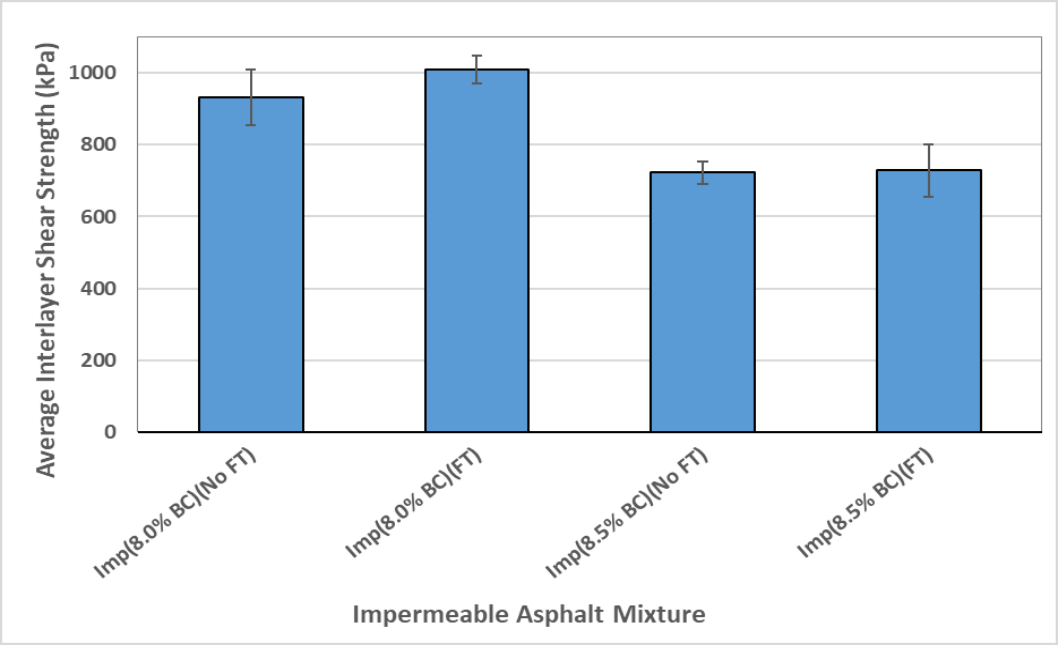

Figure 3.13: Average interlayer shear strength of impermeable asphalt samples (error bars represent one standard deviation)
Note: AC= Binder Content

3.5.5 Texture of high-density asphalt mixtures – sand patch test results

With the higher binder contents present in the impermeable asphalt mixtures, surface texture was of concern. Surface textures that are too low may result in safety concerns for drivers on the roadway. Sand patch tests were conducted according to ASTM E965 (2015) on each of the block samples to quantify the surface texture. Two replicate tests were conducted for each binder content, as well as the production mix samples. Following the tests, it was found that the mean texture depths (MTD) for samples with binder contents of 7.5%, 8.0%, 8.5% and production mix samples were 0.056 cm (0.022 in), 0.055 cm (0.021 in), 0.052 cm (0.020 in) and 0.051 cm (0.020 in), respectively. All impermeable asphalt mixtures were found to have a higher MTD than the production mix samples, which could be explained by their modified gradations, whereas the production mix samples utilized a gradation commonly used for Oregon roadways.

Previous work by Coleri et al. (2017) found the average MTD for several roadway locations in Oregon to be approximately 0.064 cm (0.025 in). A study by Noyce et al. (2007) found that the accident rate on wet roadways increases significantly at texture depths less than approximately 0.050 cm (0.020 in). The impermeable asphalt and production mix samples tested had MTDs close to those found in field locations, and each of the impermeable asphalt mixtures had MTDs

higher than the threshold for increased accident rates. These results suggest that the texture of the impermeable asphalt mixtures provides adequate skid resistance, however skid tests should also be conducted on a pilot section in the field.

3.6 SUMMARY AND CONCLUSIONS

This study focused on the development of an impermeable asphalt pavement which could be used as an overlay on concrete bridge decks to protect the deck from moisture infiltration and chloride penetration. The Bridge Deck Waterproofing Surface Course, a strategy originally developed by the New Jersey Department of Transportation, was selected for further investigation due to its claimed ability to provide an impermeable layer while maintaining strong performance with regards to cracking and rutting resistance. Three mix designs were developed based on the BDWSC method with binder contents of 7.5%, 8.0% and 8.5%. A PG76-22 binder grade was used for all mix designs.

Semi-circular bending, flow number and dynamic modulus tests were conducted to evaluate the cracking and rutting performance of the mixtures. Infiltration and rainfall simulation tests were conducted to investigate the impermeability of the mixtures. OFTT tests were conducted to evaluate bond strength at the asphalt-concrete interface for impermeable mixtures.

The analyses presented have yielded the following conclusions:

- An 8.5% binder content is required to achieve the 1.0% air void content detailed in the BDWSC specifications for a PG76-22 binder.

- A 2% air void content was the lowest air void content achieved with a PG70-22ER binder, however doing so required a 9.5% binder content, which would create issues with constructability in the field. This binder grade is not recommended for use in an impermeable asphalt mixture and it was not further evaluated in this study.

- Results for cracking and rutting tests were generally similar for 7.5% and 8.0% binder content mixtures, with significant difference existing between results for 8.0% and 8.5% binder content mixtures.

- Flow number was greatest at binder contents of 7.5% and 8.0%, however 8.5% binder content samples still possessed a flow number greater than 740 (i.e. the recommended minimum flow number for traffic levels greater than 30 million ESALs).

- The ASTM C1701 infiltration test method used was not practical for impermeable pavements.

- The moisture sensor and rainfall simulation testing system developed at Oregon State University can be used to effectively characterize moisture infiltration within asphalt samples.

- The 7.5% binder content samples experienced some moisture infiltration in the rainfall simulator, however did not become fully saturated within the five-day

analysis period. The 8.0% and 8.5% binder content samples saw no moisture infiltration within the five-day analysis period.

- The combination of a fine aggregate gradation, high binder content (8.5%) and high binder stiffness (modified PG76-22 binder) can be used to produce asphalt pavements for bridge decks in Oregon which are both impermeable and have a strong resistance to rutting and cracking.

- Sand patch testing found that impermeable asphalt mixture produced samples with a higher MTD than production mix samples, and suggested adequate texture for skid resistance on a roadway.

- Tests conducted using the Oregon Field Torque Test (OFTT) indicated that there is no significant difference in interlayer shear strength between impermeable asphalt samples which had gone through freeze-thaw cycles as compared to samples which had not gone through freeze-thaw cycles.

3.7 SUGGESTIONS FOR FUTURE WORK

Laboratory tests have shown that specialized impermeable asphalt mixtures can prevent water infiltration while also maintaining strong cracking and rutting performance. Additional materials such as commercial rubberized asphalt and elastomer modified binders should also be evaluated for their use in an impermeable asphalt mixture. The impermeable asphalt overlay strategy should be implemented in the field to investigate the relationship between field and laboratory performance. Implementation on concrete bridge decks could eliminate the early asphalt overlay failures which the Oregon Department of Transportation has currently been experiencing on bridges utilizing a waterproofing membrane to prevent water infiltration.

To conduct a field evaluation, pilot sections can be constructed using the impermeable asphalt mixtures. Automated Pavement Condition Surveys (APCS) can be performed to monitor the rutting and cracking performance over the life of the impermeable pavement. In addition, skid resistance of the surface can be quantified using a skid tester. Regular surveying can identify the onset and propagation of distresses within the pavement. Chain dragging and thermal imaging can be used to check for delamination between the impermeable pavement and the concrete bridge deck. Moisture sensors can be installed in the asphalt- concrete interface of the pavement, either at the time of construction or at a later date, to evaluate the impermeability of the asphalt over the course of its service life. Finally, strain-pressure gauges can be installed in the asphalt layer to evaluate critical strains under repeated traffic loadings.

Although the suggested asphalt mixture with 8.5% binder content and modified PG76-22 binder provides an impermeable asphalt mixture with high rutting and cracking resistance, as-built surface texture of the produced asphalt mixture after construction should be further evaluated for safety. Although the surface texture observed during laboratory sample production was high for this suggested mixture type, skid-resistance of the suggested mixture needs to be measured to make sure that surface texture is high enough to avoid any safety issues during the pavement use phase.

4.0 FINITE ELEMENT MODELING FOR BRIDGE DECKS

4.1 MODELING METHODOLOGY

In this study, finite element (FE) modeling is used to simulate the loaded truck loads on a concrete bridge deck to determine the impact of applied loads on the pavement structure. Model outputs from the simulations were used to conduct the bending beam fatigue laboratory experiments. Model details, factorial, and the results are given below.

4.1.1 Model details and modeling factorial

Axle configuration for a Class 9 truck with one steering single and two dual tandem axles (8 tires on one axle) is used to develop the moving load models.

Figure 4.1 shows the loading configuration of the Class 9 truck used in the factorial. Truck tire pressure was assumed to be 725kPa (105psi).

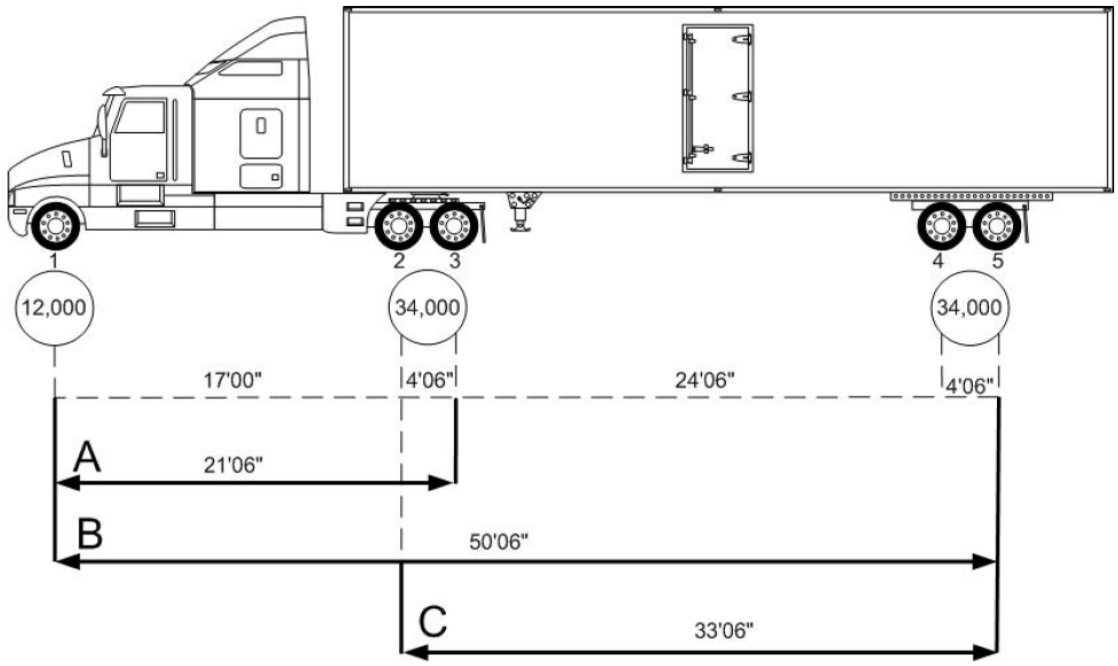

Figure 4.1: Loading configuration for the Class 9 truck (ODOT SIPP 2018) (Lengths are feet and in inches while loaded axle weights are given in circles in lb)

A dynamic finite element (FE) model was developed to determine the response of pavement structure to truck loading on a bridge deck. Abaqus™ software was used for the development of the finite element models. Due to considerable stress concentration in the asphalt layers, half models were developed to reduce the computational running time. An equivalent boundary

condition was used for the inner longitudinal side of the structure where the full-scale structure was cut into two halves. The nodes along this side were fixed in displacement and rotation except in the lateral direction. The finite-element mesh consists of Lagrange brick elements with a second-order interpolation function. The mesh is refined under the wheel path to improve accuracy. Figure 4.2 shows the meshed model structure with the truck axles.

In the developed viscoelastic FE model, linear behavior is considered (small strain domain). No nonlinearity (fatigue, permanent deformations, and cracks) is taken into account. Several factors were considered in the numerical factorial to assess the structural response under different speed, temperature, asphalt layer thickness, and asphalt layer stiffness conditions. Table 4.1 shows the numerical factorial followed for this study. A total of 16 finite element models were developed.

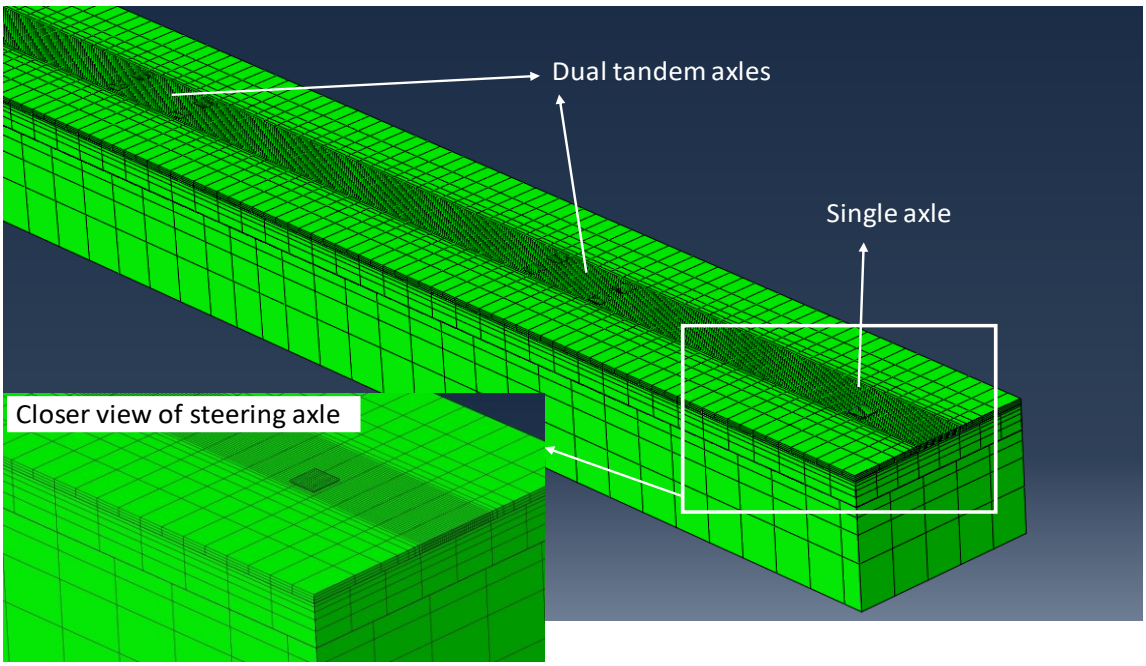

Figure 4.2: Meshed model structure in Abaqus with truck axles

Table 4.1: Numerical Modeling Factorial

Factor	Subcategories
Vehicle	Class 9 truck at the legal load limit
Speed	30 mph, 60 mph
Temperature	0ºC, 30ºC
Layer configuration	2in and 4in thick HMA on PCC deck
Asphalt type	Stiff and soft

In the finite element model, asphalt layer is placed on top of the concrete bridge deck. Bridge columns spaced 15m (45feet) apart supported the concrete bridge deck. Layer properties and finite element model input parameters are given in Table 4.2. In order to characterize the viscoelastic behavior of the stiff and soft asphalt layers, the generalized Maxwell model is used in this study to simulate the time dependency of asphalt materials used in the surface layer. The

model consists of two basic units, a linear elastic spring in series with multiple Maxwell elements (Coleri and Harvey 2013, Coleri and Harvey 2017).

Mathematically, the behavior of this model follows Prony series and is described as:

$$\boldsymbol{E(t) = E_e + \sum_{i=1}^{n} E_i\, e^{-\left(\frac{t}{\tau_i}\right)}}$$

(4-1)

Where

E_e is the equilibrium modulus of the elastic spring, E_i and τ_i are the relaxation modulus and relaxation time of the i[th] member among n Maxwell elements.

The viscoelastic behavior of the stiff and soft asphalt materials were characterized using the falling weight deflectometer (FWD) test (a nondestructive field test to determine material properties through backcalculation) results from two pavement sections (one with stiff and other with soft asphalt layers on the surface). Using the relaxation modulus outputs, the constants of Prony series were back-calculated and then imported into the finite element models as the inputs to model the asphalt behavior (Coleri and Harvey 2013, Coleri and Harvey 2017).

The temperature dependency of the asphalt mix is defined by using the Williams-Landel-Ferry (WLF) equation, given as follows (Ferry 1980).

$$\boldsymbol{\log(a_T) = \frac{-C_1(T - T_{ref})}{C_2 + (T - T_{ref})}}$$

(4-2)

Where,

a_T = the time-temperature shift factor,

C_1 and C_2 = regression coefficients,

T_{ref} = the reference temperature, and

T = test temperature.

To optimize the regression coefficients C_1 and C_2, the shear modulus data were first fitted to a sigmoid function, in the form of:

$$\log(G(\xi)) = \delta + \frac{\alpha}{1 + \exp(\beta + \gamma \log(\xi))}$$

(4-3)

Where,

α, β, γ and δ = regression coefficients, and

ζ=reduced time.

Shift factors are calculated by fitting the measured or back-calculated modulus to the sigmoidal function (Eqn. 4.3). Finally, the dynamic modulus master curve for each section was obtained by processing the test results for the stiff and soft asphalt materials used in this study. Back calculated input parameters for finite element model development are given in Table 4.2.

Table 4.2: Finite Element Model Input Parameters for each Layer

Material	Long term elastic modulus [MPa]	Poisson's ratio	Density [Tonne/mm^3]	Viscoelastic model inputs		WLF model coefficients		
				g_i	τ_i	T_{ref}	C_1	C_2
Soft Asphalt	2,447	0.35	2.3E-09	0. 28	6.4E-05	19	11.03	123.81
				0.31	0.01			
				0.17	2.6E-07			
				0.14	1.33			
				0.08	152.31			
Stiff Asphalt	20,414	0.35	2.3E-09	0.21	4.6E-05	19	16.17	283.73
				0.23	0.003			
				0.15	3.9E-07			
				0.25	0.18			
				0.15	71.2			
Steel	210,000	0.25	8.5E-09	-	-	-		
PCC	40,169	0.20	2.4E-09	-	-	-		

The tire is represented by a square stiff thin deformable body that moves over the surface of the pavement (dynamic loading). The projected contact pressure from tires are applied on the simplified square body. In order to simulate moving loads in the viscoelastic FE model, a displacement boundary condition was applied to the loading body to simulate the constant-speed passage of axles over the pavement section. The distribution of contact pressure on the tire is assumed constant.

4.1.2 Modeling results

Outputs for all the models are presented in this section. The critical (highest along the bridge deck) vertical displacement on the surface of the pavement under the vehicle tire was used as the model output to determine the laboratory bending beam fatigue test strain/displacement levels. Figure 4.3 shows the change in critical vertical surface displacement with time. Since dynamic

loading scheme was used in this study to better simulate the passage of a truck, displacement outputs had some noise. A Matlab algorithm was used to process the output to reduce the output noise level. Figure 4.3 shows both the raw and smoothened model outputs. Processed outputs were used for extracting critical (peak) displacements from all 16 modeled cases.

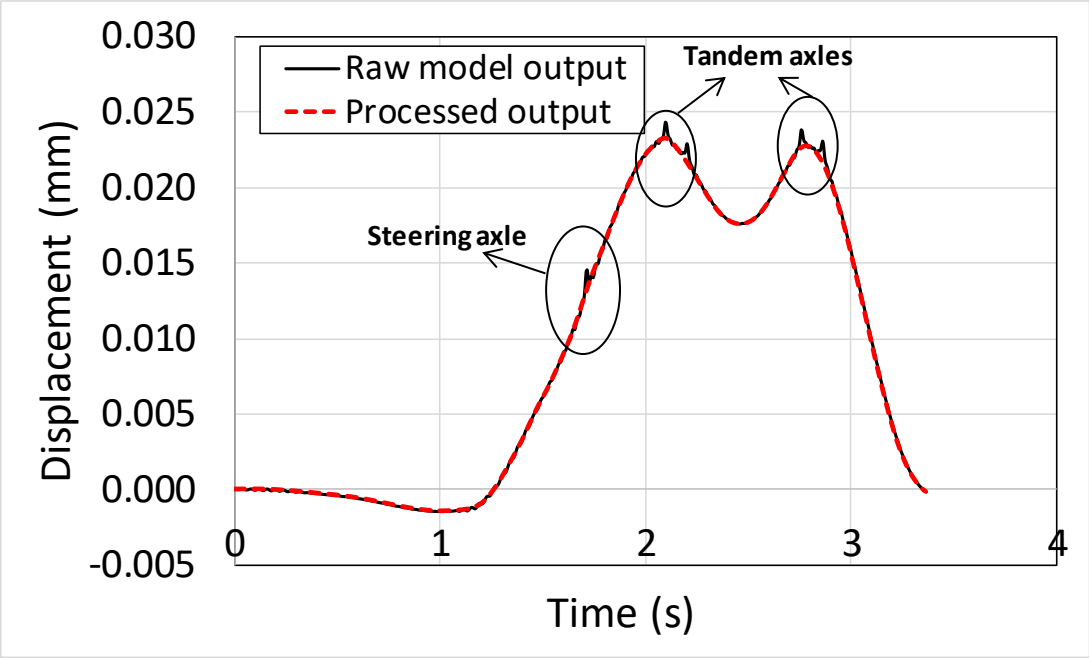

Figure 4.3: Vertical displacement response for the case with 2inch thick stiff asphalt layer at 0°C temperature and 30mph speed (raw and processed outputs are shown together).

Figure 4.4 shows the displacement outputs for all 16 cases. By comparing Figure 4.4a to Figure 4.4b, it can be observed that increasing the thickness of the asphalt layer is significantly reducing the surface displacement and layer bending when the asphalt layer is stiff. For the cases with soft asphalt layer, thickness does not have any significant effect on surface vertical deformation. However, it should be noted that these results are only considering the viscoelastic properties of asphalt layers. Rut resistance of asphalt layers and the impact of asphalt layer thickness on rutting performance were not simulated in these finite element models. It is expected that surface rutting will linearly increase with increasing layer thickness since the underlying layer is concrete. Two times higher surface rutting is expected for a section with 4inch layer thickness when compared to a section with 2inch layer thickness when both sections were exposed to identical climatic conditions and traffic loading (Coleri et al. 2012).

It can also be observed from Figure 4.4 that increasing temperature increases displacements and strains since asphalt gets softer with increasing temperature. In addition, increasing speed reduced surface displacements due to the viscoelastic nature of asphalt layer. This observed reduction in displacement with increasing speed is lower for the cases with soft asphalt. Based on the results of the analysis, highest level of vertical displacement (0.03mm) was observed for the case with soft asphalt layer with 2inch thickness, 30mph speed level at 30°C temperature. Laboratory beam samples were also tested with 0.03mm critical surface deformation.

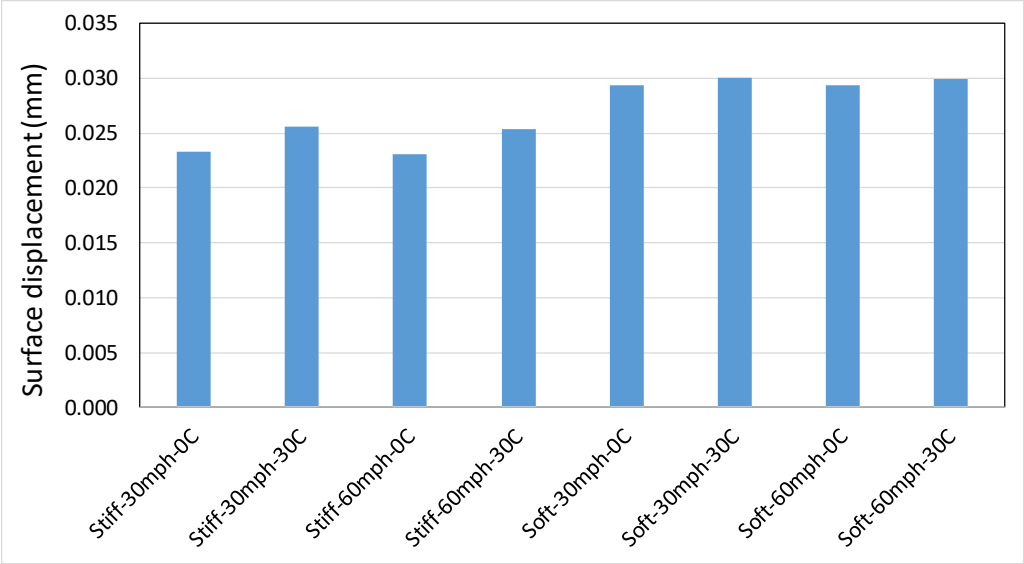

(a)

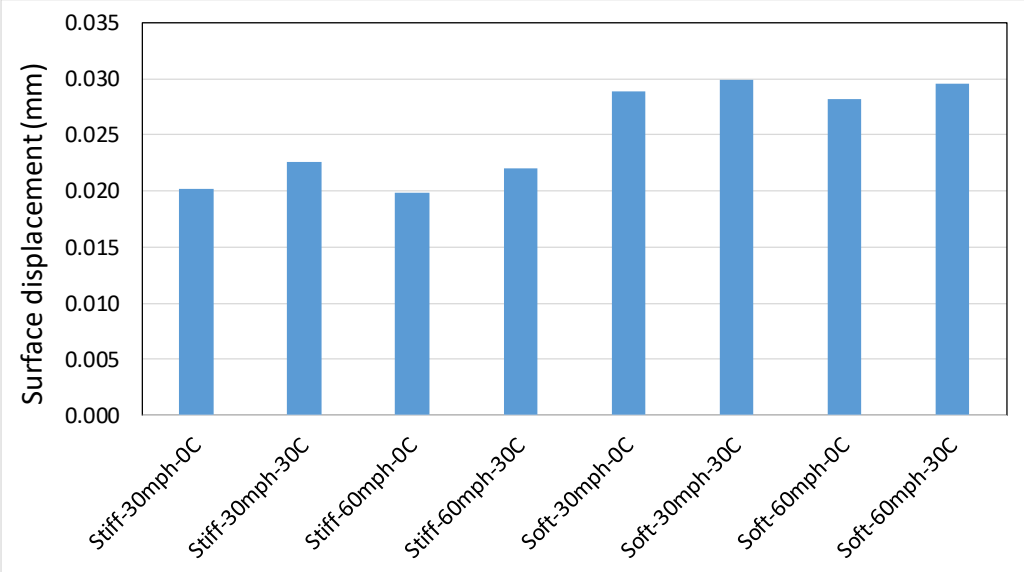

(b)

Figure 4.4: Critical vertical displacement outputs for all models (a) Cases with 2inch thick asphalt layer (b) Cases with 4inch thick asphalt layer.

5.0 EVALUATION OF WATERPROOFING MEMBRANE STRATEGIES TO PROTECT AND SEAL CONCRETE BRIDGE DECKS

5.1 INTRODUCTION

The installation of waterproofing membranes on concrete bridge decks is a commonly used strategy to prevent water on the roadway surface from penetrating into the deck and to reduce the load and freeze-thaw related damage to the bridge deck. Detailed literature on waterproofing membranes is given in Section 2.0 in this report. Typically, an asphalt layer is paved over the waterproofing membrane to prevent damage from heavy vehicles. The early failure of asphalt pavement overlays on concrete bridge decks with waterproofing membranes has been recognized as a significant issue by the Oregon Department of Transportation (ODOT). Potential reasons for the failure of the asphalt overlay were thought to be due to poor adhesion between the waterproofing membrane and the asphalt wearing course, and the material properties of the asphalt layer. By determining the most effective waterproofing methods and strategies, this research will serve to decrease repair and replacement costs, and increase the service life of asphalt overlays on concrete bridge decks in Oregon. The main goals of this study are to provide the industry and ODOT with better insight on the failure mechanisms of asphalt overlays on concrete bridge decks and establish field and laboratory experiments to evaluate the performance of these overlays. From the results of this study, a poured waterproofing membrane was recommended as an ideal membrane for use on concrete bridge decks due to its ease of installation, complete impermeability, relatively lower cost, and high bond strengths between the concrete deck, membrane layers and asphalt overlay.

5.2 OBJECTIVES

The main objectives of this study are to:

- Determine the asphalt overlay failure mechanisms on concrete bridge decks;
- Develop laboratory and field experiments to measure bond performance and delamination on bridge decks;
- Quantify the impact of bonding on asphalt overlay performance;
- Identify laboratory experiments to measure waterproofing membrane impact on cracking and rutting performance;
- Develop a laboratory test to evaluate the impermeability of waterproofing membranes;

- Determine the impact of freeze-thaw cycles on the performance of waterproofing membranes; and

- Identify the most effective waterproofing membranes for use on concrete bridge decks.

5.3 MATERIALS AND METHODS

In this study, four waterproofing membrane strategies were evaluated to characterize cracking, rutting and bond performance as well as impermeability of the evaluated strategies. Evaluated waterproofing membrane strategies are listed in Table 5.1. Strategies 1 and 2 are liquid applied membranes. Strategy 3 is a preformed sheet membrane. Strategy 4 is based off of a German bridge waterproofing method and consists of an impermeable mastic asphalt layer constructed on top of a preformed sheet membrane (EAPA 2013).

Table 5.1: Waterproofing Bridge Deck Strategies Evaluated

Strategy 1-	Sprayed Waterproofing Membrane (Figure 5.1)
Strategy 2-	Poured Waterproofing Membrane (Figure 5.3)
Strategy 3-	Roll-On Waterproofing Membrane (Figure 5.5)
Strategy 4-	Mastic Asphalt Layer with Roll-On Membrane (Figure 5.7)

Samples produced in the laboratory consisted of a bottom concrete block slab representative of a concrete bridge deck. Concrete was mixed and poured into custom molds to cure for 28 days. Texture was then introduced to the concrete surface by sand blasting and the waterproofing membrane was constructed on top of the slab following manufacturer's recommendations for each membrane. For the Roll-On membrane, a thin asphalt leveling course was compacted on top of the concrete slab prior to membrane installation, as per ODOT Standard Specifications (ODOT 2015). Tack coat was applied to each membrane and a typical Oregon production mix asphalt was compacted on top of the slab using a hydraulic roller compactor. Thicknesses for each layer for all tested membrane strategies are shown in Table 5.2. The final dimensions of prepared samples were 40 cm (length) by 26 cm (width) by 10 cm (height).

Table 5.2: Layer Thicknesses for Selected Strategies (mm)

Strategy	Concrete Thickness	Bottom Layer Thickness (Asphalt) (mm)	Top Layer Thickness (Asphalt + Membrane) (mm)
S1- Sprayed	50.8mm	N/A	49.2mm
S2- Poured	50.8mm	N/A	49.2mm
S3- Roll On	25.4mm	25.4mm	49.2mm
S4- Mastic Asphalt Layer	50.8mm	N/A	49.2mm[1]

Note: [1]This thickness corresponds to the thickness of the roll-on membrane, mastic asphalt layer and traditional production mix asphalt layer.

All materials for the sprayed, poured and roll-on waterproofing membranes were obtained from Jonnic Construction. Shot blasting of concrete slabs and installation of sprayed, poured and roll-on membranes were also completed by Jonnic Construction.

5.3.1 Aggregate, asphalt binder, and production mix materials

All the materials used in this study were obtained from local sources. Virgin aggregates used for the mastic asphalt mixture production were obtained from a local quarry near Pendleton, Oregon. The virgin aggregates were delivered in three gradations, namely coarse (1/2" to #4), medium (#4 to #8), and fine (#8 to zero). To determine the gradation of each stockpiled aggregate, wet-sieve and dry-sieve analyses were performed on multiple samples of each stockpile following AASHTO T 27-11 (2011).

A local producer in Oregon provided the virgin modified PG70-22ER binder to be used for producing the mastic asphalt layer in this study. The binder was modified with polymers, allowing for the use of higher binder contents while maintaining enough stiffness to allow for adequate rutting resistance. Temperature curves, mixing temperatures and compaction temperatures were provided by the producer as well. Laboratory mixing and compaction temperatures were estimated by using the viscosity-temperature lines following the procedure described in Asphalt Institute guidelines (2016) and AASHTO T 316-11 (2011).

A ½" (12.7 mm) dense graded production asphalt mixture was sampled from River Bend Sand and Gravel-Oldcastle Materials in Salem, OR for this study. Prior to compaction, sampled production mix was heated and put through a mechanical splitter in order to obtain uniform sampling of the mixture. The theoretical maximum specific gravity (G_{mm}) of the mixture was measured in the lab using a CoreLok device according to AASHTO T-209 (AASHTO 2012). Three replicate G_{mm} measurements (2.520, 2.494, and 2.515) were taken and the average (2.510) was used as the asphalt mixture G_{mm}. Required amounts for first and second lift compactions were then weighed out based on the measured average G_{mm} of the mixture and the selected 7% air void content. The 7% air void content was chosen since it is commonly specified during construction in Oregon. Weighed amounts were split equally into two pans to facilitate homogeneous heating of the mixture to compaction temperature.

5.3.2 Sprayed membrane installation and materials

A spray membrane is a liquid applied membrane which can be applied to a multitude of bridge deck shapes, and can easily coat the sides of drainage curbs to prevent water penetration from the bridge deck perimeter. While spray membranes are more challenging and costly to install than roll-on membranes due to the need for specialized spraying equipment, careful mixing and application practices can result in installations with seamless impermeable layers. The Oregon Department of Transportation (ODOT) utilizes a two-component polyurea waterproofing membrane which is sprayed over the top of a primer layer on a shot blasted concrete bridge deck. The membrane is evenly sprayed over the deck to obtain a uniform coverage of 0.45 gallons/yd^2 (2.0 L/m^2). ODOT recommends that the membrane should be paved over using a minimum of 3 inches (7.6 cm) of asphalt concrete with a PG64-22 binder (ODOT 2015). The sprayed waterproofing membrane evaluated in this study was comprised of the layers shown in Figure 5.1.

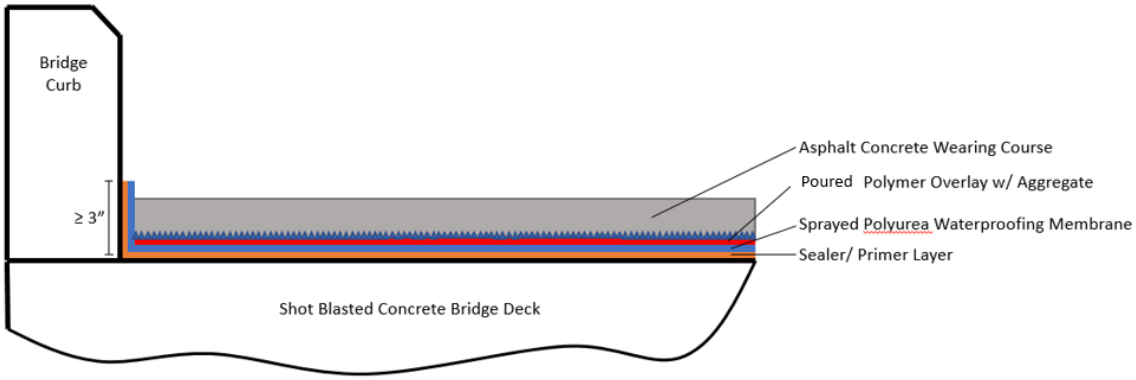

(a)

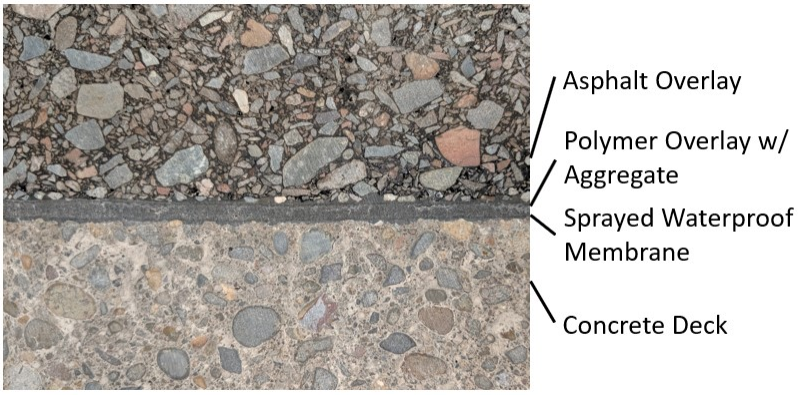

(b)

Figure 5.1: Strategy 1 - Sprayed membrane (a) Diagram and (b) Cross-section of the produced laboratory sample

The sprayed membrane installation process can be seen in Figure 5.2. For the installation of sprayed waterproofing membrane samples used for this study, concrete block slabs were first produced in the laboratory and allowed to cure for 28 days. The slabs were then sand blasted to create texture by following a system identical to the ones used in the field during construction (Figure 5.2a). A paint roller was then used to apply a basic primer to the slabs. The primer was let to cure for 30 minutes in order to allow infiltration into the top surface of the concrete to create a strong bond (Figure 5.2b). The two-component sprayed membrane was then sprayed over the primer (Figure 5.2c). A Grako XP2 Proportioning Unit was used to mix the two components, control the temperature of the membrane and control the pressure at which the membrane was being sprayed onto the blocks. Once the membrane has been sprayed onto the blocks, it hardens in 5 minutes. Using a paintbrush, the polymer overlay was distributed over the top of the membrane (Figure 5.2d) and #4 to #16 aggregate was broadcast over the top until 95% coverage was achieved (Figure 5.2f).

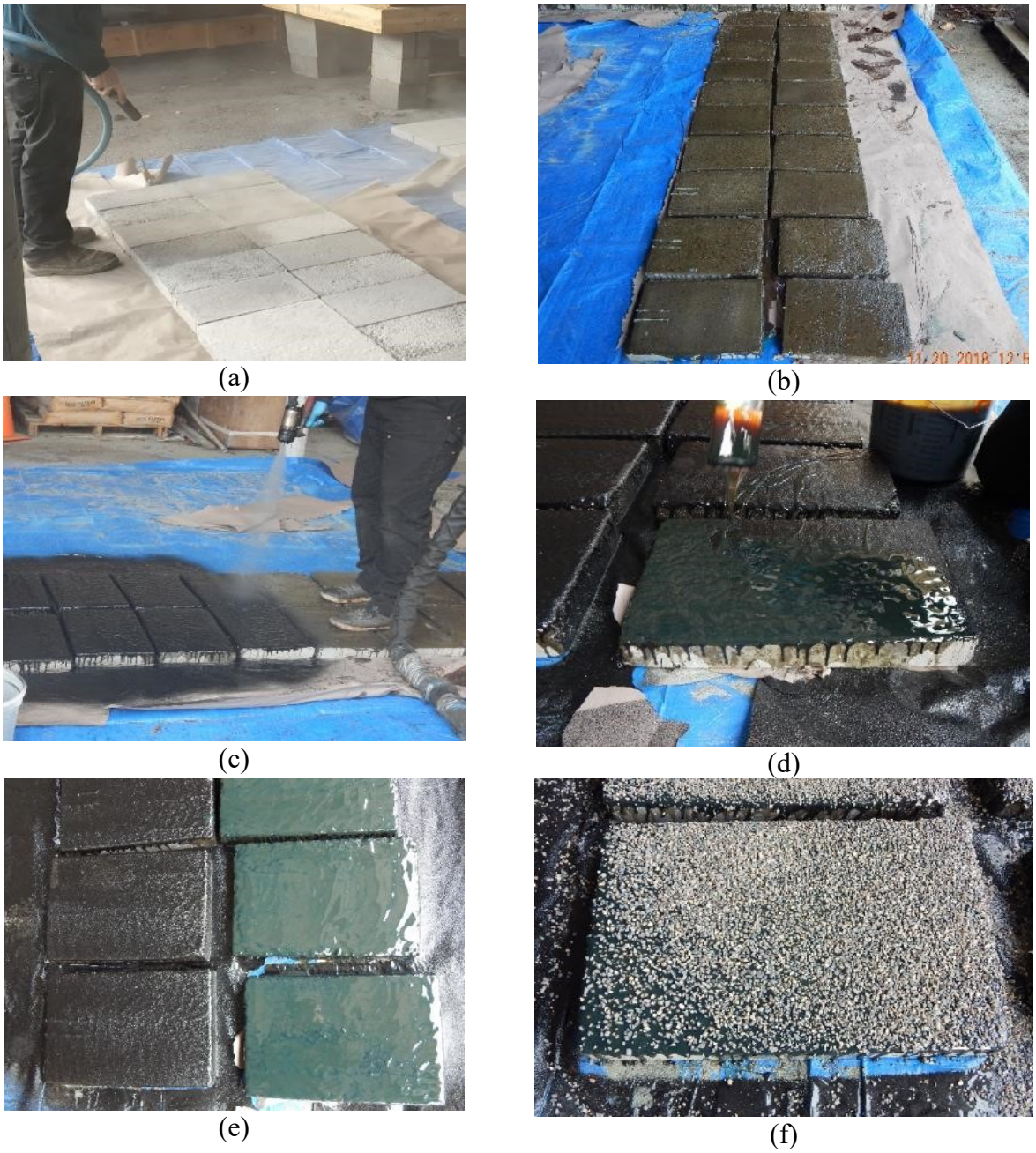

Figure 5.2: Sprayed membrane installation (a) Shot blasting concrete slabs (b) Primer poured onto slabs (c) Waterproof membrane sprayed onto primer (d) Polymer overlay brushed over membrane (e) Slabs with spray membrane (left) and polymer overlay (right) (d) Aggregate broadcast over polymer overlay

5.3.3 Poured membrane installation and materials

Multiple variations of poured membranes exist, however the most common one utilizes an impermeable liquid polymer layer to prevent moisture infiltration into a bridge deck. These membranes are advantageous because they are more cost effective than the sprayed membrane

since a smooth and uniform coverage can be achieved without the need for the expensive equipment used to install the sprayed membrane. However, the poured membrane is much less flexible than the sprayed membrane. During the installation process for the poured membrane in the field, existing asphalt is first ground off the bridge deck, leaving the exposed concrete deck. The deck is then swept and shot blasted until a 1/16-inch (1.6 mm) surface texture depth profile has been achieved. A primer coat is poured and spread over the bridge deck and the primer layer is allowed to penetrate into the concrete deck for a minimum of 15 minutes. The epoxy polymer waterproofing membrane resin is then poured over the primer layer, covering a maximum area of 0.18 gallons/yd^2 (0.82 L/m^2) and achieving a minimum membrane thickness of 3/16 inches (4.8 mm). Aggregate is broadcast over the resin to complete coverage. Pull tests are conducted to check for a minimum bond strength of 175 psi (1.21 MPa). Chain dragging and coring may also be used to check for delamination and bond failure. Traffic is allowed on the membrane for up to 7 days before the bridge deck was paved using conventional paving methods (ODOT 2015). The poured waterproofing membrane evaluated in this study was comprised of the layers shown in Figure 5.3.

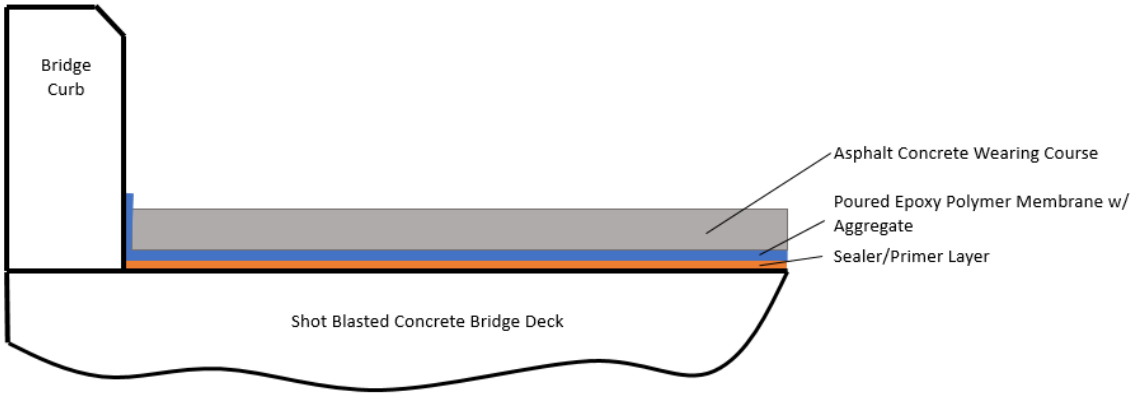

(a)

(b)

Figure 5.3: Strategy 2 - Poured membrane (a) Diagram and (b) Cross-section of the produced laboratory sample

The sprayed membrane installation process can be seen in Figure 5.4. For the installation of sprayed waterproofing membrane samples used for this study, concrete block slabs were first

produced in the laboratory and allowed to cure for 28 days. The slabs were then sand blasted to create texture by following a system identical to the ones used in the field during construction (Figure 5.4a). A paint roller was then used to apply a basic primer to the slabs. The primer was let to cure for 30 minutes in order to allow penetration into the top surface of the concrete to create a strong bond (Figure 5.4b). The poured membrane was applied on top of the primer using a paint roller and left to partially cure for 30 minutes before applying aggregates (Figure 5.4c). By letting the membrane partially cure, aggregates placed over the top would remain near the surface of the membrane and not sink through to the primer layer. After 30 minutes, #4 to #16 aggregate was broadcast over the top until 95% coverage was achieved (Figure 5.4d).

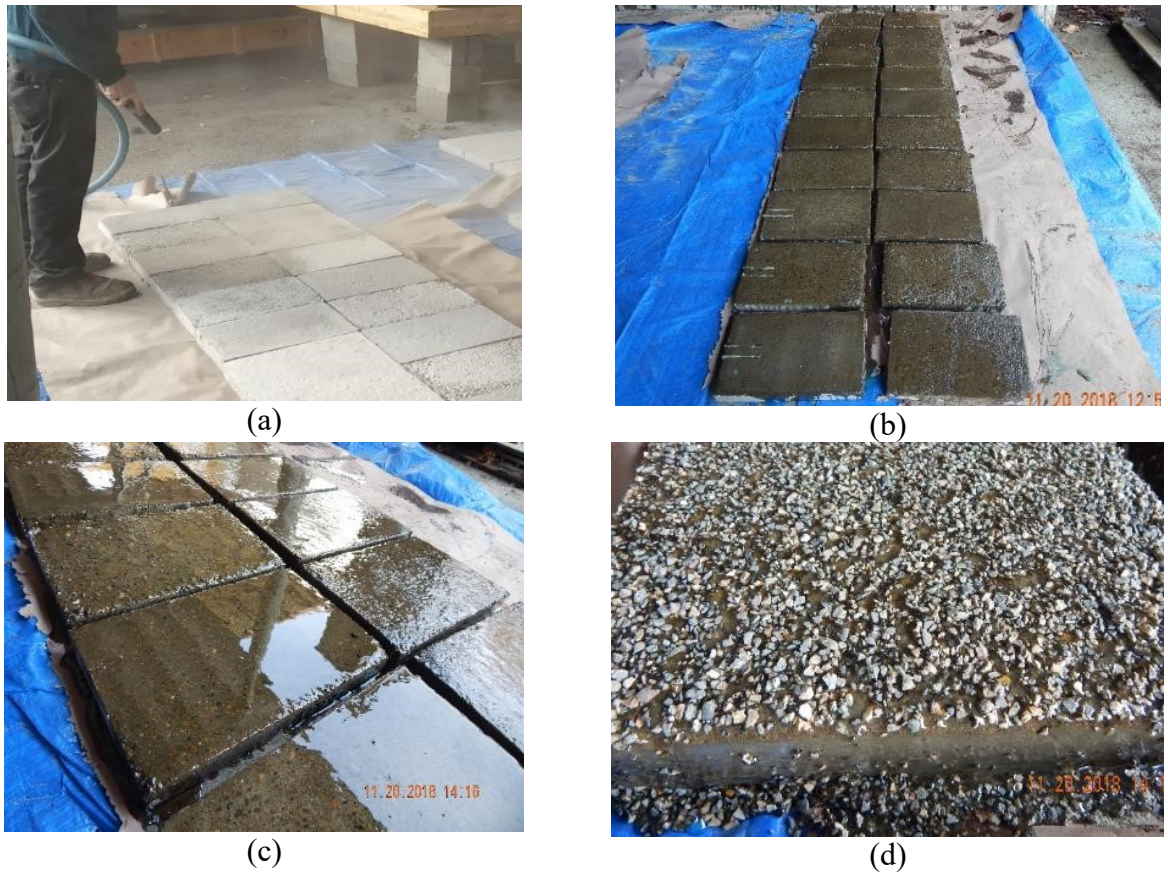

Figure 5.4: Poured membrane installation (a) Shot blasting concrete slabs (b) Primer poured onto slabs (c) Waterproof polymer membrane poured onto primer (d) Aggregates broadcast over membrane

5.3.4 Roll-on membrane installation and materials

Roll-on membranes consist of a preformed waterproof sheet which is usually applied longitudinally onto a concrete bridge deck surface. These sheets come in rolls ranging in size from 3 to 5 feet (0.9 to 1.5 m) wide and 30 to 50 feet (9.1 to 15.2 m) long, which are produced in a factory by following different quality standards thereby reducing the risk of inconsistencies between sheets (Manning 1995). They come in uniform thicknesses and installation is straight-

forward, with sheets being rolled out side-by-side with a slight overlap along the deck. These overlaps, however, create seams in the waterproofing membrane through which water can penetrate if the sheets are not properly adhered to one another (Frosch et al. 2013). Membrane sheets are bonded to the concrete deck in a variety of ways. Adhesive backings, which are either directly applied or first heated with a blow torch to activate the adhesive, are the most common method for bonding a roll-on membrane to the pavement surface. Another installation strategy is to pour hot oxidized bitumen onto the concrete deck in front of the membrane as it is being rolled out (Manning 1995). Some roll-on membranes also require a primer layer to be put down prior to membrane installation. Once in place, the membranes are paved over using traditional paving methods (Russell 2012). The Oregon Department of Transportation (ODOT) requires that a thin asphalt pavement leveling course is put down on the deck to reduce irregularities prior to the installation of a roll-on membrane system (ODOT 2015). The poured waterproofing membrane evaluated in this study was comprised of the layers shown in Figure 5.5.

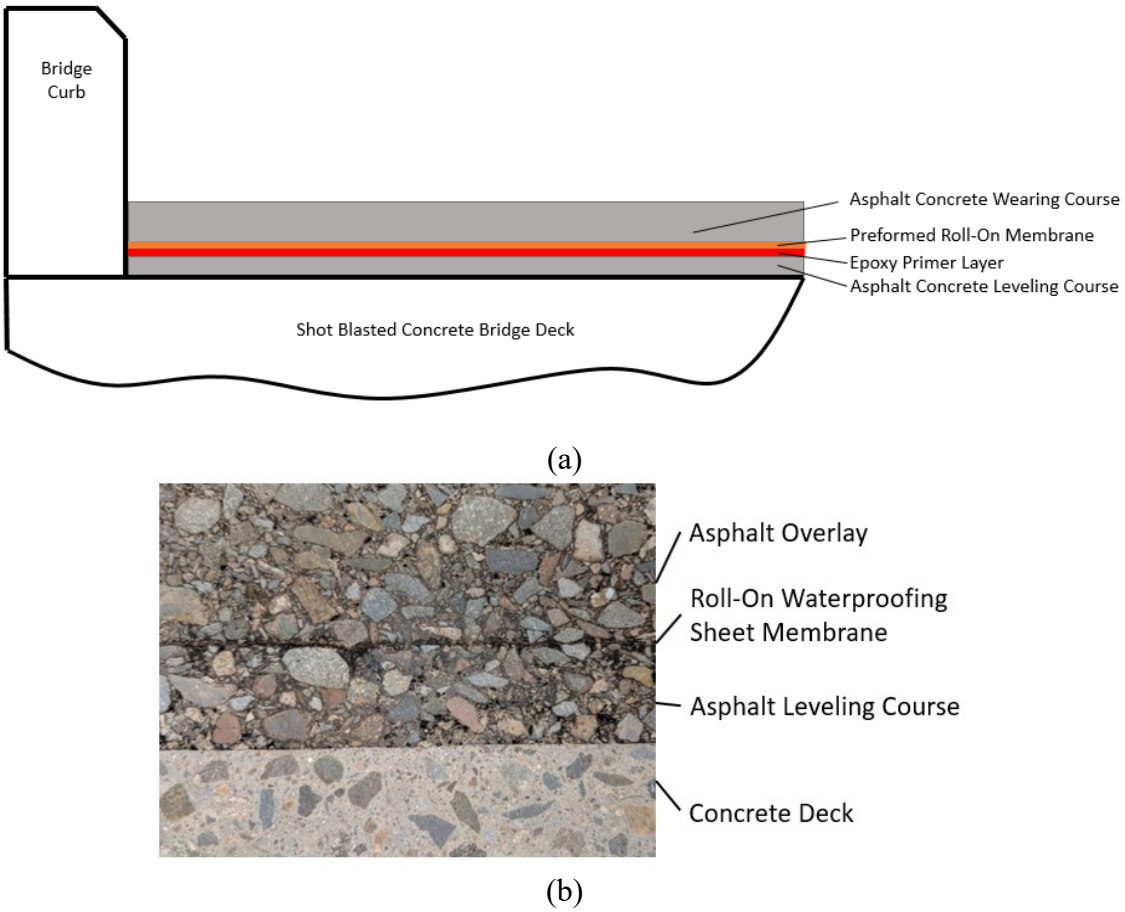

Figure 5.5: Strategy 3 - Roll-on membrane (a) Diagram and (b) Cross-section of the produced laboratory sample

The sprayed membrane installation process can be seen in Figure 5.6. For the installation of sprayed waterproofing membrane samples used for this study, a grinder was first used on the concrete block slabs to create texture on the concrete slab representative of a milled surface. The surface was ground to a mean texture depth (MTD) of 1.6 mm (0.0625 in) (ODOT 2015) as

determined by sand patch testing in accordance with ASTM E965-15 (2015). A high-performance tack coat was then uniformly applied to the concrete slab using an application rate of 0.36 L/m^2 (0.08 gal/yd^2). This application rate was determined as an optimal application rate for high texture surfaces through studies by Coleri et al. (2017) and Covey et al. (2017). A 25 mm (0.98 in) asphalt leveling course was then compacted over the concrete block using a hydraulic roller compactor. The general process for hydraulic roller compaction is described in Section 5.3.6. After the asphalt leveling course was in place, a paint roller was used to apply a specialized asphalt primer to the slabs to complete coverage (Figure 5.6a). The roll-on membranes were cut and the plastic covering over the bituminous backing of the membranes was removed (Figure 5.6b). Membranes were placed on the slabs (Figure 5.6c) and a heat gun was used to partially melt and adhere the bituminous backing of the membranes (Figure 5.6d). Complete adhesion occurs when hot asphalt is later compacted over the top of the membrane.

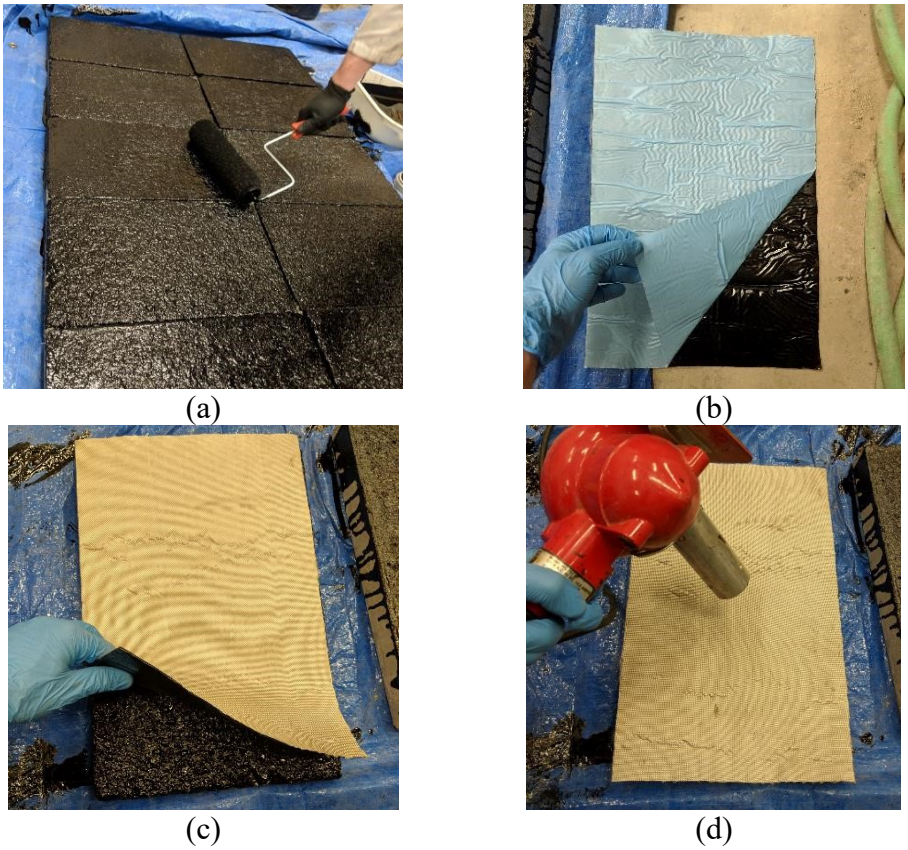

Figure 5.6: Roll-on membrane installation (a) Primer brushed over asphalt leveling course (b) Plastic peeled off roll-on membrane to expose bituminous backing (c) Membrane placed onto asphalt leveling course (d) Membrane heated to partially adhere bituminous backing

It should be noted that installation of roll-on membrane systems requires less effort during construction when compared to poured and sprayed membrane strategies due to easier surface preparation. Shot blasting and hand tooling are generally required to prepare the bridge deck surface before the installation of poured and sprayed membranes. These surface preparation steps

require a substantial amount of time and effort. Achieving a clean surface before the application of poured and sprayed membranes is also critical.

5.3.5 Mastic asphalt layer with roll-on membrane installation and materials

According to a 2013 report published by the European Asphalt Pavement Association (EAPA), Germany employs a concrete bridge deck waterproofing system consisting of a waterproofing bitumen sheet underneath two layers of asphalt. Shot blasting is first used to introduce texture to the concrete deck. An epoxy resin primer gritted with 300-500 g/m^2 (8.85 – 14.75 oz/yd^2) quartz sand is spread over the deck to penetrate and seal the concrete pores. A bitumen sheet waterproofing layer (4.5-5.5mm thickness) (0.18 – 0.22 in) is then rolled onto the deck over the primer and a mastic asphalt layer is poured onto the deck at a thickness of 35-40mm (1.38-1.58 in) to act as an impermeable protective layer for the bitumen sheets. Finally, a surface layer is constructed which acts as a suitable wearing course for vehicles. This surface course has a minimum thickness of 35-40mm (1.38-1.58 in) and can be constructed of traditional asphalt concrete (EAPA 2013). The mastic asphalt layer and roll-on membrane system evaluated in this study was comprised of the layers shown in Figure 5.7.

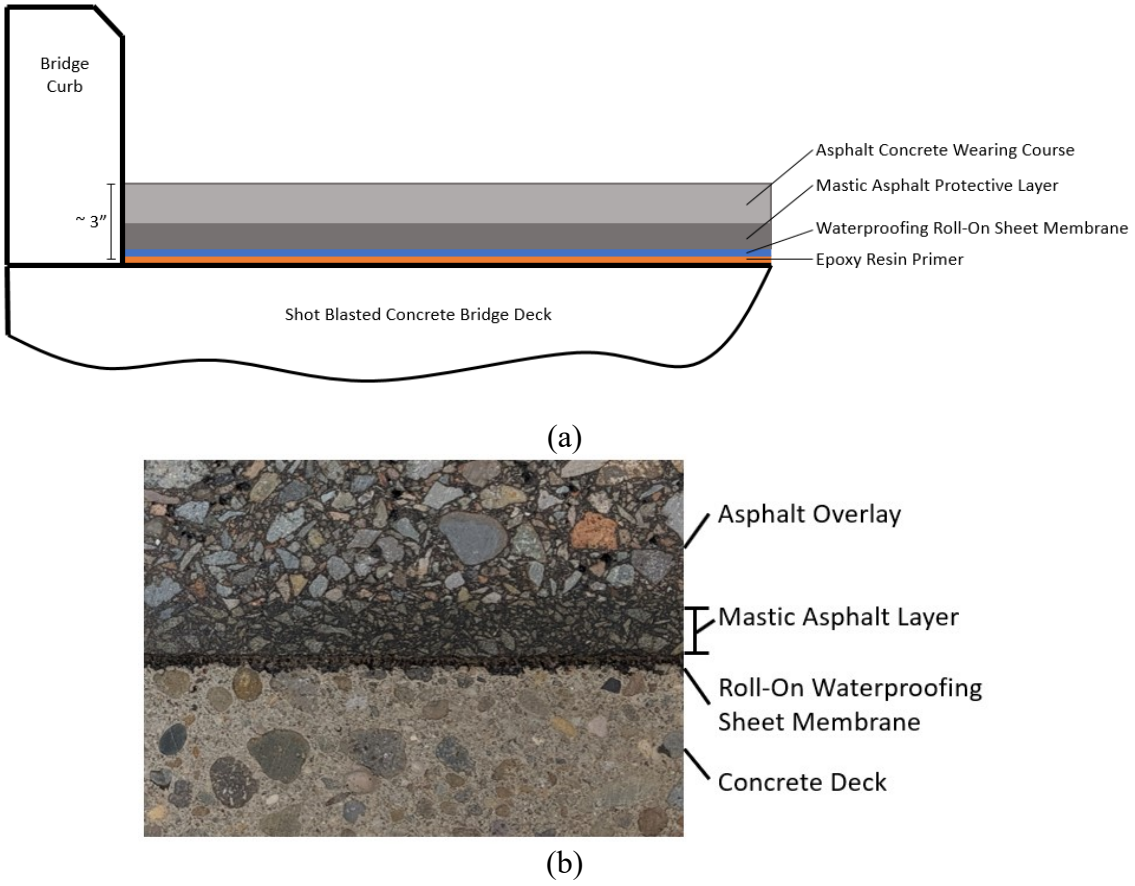

Figure 5.7: Strategy 4 - Mastic asphalt with roll-on membrane (a) Diagram and (b) Cross-section of the produced laboratory sample

5.3.5.1 Mastic asphalt design and compaction

For the production of mastic waterproofing membrane samples used for this study, concrete block slabs were first produced in the laboratory and allowed to cure for 28 days. The slabs were then sand blasted to create texture by following a system identical to the ones used in the field during construction. The same roll-on membrane used in Section 5.3.4 was then installed on concrete. Installation of the roll-on membrane for this strategy followed the procedure described in Section 5.3.4, with the only exception being that the primer and membrane was placed directly onto the shot-blasted concrete slabs as opposed to being placed on an asphalt leveling course. For the design of the mastic asphalt layer, the goal was to design a thin layer with no air voids and a low viscosity that could be poured over the block samples. These characteristics were achieved by using a high binder content and a fine gradation in the mastic asphalt mixture. The final mixture for the mastic layer utilized a binder content of 11.0%, a binder grade of PG70-22ER and a nominal maximum aggregate size (NMAS) of 2.38 mm (0.09 in). The mastic asphalt layer was compacted to a height of 10 mm (0.4 in) on top of the roll-on membrane.

The mastic asphalt mixing and placement process can be seen in Figure 5.8. To construct the mastic asphalt on top of the roll-on sheet membrane, aggregates and PG70-22ER binder were placed in an oven set to 160°C (320ºF) for 2 hours, as recommended by the binder manufacturer for mixing. Aggregates were removed from the oven and placed in a bucket mixer (Figure 5.8a). Binder was removed from the oven and added to the aggregates until a binder content of 11.0% (by weight of the total mixture) was reached (Figure 5.8b). The materials were mixed until an even coating of binder was achieved around all aggregates (Figure 5.8c). The mastic mixture was poured into a pan and put back in the oven at 152°C (305.6 ºF) for 2.5 hours to reach a uniform compaction temperature, as recommended by the binder manufacturer. At this time, a high-performance tack coat was uniformly applied to the top of the roll-on membrane using an application rate of 0.23 L/m^2 (0.05 gal/yd^2) (Figure 5.8d). This application rate was deemed optimal such that complete coverage was achieved without creating puddling of tack coat on the membrane surface. Once compaction temperature was reached, the mixture was removed from the oven and poured into a mold over the concrete slab and roll-on membrane. A spreader and roller were used to evenly distribute the mastic asphalt over the roll-on membrane (Figure 5.8e), and heavy rectangular steel spacers were placed in the mold on top of the mastic mixture to ensure complete compaction and even distribution of the mixture as it cooled (Figure 5.8f).

Figure 5.8: Mastic asphalt mixing and compaction (a) Heated aggregates placed in bucket mixer (b) Binder added to achieve 11.0% binder content (c) Materials mixed to achieve uniform binder coverage around aggregates (d) Tack coat spread onto block sample and sample placed in mold (e) Mastic asphalt mix distributed over block sample using spreader and roller (f) Metal plates placed on top of mastic mixture

5.3.6 Compaction of asphalt production mix over waterproofing membrane strategies

After installing waterproofing membrane strategies on the concrete slabs, an asphalt production mix (sampled from a local plant), typical of that used for constructions on Oregon highways, was compacted on top of the block samples using a hydraulic roller compactor. The compaction process for waterproofing membrane samples can be seen in Figure 5.9. Two and a half hours prior to compaction, predetermined quantities of loose production mix asphalt were placed in an oven at 144°C. At this time, a high-performance tack coat was applied to the surface of the waterproofing membranes (Figure 5.9a). For the sprayed and poured membranes, which had a high surface texture, the tack coat was applied at an application rate of 0.32 L/m^2 (0.07 gal/yd^2) as recommended by Covey et al. (2017) and Coleri et al. (2017). For the roll-on membrane and mastic layer, which had low surface texture, the tack coat was applied at a rate of 0.23 L/m^2 (0.05 gal/yd^2) to prevent puddling. During compaction, the concrete block sample was placed into a metal mold with a height of 100 mm (3.9 in) (Figure 5.9b). Once the block was in place, the loose asphalt mix was poured into the mold and spread around such that an even amount of asphalt was covering all parts of the block (Figure 5.9c). A collar was placed around the mold and the mold was placed in the hydraulic roller compactor (Figure 5.9d). Compaction pressure was increased with each pass of the hydraulic roller and compaction ceased once the mold height was reached. After compaction, the sample was allowed to cool overnight prior to cutting or coring.

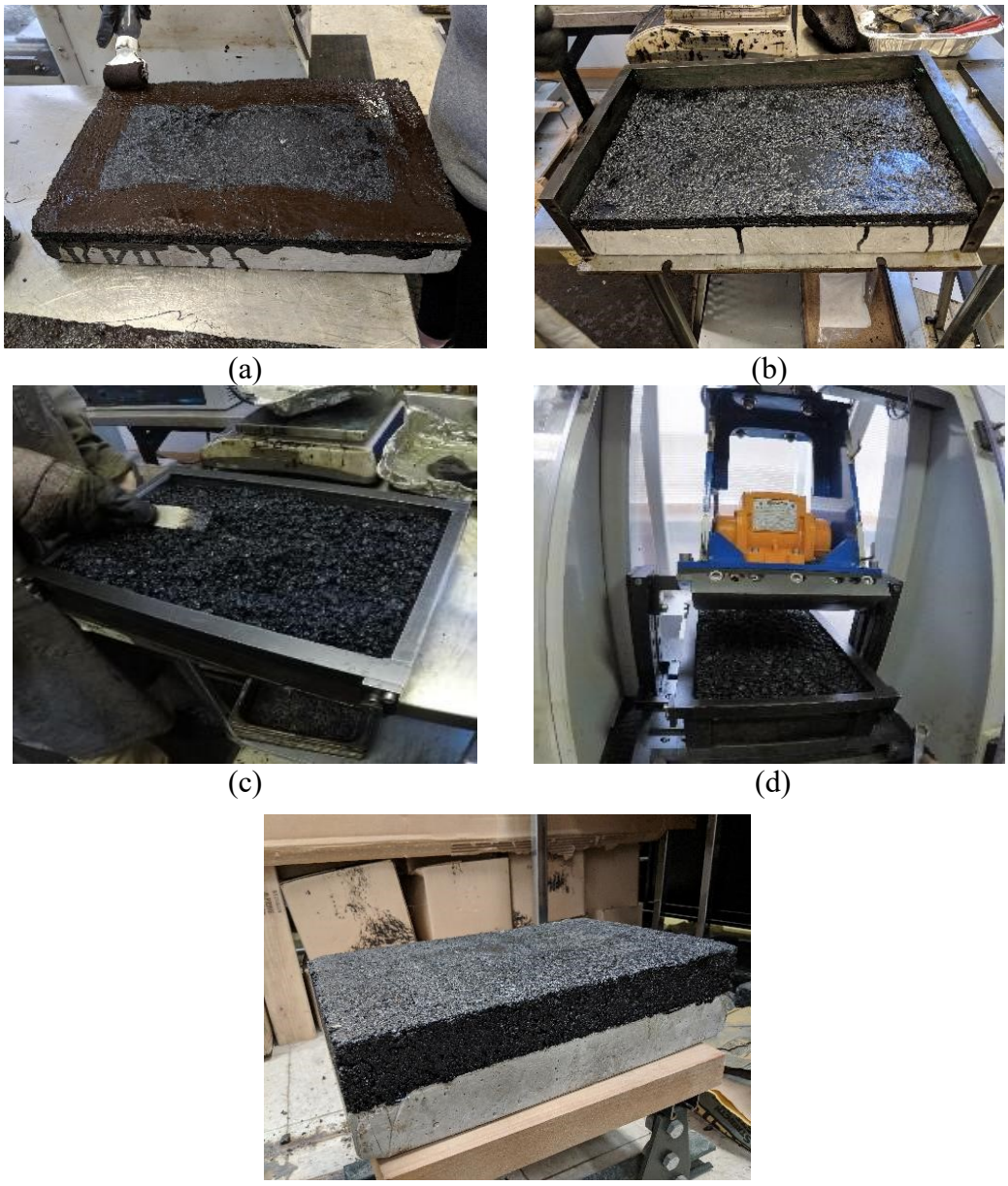

Figure 5.9: Asphalt overlay compaction for waterproofing membranes (a) Tack coat applied to waterproofing membrane surface (b) Concrete slab placed in roller compactor mold (c) Loose production mix asphalt poured into mold and evenly distributed (d) Uncompacted sample placed in roller compactor (e) Compacted concrete-waterproofing membrane-asphalt block sample.

5.4 EXPERIMENTAL DESIGN AND TEST METHODS

A total of 64 sample blocks were produced for the evaluation of four different bridge deck waterproofing strategies. A list of the four waterproofing strategies can be referenced in Table 5.1. Each complete block sample had dimensions of 40 cm (length) x 26 cm (width) x 10 cm (thickness) (15.8 in x 10.2 in x 3.9 in). Each block sample was comprised of a 50 mm (2.0 in)

concrete layer overlaid with one of four waterproofing strategies. An approximately 50 mm (2.0 in) asphalt wearing course was constructed over the top of each waterproofing strategy. Variations in construction existed for both Strategy 3 (roll-on membrane) and Strategy 4 (mastic asphalt layer with roll-on membrane), which are detailed in Section 5.3.4 and Section 5.3.5, respectively. Following construction, two blocks from each strategy were instrumented with moisture sensors for moisture infiltration testing with the rainfall simulator.

Oregon Field Torque Test (OFTT) tests, flow number (FN) tests, three-point flexural fatigue tests and Hamburg Wheel Tracking (HWT) tests were conducted on sets of samples which both had and had not been exposed to freeze-thaw cycle effects. To investigate the effect of freeze-thaw on waterproofing membranes, half of the tested samples were subjected to a series of 15 freeze-thaw cycles. For freeze-thaw cycling, samples were first placed under the rainfall simulator and underwent a simulated rainfall event for a period of 48 hours. Samples were then placed in a freezer set at -20 °C (-4 °F) for 14 hours. The frozen samples were removed from the freezer to thaw for 10 hours at 20 °C (68 °F). This process was repeated for 15 days to simulate 15 freeze-thaw cycles. Samples tested for moisture infiltration were not subjected to freeze-thaw cycles. The experimental plan followed in this study is given in Table 5.3. Sample preparation and testing procedures for individual tests are outlined in the following sections.

Table 5.3: Experimental Plan for Evaluated Waterproofing Membranes

Test Type	Strategies[1]	Test Variations[2]	Replicates	Total Tests	Total Block Samples
Moisture Infiltration Test	1,2,3,4	None	2	8	8
Freeze-Thaw Simulation	1,2,3,4	None	4	16	16
Oregon Field Torque Test	1,2,3,4	w/ F-T, w/o F-T	6	48	8
Flow Number Test	1,2,3,4	w/ F-T, w/o F-T	3	24	16
3-Point Flexural Fatigue Test	1,2,3,4	w/ F-T, w/o F-T	3	24	8
Hamburg Wheel Tracking Test	1,2,3,4	w/ F-T, w/o F-T	3	24	24

Note: [1]Strategy number correspond to those found in Table 5.1
[2]w/ F-T denotes that half of samples have undergone freeze-thaw cycles prior to testing

5.4.1 Rainfall simulation and moisture infiltration tests

5.4.1.1 Rainfall simulation and moisture infiltration sample preparation

The complete moisture sensor setup is depicted in Figure 5.10. For moisture infiltration laboratory experiments, two holes were drilled into the block samples for the different

waterproofing strategies. Holes were drilled at the top of the concrete slab and below the waterproofing membrane such that the top of the hole was exposed to the bottom of the membrane. A moisture sensor was inserted into the holes at the membrane-concrete interface of the block samples, and fine sand was used to fill remaining voids around the sensor nodes and provide a medium through which any infiltrated water could reach the nodes (Figure 5.10a). The moisture sensor was then sealed using a silicone gel to prevent water from reaching the sensor from the exterior, as opposed to reaching the sensor by permeating through the asphalt overlay (Figure 5.10b). The sensor was wrapped in plastic wrap (Figure 5.10c), and protective covers were placed over the edges of the block to further ensure that no moisture reached the sensor from the sides of the sample or from the insertion point of the sensor nodes (Figure 5.10d). Properly sealing the sides of the blocks and exterior of the moisture sensor was critical to ensure that any moisture being detected by the sensor had passed through both the asphalt overlay and the respective waterproofing membrane to reach the sensor.

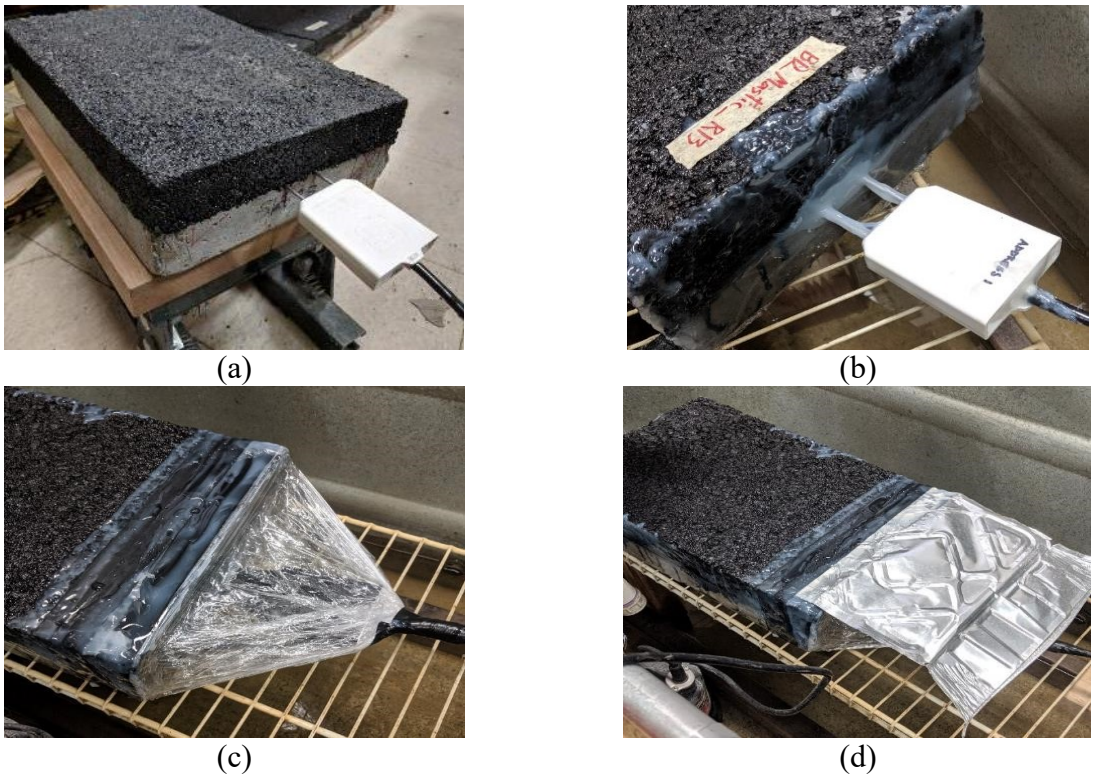

(a) (b) (c) (d)

Figure 5.10: Sealing the moisture sensor to prevent external moisture readings (a) Sensor inserted into layer interface (b) Exposed sensor nodes and surrounding sample sealed with silicone gel (c) Sensor wrapped in plastic wrap and sealed (d) Protective covering placed over sensor area

5.4.1.2 Rainfall simulation and moisture infiltration testing procedure

For this test, samples were placed under the rainfall simulator and subjected to a steady simulated rainfall event over a five-day span. A depiction of the rainfall simulator test setup is shown in Figure 5.11. A customized moisture sensor imbedded at the sample

asphalt-concrete interface, below each respective waterproofing surfacing strategy, was used to continually log data for the test and consisted of two main components. The sensor component consisted of a CS655 Water Content Reflectometer produced by Campbell Scientific, Inc. The CS655 possessed two 30 cm long (11.8 in) nodes and was capable of measuring volumetric water content, bulk electrical conductivity and temperature. The data logger component, capable of running up to four serial data interface (SDI-12) sensors (such as the CS655) simultaneously, was developed. The SDI-12 data logger runs on an open source Python script and can collect continuous data for months at a time (Liu 2017).

The moisture sensor used for the tests was calibrated to take moisture readings every 10 seconds and export the readings to a spreadsheet. Moisture readings were directly measured by reading the dielectric permittivity within a sample, then converting the reading to a volumetric water content (m^3/m^3). From the output, the amount of water present at the asphalt-concrete interface could be tracked over time, allowing one to determine at what point water had infiltrated the sample (Liu 2017). If the waterproofing membranes installed on the samples were functioning as designed, no moisture infiltration should be detected by the sensors over the analysis period.

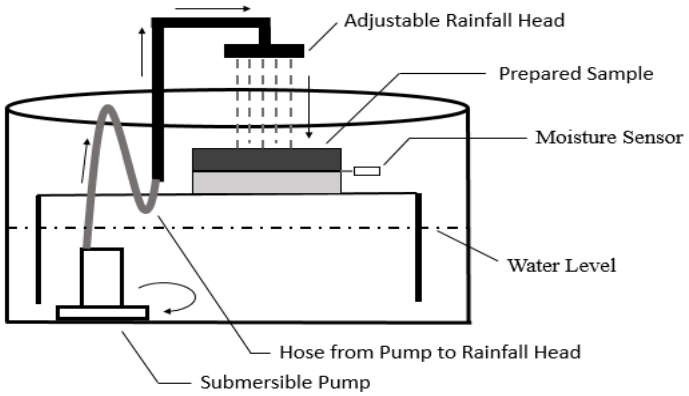

(a)

(b)

Figure 5.11: Rainfall simulator test setup (a) Rainfall simulator diagram (b) Sample undergoing infiltration test

5.4.2 Freeze-thaw cycling

The freeze-thaw cycling procedure involved placing respective test samples (blocks with asphalt, concrete, and membranes) under the rainfall simulator to saturate the samples, then subjecting them to repeated extreme temperature cycles. To prepare samples for freeze-thaw cycling, the samples had to be completely sealed from the sides and bottom. Doing so ensured that moisture that had infiltrated through the asphalt stayed within the sample to freeze and re-freeze as opposed to simply draining out of the sample after several cycles. To seal the bottom of samples, a thick plastic covering was taped in place, covering the bottom and extending 25 mm (0.98 in) up the sides of each sample. Silicone gel was then spread along the sides of the sample to completely seal it and prevent water from escaping the sides or bottom. Samples were then placed under the rainfall simulator for 48 hours, which was long enough to ensure complete saturation of the asphalt overlay on the sample (Haynes et al. 2019). After becoming fully saturated, samples were placed into a freezer set to -20 ºC (-4 ºF) for 14 hours. The frozen samples were removed from the freezer to thaw for 10 hours at 20 ºC (68 ºF). This freezing and thawing process was repeated for 15 days to simulate 15 freeze-thaw cycles.

5.4.3 Oregon Field Torque Test (OFTT) tests

5.4.3.1 Oregon Field Torque Test (OFTT) sample preparation

OFTT samples were cored using a 2” core drill to a depth of a few millimeters below the base of the membrane (i.e. a few millimeters into the concrete slab). This allowed the platen for the OFTT test to be adhered to an isolated area of the waterproofing system for testing and allowed failures to occur at the interface between the waterproofing membrane and adjacent layers. Six OFTT tests were conducted on a single block for each waterproofing strategy. After coring of OFTT blocks, platens were glued to the top of the cores using a fast-setting epoxy. Block coring and gluing of platens can be seen in Figure 5.12.

(a) (b)

Figure 5.12: (a) Block coring for OFTT test and (b) Gluing of OFTT platens

5.4.3.2 Oregon Field Torque Test (OFTT) testing procedure

The OFTT in-situ torque tester developed by Coleri et al. (2017) was used to characterize the interlayer shear strength of a multi-layer sample. In this study, the bonds being investigated were those between the concrete slab and respective waterproofing membrane, and between the waterproofing membrane and asphalt overlay. The hardware of the OFTT device consists of an automatic step motor, planetary gearbox, transducers, torque sensor and amplifier, data acquisition and control systems, and an adjustable frame (Figure 5.13a). A software was developed to control the loading and rotation speed of the system.

To conduct the test, the OFTT test system was placed on the platens and the torque frame was adjusted to match the platens (Figure 5.13b). Using the control software, the torque transducer was rotated at 2^{o} per second until the interlayer bond within a sample was completely broken (Figure 5.13c). The OFTT recorded the peak torque stress (strength) at the interface between pavement layers (Figure 5.13d). Using the rotation angle versus applied torque, peak torque at failure was determined. After obtaining the peak torque at failure for each sample, the measured torque value (Nm) was converted to OFTT shear strength (kPa) using Equation **Error! Reference source not found.**) given below (Muslich 2009):

$$\boldsymbol{\tau = \frac{12M \times 10^{6}}{\pi D^{3}}} \qquad \textbf{(5-1)}$$

Where;

τ is the interlayer shear strength (OFTT shear strength) (kPa);

M is the peak torque at failure (N.m), and

D is the diameter of the core (mm).

The OFTT test setup can be observed in Figure 5.13.

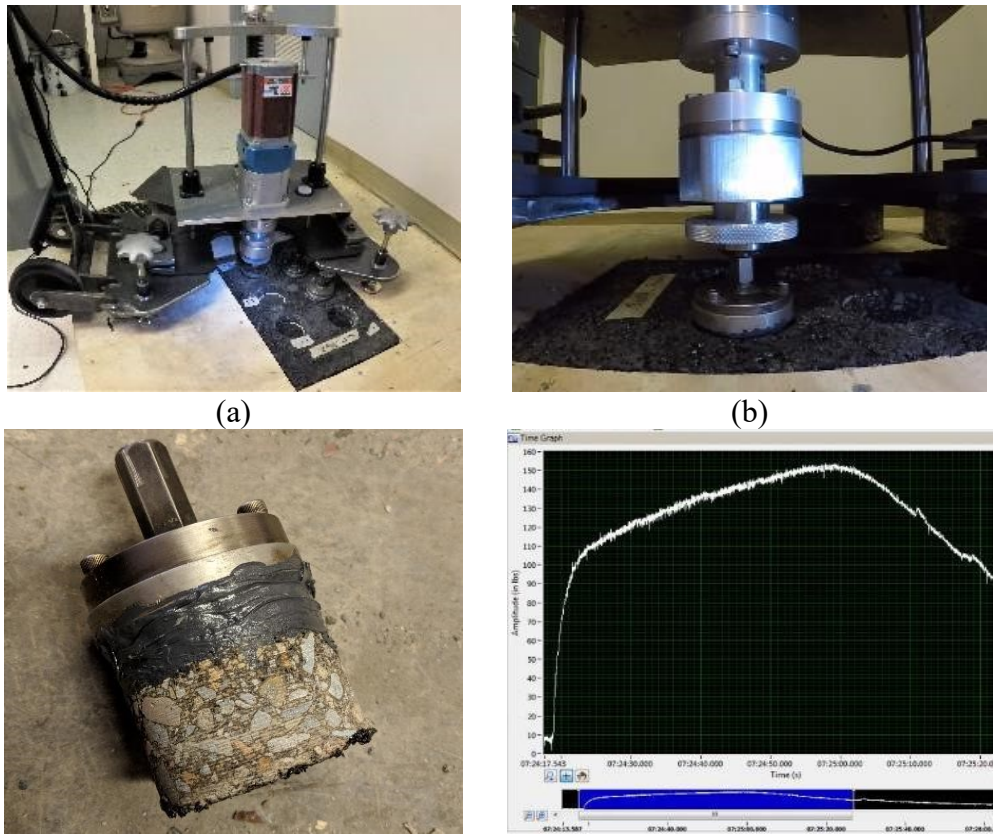

Figure 5.13: Oregon Field Torque Test Procedure (a) OFTT placed over block sample (b) Torque frame lowered onto platen (c) Failure from membrane bond after torque is applied (d) Peak torque stress determined from software

5.4.4 Flow number (FN) tests

5.4.4.1 Flow number (FN) sample preparation

To prepare samples for flow number testing, block samples were cut in half transversely using a high accuracy saw (Figure 5.14a). Samples were allowed to dry for several days, then placed in the Universal Testing Machine (UTM) for conditioning. Prior to testing, a rubber sheet and metal load plate were positioned on top of the sample to facilitate an even load distribution similar to a truck tire load.

(a) (b)

Figure 5.14: FN sample preparation and testing (a) Cutting of FN samples (b) FN sample positioned in UTM

5.4.4.2 Flow number (FN) testing procedure

The flow number (FN) test was utilized to evaluate the rutting resistance of samples comprised of a concrete slab, waterproofing membrane and asphalt overlay. In this test, a constant deviator stress was applied at each load cycle on the test sample and permanent strain at each cycle was measured. Permanent deformation of asphalt pavement has three stages: 1) primary or initial consolidation, 2) secondary and 3) tertiary or shear deformation (Figure 5.15) (Biligiri et al. 2001). FN is the loading cycle at which the tertiary stage starts after the secondary stage.

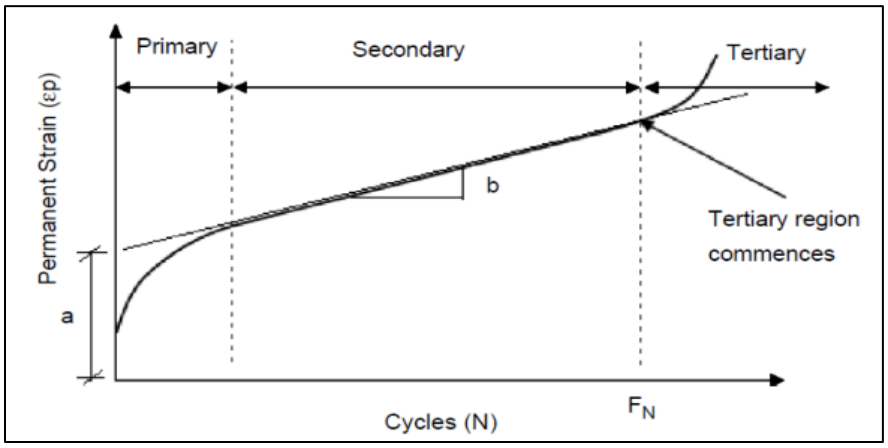

Figure 5.15: Stages of permanent deformation in asphalt pavement (Biligiri et al. 2001)

In this study, testing conditions and requirements for FN testing described in AASHTO TP 79-13 (2013) for unconfined tests were followed. The recommended test temperature, determined by LTPPBind Version 3.1 software, is the average design high pavement temperature at 50% reliability for cities in Oregon with high populations and at a depth of 20 mm (0.79 in) for surface courses (Rodezno et al. 2015). Tests were conducted at a temperature of 54.7ºC (130.5ºF) with average deviator stress of 600 kPa (87.0 psi) and

minimum (contact) axial stress of 30 kPa (4.4 psi). For conditioning, samples were kept in a conditioning chamber at the testing temperature for five hours prior to testing. To calculate FN in this study, the Francken model was used (Francken 1977).

5.4.5 Three-point flexural fatigue tests

5.4.5.1 Three-point flexural fatigue sample preparation

To prepare samples for three-point flexural fatigue testing, block samples were cut into thirds longitudinally using a high accuracy saw (Figure 5.16a). Samples were allowed to dry for several days, then placed in the Universal Testing Machine (UTM) for conditioning. A specialized loading frame was developed at OSU for testing the composite samples (Figure 5.16b). The frame consisted of two rollers positioned underneath the sample on either side to allow freedom of movement during bending of the sample. A custom load plate was centered on top of the sample to evenly distribute applied loads along its width.

(a) (b)

Figure 5.16: Three-point bending sample preparation and testing (a) Cutting of three-point bending sample (b) Three-point bending sample positioned in UTM

5.4.5.2 Three-point flexural fatigue testing procedure

The three-point flexural fatigue test was utilized to evaluate the cracking and deformation resistance of the samples. Additionally, this test allowed for the observation of any delamination that would occur at the waterproofing membrane interface as a result of repeated flexural bending due to heavy truck loads. To conduct the test, samples were placed on the loading frame in the UTM and allowed to condition for two hours at a temperature of 25°C (77°F). The actuator of the UTM was then lowered down and a repeated cyclic load was applied at the center of the beam sample. Repeated loads were applied with a force of 0.8kN and at a loading frequency of 10Hz (10 loading cycles per second). This frequency corresponds to the loading time of a vehicle tire at a single point on an asphalt pavement if that vehicle were travelling at approximately 97 kph (60 mph). Tests were run for 10 hours (360,000 cycles). Displacement of the actuator within the UTM was tracked throughout the duration of the test. Following the test, peak

displacement was determined and comparisons were drawn between waterproofing membrane strategies.

5.4.6 Hamburg Wheel Tracking (HWT) tests

5.4.6.1 Hamburg Wheel Tracking (HWT) sample preparation

To prepare samples for HWT testing, block samples were placed in the testing mold. Since the width of the produced test blocks were about 2inches shorter than the width of the testing mold, the gap between the block and the mold was filled with plaster. After the plaster cured in about 16 hours, sample was placed in the HWT test system for conditioning. After conditioning, test system automatically starts the tests. It takes about 7 hours to conduct one experiment and two samples can be tested at the same time.

5.4.6.2 Hamburg Wheel Tracking (HWT) testing procedure

The Hamburg Wheel-Tracking Device (HWTD) was developed to measure rutting and moisture damage (stripping) susceptibility of an asphalt concrete sample. In this study, tests were conducted by immersing the asphalt concrete blocks in a hot water bath at 50°C and rolling a steel wheel across the surface of the sample to simulate vehicle loading. 20,000 wheel passes were applied to determine the rutting resistance of a sample. Figure 5.17 shows the HWT test system used for running experiments in this study and a tested sample.

(a) (b)

Figure 5.17: Hamburg wheel tracking test (a) Test system used for conducting experiments (b) Tested block sample.

The HWTD test is one option to characterize the structural resistance of various waterproofing bridge deck strategies. It could be particularly useful when the waterproofing strategy being tested is an impermeable (mastic) pavement. Impermeable pavements generally employ a high-density asphalt mixture which is achieved by using a softer asphalt binder or higher binder content. These factors make the asphalt pavement

more susceptible to rutting from repeated vehicle loading. Since the HWTD test simulates vehicle tire loading, it could be ideal for evaluating susceptibility of impermeable asphalt pavement mixtures on concrete bridge decks.

5.5 RESULTS AND DISCUSSION

5.5.1 Rainfall simulation and moisture infiltration results

Moisture infiltration tests were conducted in the rainfall simulator over a five-day analysis period, with sensors continually logging any moisture infiltration to the membrane-concrete interface over that time. To observe the trends associated with infiltration times of each sample, bar charts were developed displaying the duration of rainfall testing required to reach initial infiltration and 50% total volumetric water content (i.e. 50% saturation). Figure 5.18 outlines the times required for the moisture sensor to initially detect moisture at the membrane-concrete interface of samples for each waterproofing strategy. Following the tests, it was observed that neither sprayed nor poured membrane samples saw any infiltration over the course of the five-day analysis period. One of the two roll-on membrane samples tested saw no moisture infiltration, however the other roll-on sample saw initial moisture infiltration after approximately 13.8 hours. Similarly, one of the mastic asphalt (with roll-on membrane) samples saw no moisture infiltration, however the other saw initial moisture infiltration after approximately 41.8 hours.

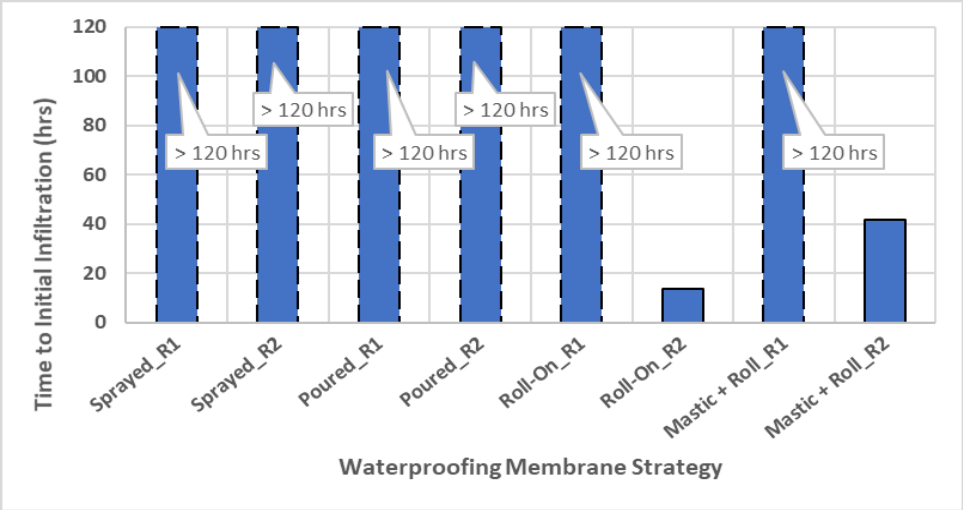

Figure 5.18: Time to reach initial water infiltration for rainfall samples
Note: R1 and R2 indicate Replicate 1 and Replicate 2
Samples indicating a time of 120 hours saw no infiltration

Figure 5.19 outlines the times required to reach 50% of the total volumetric water content. For this case, the roll-on membrane strategy reached 50% of its total volumetric water content (i.e. became 50% saturated) after approximately 22.6 hours and became fully saturated after 45.8 hours. The mastic asphalt and roll-on membrane sample, however, experienced continued infiltration at a much slower rate, and did not reach a 50% saturation level within the five-day analysis period.

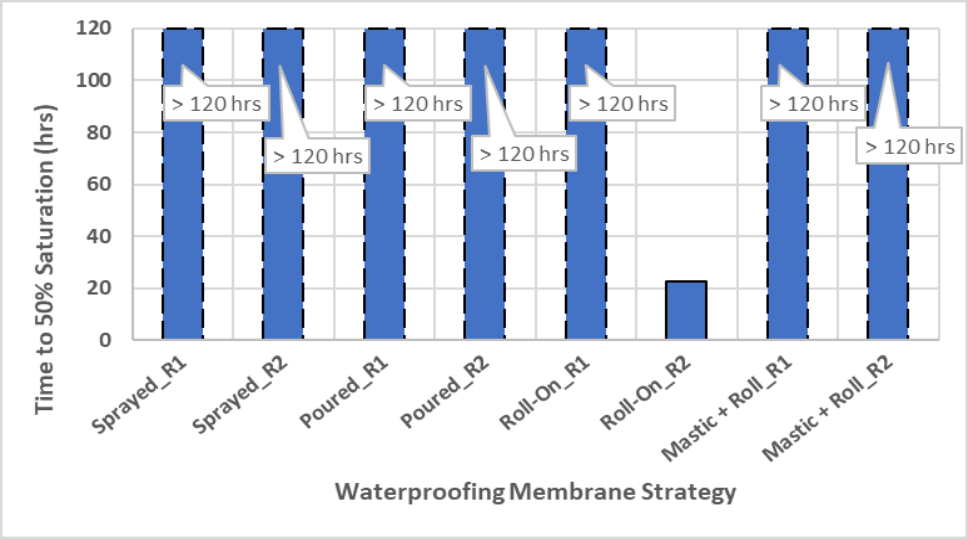

Figure 5.19: Time to reach 50% of total volumetric water content for rainfall samples
Note: R1 and R2 indicate Replicate 1 and Replicate 2
Samples indicating a time of 120 hours did not reach 50% saturation

5.5.2 Oregon Field Torque Test (OFTT) results

Oregon Field Torque Test (OFTT) were conducted on samples for each waterproofing membrane strategy. For all four strategies, one set of tests was conducted on blocks that had not been subjected to freeze-thaw cycles, and another set of tests was conducted on blocks which had been subjected to freeze-thaw cycles. From the OFTT tests, the average interlayer shear strengths at the failure interface were determined for each sample. These results can be seen in Figure 5.20.

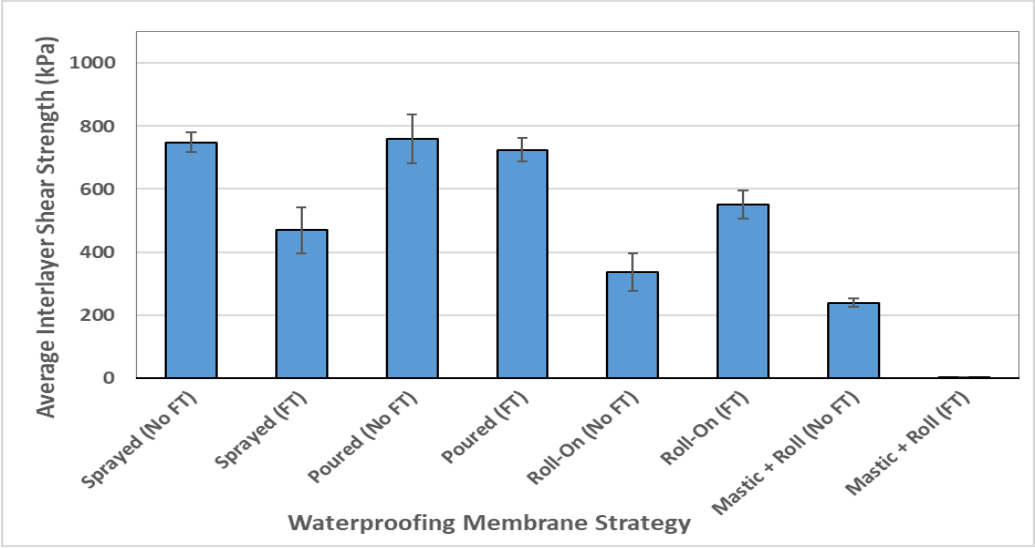

Figure 5.20: Oregon Field Torque Test (OFTT) results
Note: Length of error bars represent one standard deviation
FT = Sample underwent freeze-thaw cycles prior to testing

From the results, it can be observed that for both the sprayed and poured membrane cases, average interlayer shear strength was lesser for samples that had been subjected to repeated freeze-thaw cycles, indicating that these extreme temperature cycles deteriorated the bond between the membrane and the asphalt overlay. The difference is greatest between the two sprayed membrane cases, which may be due to the fact that the sprayed membrane had a lower surface texture compared to the poured membrane. For the roll-on membrane cases, the bond strength was greater for the sample that had gone through freeze-thaw cycles. This unexpected outcome may be the result of some inconsistency during the construction of the membrane and additional test should be conducted to assess the accuracy of these results. For the mastic with roll-on membrane samples which had been subjected to freeze-thaw cycles, all samples failed during the sample coring process described in Section 5.4.3.1. The small amount of torque applied in the coring process was enough to break each of these samples at the roll-on membrane – concrete interface. Typically, a roll-on membrane is constructed on an asphalt surface, however for these samples, it was placed directly on a concrete slab. The lower texture of the concrete slab, combined with deterioration from freeze-thaw cycle effects, likely decreased the bond strength at this interface and resulted in the early failures.

It is also possible that the differences in the coefficient of thermal expansion between asphalt and concrete layers were responsible for the bond failures in the mastic asphalt samples. The coefficient of thermal expansion for a high binder content asphalt mixture, such as the one used for the mastic layer, is approximately 2.046*10-5/°C (1.137*10-5/°F), whereas the coefficient of thermal expansion for a typical Portland Cement Concrete ranges from 7.4*10-6/°C to 13.0*10-6/°C (4.1*10-6/°F to 7.3*10-6/°F) (Mamlouk et al. 2005, FHWA 2016). Greater expansion of the concrete slab due to its higher coefficient of thermal expansion likely introduced additional stresses at the bond interface during freeze-thaw cycles and could have contributed to the early failures. Bond failure locations with number of samples for each of the tested membrane strategies are outlined in Table 5.4.

Table 5.4: Membrane Failure Locations after OFTT Testing

Membrane Type	Bond Failure Location
Sprayed Membrane (No Freeze-Thaw)	Sprayed Membrane – Asphalt Interface (All Tests)
Sprayed Membrane (Freeze-Thaw)	Sprayed Membrane – Asphalt Interface (All Tests)
Poured Membrane (No Freeze-Thaw)	Poured Membrane – Asphalt Interface (All Tests)
Poured Membrane (Freeze-Thaw	Poured Membrane – Asphalt Interface (All Tests)
Roll-On Membrane (No Freeze-Thaw)	Roll-On Membrane – Asphalt Overlay Interface (All Tests)
Roll-On Membrane (Freeze-Thaw)	Roll-On Membrane – Asphalt Overlay Interface (All Tests)
Mastic + Roll-On (No Freeze-Thaw)	Roll-On Membrane – Concrete Interface (2 Tests) Roll-On Membrane – Mastic Layer Interface (4 Tests)
Mastic + Roll-On (Freeze-Thaw)	Roll-On Membrane – Concrete Interface (all failed during coring of samples)

Note: Number of tests which failed at the specified interface are given in parenthesis

5.5.3 Flow number (FN) results

Flow number tests were conducted for the each of the waterproofing membrane strategies with and without freeze-thaw conditioning. The results from flow number testing are outlined in Figure 5.21.

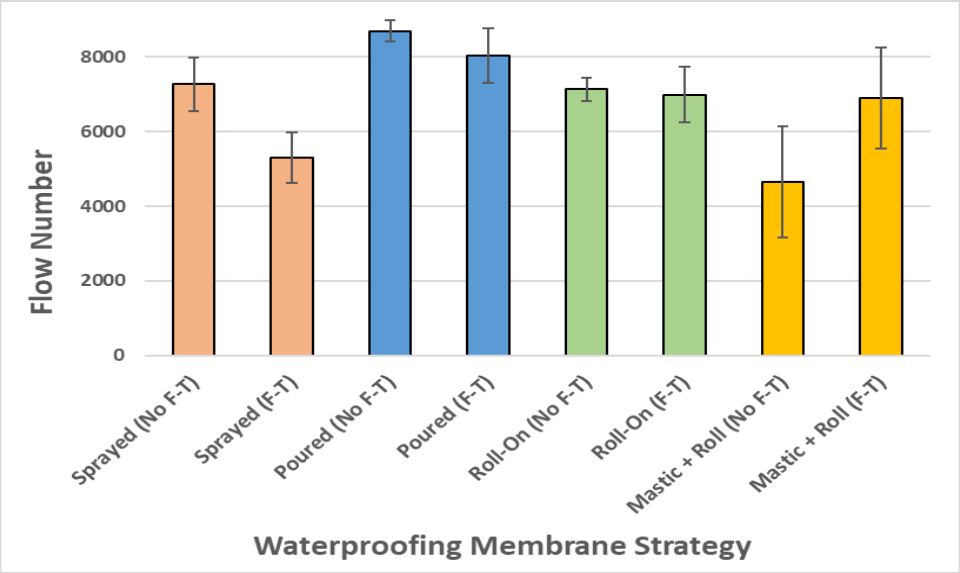

Figure 5.21: Flow number (FN) results
Note: Length of error bars represent one standard deviation
FT = Sample underwent freeze-thaw cycles prior to testing

From the results, it can be seen that samples which had been subjected to freeze-thaw cycles generally produced lower flow numbers. If the freeze-thaw cycles deteriorate the bond at the asphalt – waterproofing membrane interface, the sample may stop acting as a monolithic structure and the asphalt layer would be able to flow independently, likely resulting in greater deformation. It is likely that bond damage was happening at the asphalt-impermeable layer interface for all samples except the mastic sample due to freeze-thaw cycles. Since the asphalt layer is not impermeable, water infiltrates through the asphalt layer and stands on top of the impermeable interface. Freezing expands the water and damages the bond. The samples with a mastic asphalt layer produced highly variable and inconsistent flow numbers, with a high standard deviation. This variation is likely due to the high binder content in the mastic layer making it more prone to flowing unpredictably, especially at the high test temperatures (54.7°C). Figure 5.22 depicts the deformation present in a tested mastic asphalt sample at the conclusion of the flow number test, with the red line representing the interface between the deformed mastic asphalt layer and the traditional asphalt layer. It appears that the majority of deformation within the sample is occurring at the mastic asphalt interface.

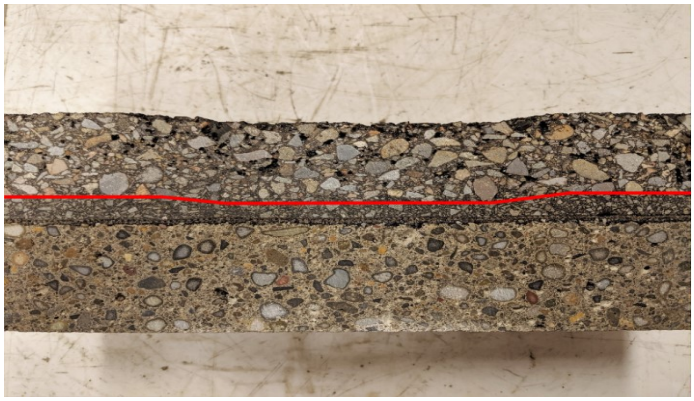

Figure 5.22: Mastic asphalt sample cross-section after flow number testing

5.5.4 Three-point flexural fatigue results

Three-point flexural fatigue tests were conducted to determine the cracking resistance of samples for each waterproofing membrane strategy (samples with and without freeze-thaw conditioning). Tests were conducted for 10 hours, applying a 0.8 kN load to the center of a beam sample at a frequency of 10 Hz. Following the conclusion of the test, bending deformation in the middle of the beam was reported.

Average deformations for each membrane strategy are presented in Figure 5.23. From the test results, it can be observed that all samples experienced minute permanent bending, likely due to the high strength of the concrete layer. There appeared to be small differences between samples that had been subjected to freeze-thaw cycles and sample which had not. Sprayed, poured and roll-on membrane samples all observed similar average deformations between 0.74 mm (0.029 in) and 0.87 mm (0.034 in). Permanent deformation in the samples with the mastic asphalt layer were significantly higher, averaging about 1.21 mm (0.048 in). This may be a result of the increased bending of the beam under the constant load due to the soft mastic asphalt layer.

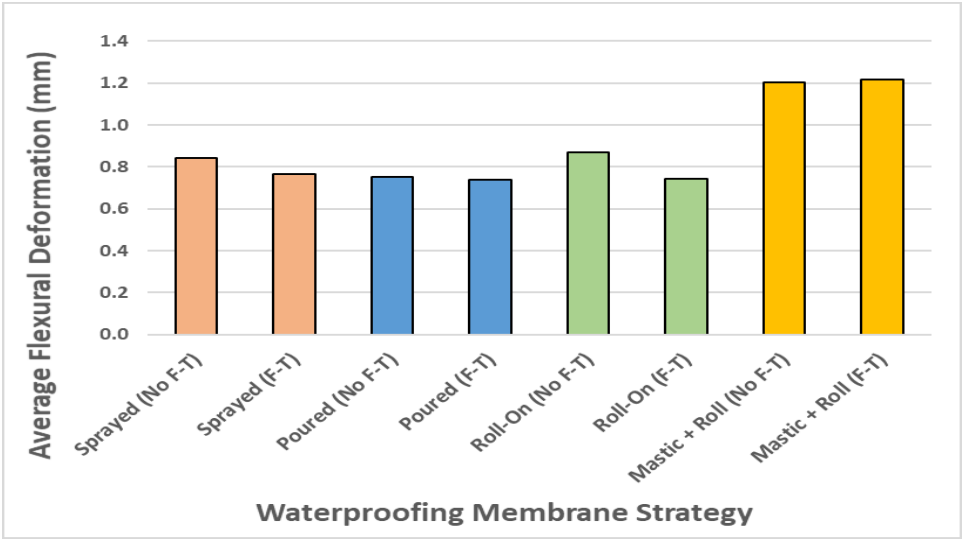

Figure 5.23: Three-point flexural fatigue test results

5.5.5 Hamburg Wheel Tracking (HWT) results

HWT tests were conducted for each of the waterproofing membrane strategies with and without freeze-thaw conditioning. The results from HWT testing are outlined in Figure 5.24.

HWT test results mostly agree with the FN test results. HWT test samples which had been subjected to freeze-thaw cycles generally produced higher deformations after 20,000 wheel passes. If the freeze-thaw cycles deteriorate the bond at the asphalt – waterproofing membrane interface, the sample may stop acting as a monolithic structure and the asphalt layer would be able to flow independently, likely resulting in greater deformation. It is likely that bond damage was happening at the asphalt- waterproofing membrane interface for all samples except the mastic sample due to freeze-thaw cycles. Since the asphalt layer is not impermeable, water infiltrates through the asphalt layer and stands on top of the impermeable interface. Freezing expands the water and damages the bond.

The samples with a mastic asphalt layer were not affected by freeze-thaw cycles since water could not reach the mastic-impermeable membrane interface due to the low air void content of the mastic layer. However, the samples with mastic layers had significantly higher surface deformation than all other strategies due to the high binder content and low stiffness of the mastic layer. It should also be noted that the impact of freeze-thaw cycles on surface deformation for the samples with poured membranes was significantly less than the sprayed membrane samples (agreeing with the OFTT test results). This result suggested that sprayed membrane sections are more vulnerable to freeze-thaw cycles when compared to other strategies.

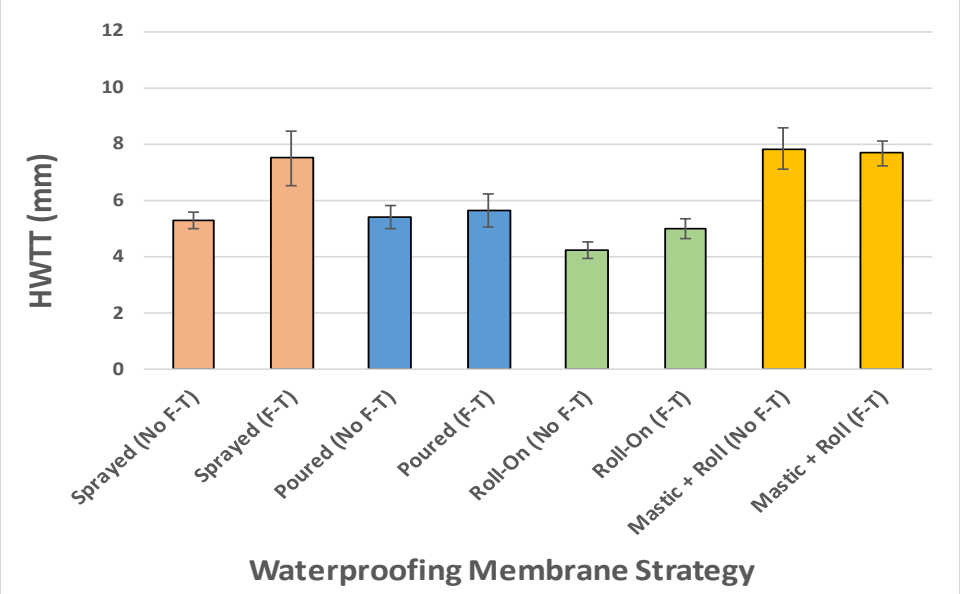

Figure 5.24: HWT test results

5.6 SUMMARY AND CONCLUSIONS

In this study, four different waterproofing membrane strategies were evaluated based on their resistance to cracking and rutting, interlayer bond strength, and their ability to remain

impermeable over extended rainfall events. To produce samples for laboratory testing, concrete slabs were cast in custom molds and membranes were constructed on top of slabs. An asphalt overlay was constructed on top of the membranes using a hydraulic roller compactor. Prior to testing, select samples were subjected to a series of freeze-thaw cycles to investigate the effects of extreme temperature cycling on overall structural performance. Flow number (FN) and Hamburg Wheel Tracking (HWT) tests were conducted to evaluate rutting resistance of samples. Three-point bending flexural fatigue tests were conducted to evaluate cracking resistance. The Oregon Field Torque Tester (OFTT) was used to compare the bond strength of different membranes and identify where failures due to delamination were likely to occur. A rainfall simulator and moisture sensor system were developed in this study to subject samples to a simulated rainfall event and measure moisture infiltration over a five-day analysis period.

The following important conclusions were obtained from this study:

- The moisture sensor and rainfall simulation testing system developed at Oregon State University can be used to effectively characterize moisture infiltration within asphalt samples constructed over a waterproofing membrane.

- Samples which incorporated a roll-on waterproofing membrane experienced some moisture infiltration through the membrane during a simulated extended rainfall event. Samples which has a mastic asphalt layer over the roll-on membrane experienced moisture infiltration at a much slower rate. Overall, the roll-on membrane systems did not provide adequate impermeability. However, it should be noted that only two replicate samples were tested for moisture infiltration in this study. Additional laboratory and/or field testing are required to validate the results.

- Installation of roll-on membrane systems requires less effort during construction when compared to poured and sprayed membrane strategies due to easier surface preparation. Shot blasting and hand tooling are generally required to prepare the bridge deck surface before the installation of poured and sprayed membranes. These surface preparation steps require a substantial amount of time and effort. Achieving a clean surface before the application of poured and sprayed membranes is also critical.

- Spray-on and poured waterproofing membranes both exhibited impermeability during moisture testing through a simulated extended rainfall event.

- Samples subjected to freeze-thaw cycles generally had a lower rutting resistance and interlayer shear strength as compared to samples not subjected to temperature cycling.

- Membrane surface texture has a significant impact on interlayer shear strength at the membrane-asphalt interface. High surface textures on the spray-on and poured membranes produced a much stronger bond with the asphalt overlay as compared to the smooth-textured roll-on membrane.

- Samples with a mastic asphalt layer produced flow number values significantly lower than those without a mastic asphalt layer. The high binder content in the mastic layer is likely responsible for increased flow and deformation.

- Beam samples with a mastic asphalt layer saw higher deformation following flexural fatigue tests as compared to samples without a mastic asphalt layer.

- HWT test results showed that the samples with a mastic asphalt layer were not affected by freeze-thaw cycles since water could not reach the mastic-impermeable membrane interface due to the low air void content of the mastic layer. However, the samples with mastic layers had significantly higher surface deformation than all other strategies due to the high binder content and low stiffness of the mastic layer.

- HWT test results also showed that the impact of freeze-thaw cycles on surface deformation for the samples with poured membranes was significantly less than the sprayed membrane samples.

The roll-on and mastic layer + roll-on strategies both saw moisture infiltration that reached the concrete surface during rainfall testing, and it was determined that the low texture on the roll-on membrane creates a poor bond with the asphalt overlay. Additionally, there was a large amount of variability in flow number results for mastic samples due to the high binder content of the mastic layer. Both the sprayed membrane and poured membrane performed well in all laboratory tests conducted. A slightly higher bond strength to the asphalt overlay was observed for the poured membrane, likely due to the higher surface texture. Rutting resistance of the asphalt mixture on the poured membrane system was also higher than the asphalt layer on the sprayed membrane system. Additionally, the installation process for the poured membrane is much simpler than that of the sprayed membrane. Whereas the sprayed membrane required specialized equipment to control the temperature and pressure at which the membrane is being sprayed, the poured membrane only requires a paint roller and notched squeegee to distribute over the surface of a concrete bridge deck. However, it should be noted that installation of roll-on membrane systems requires less effort during construction when compared to poured and sprayed membrane strategies due to easier surface preparation. Shot blasting and hand tooling are generally required to prepare the bridge deck surface before the installation of poured and sprayed membranes. These surface preparation steps require a substantial amount of time and effort. Achieving a clean surface before the application of poured and sprayed membranes is also critical.

While the sprayed and poured membranes performed well in laboratory testing, their performance should be further quantified through field implementation and testing. Additional field testing is also required to validate the moisture infiltration of roll-on membranes. To conduct a field evaluation, pilot sections can be constructed on a bridge using each of the waterproofing membranes. Automated Pavement Condition Surveys (APCS) can be performed to monitor the rutting and cracking performance over the life of the bridge section. Chain dragging and thermal imaging can be used to check for delamination between the waterproofing membrane and the asphalt overlay. Finally, moisture sensors can be installed in the membrane-concrete interface of the pavement prior to installation of the membrane in order to validate the impermeability of the membrane over the course of its service life.

6.0 COST COMPARISON OF WATERPROOFING MEMBRANE STRATEGIES

Material and installation costs of each of these membrane strategies are an important factor to consider in addition to the performance of the waterproofing membrane strategy. An ideal membrane system is not only effective at performing its designed function- it is also cost effective and inexpensive to install. The material cost of membranes, and the cost of equipment required to install the membranes, varies greatly between systems. A cost comparison of the roll-on, sprayed and poured membrane systems is provided below. Approximate material costs are determined for a hypothetical 10,000 square foot bridge deck.

Material costs for a typical roll-on membrane are approximately $0.85 per square foot. The crew size for installation of a roll-on membrane typically ranges from five to twelve people, depending on the size of the bridge structure. In some cases, an asphalt leveling course must be constructed on the bridge deck prior to installation, increasing installation time and cost. An asphalt primer is typically used prior to membrane installation when the asphalt leveling course is used. The membrane material cost for a 10,000 square foot bridge, not including the cost of the asphalt leveling course, would be approximately $8,500. For the roll-on membrane used in this study, a heat gun (~$150) was the only additional piece of equipment required to install the membrane.

There are several components which make up the sprayed membrane system used in this study. The primer layer costs approximately $30 per gallon and is applied at a rate of 150 square feet per gallon. The membrane layer costs approximately $45 per gallon and is applied at a rate of 16 square feet per gallon. The overlay topcoat costs approximately $30 per gallon and is applied at a rate of 32 square feet per gallon. The total sprayed membrane material cost for a 10,000 square foot bridge deck would be approximately $39,500. The initial investment for the equipment required to install the sprayed membrane systems is much greater than that of the roll-on system. A specialized sprayer, feed pump and generator are required to install the membrane. In total, these three pieces of equipment cost approximately $87,000. Due to their higher installation costs, sprayed membranes come with a warranty in Oregon to ensure quality and performance of the system being put down.

For poured membranes, the primer layer costs approximately $30 per square foot and is applied at a rate of 100 square feet per gallon. The top coat membrane costs approximately $30 per square foot and is applied at a rate of 40 square feet per gallon. The total poured membrane material cost for a 10,000 square foot bridge deck would be approximately $10,500. Installation can be completed with a mechanical mixer and a notched squeegee, making it a very cost-effective option.

The costs associated with each membrane strategy are outlined in Table 6.1.

Table 6.1: Membrane Strategy Costs

Membrane Type	Membrane Manufacturer	Membrane Name	Total Material Cost ($/sq. ft.)	Installation Equipment Cost ($)
Roll-On	Crafco	GeoTac HS	$0.85	$150
Sprayed	Olin Polycarb	Mark 155/154	$3.95	$87,000
Poured	E-Chem	EPX 50	$1.05	$1,000

7.0 SUMMARY AND CONCLUSIONS

This study focused on the evaluation of several strategies used to preserve the integrity of concrete bridges, namely through the use of waterproofing membranes and impermeable pavement overlays. Laboratory samples were produced which were representative of a concrete bridge deck and implemented five different waterproofing systems. Moisture infiltration tests were used to evaluate the impermeability of the waterproofing systems. Cracking and rutting tests were used to compare the performance of waterproofing systems under traffic loadings. Torsional tests were used to quantify the bond strength between asphalt, membrane and concrete layers in the evaluated waterproofing systems.

The research study presented in this report seeks to provide the industry and ODOT with better insight on the failure mechanisms of asphalt overlays on concrete bridge decks and establish field and laboratory experiments to evaluate the performance of these overlays. The most effective deck waterproofing systems and overlay strategies were determined for concrete bridge decks in Oregon. An ideal waterproofing system is one in which there is no early failure of the asphalt overlay, adequate bonding exists between the waterproofing membrane, asphalt and concrete layers, and one that is simple and cost effective to construct in the field.

The major conclusions based on the experimental and analytical findings of this study are as follows:

Impermeable asphalt concrete layer to protect and seal concrete bridge decks

1. An 8.5% binder content is required to achieve the 1.0% air void content detailed in the BDWSC specifications for a PG76-22 binder.

2. A 2% air void content was the lowest air void content achieved with a PG70-22ER binder, however doing so required a 9.5% binder content, which would create issues with constructability in the field. This binder grade is not recommended for use in an impermeable asphalt mixture and it was not further evaluated in this study.

3. Results for cracking and rutting tests were generally similar for 7.5% and 8.0% binder content mixtures, with significant difference existing between results for 8.0% and 8.5% binder content mixtures.

4. Flow number was greatest at binder contents of 7.5% and 8.0%, however 8.5% binder content samples still possessed a flow number greater than 740 (i.e. the recommended minimum flow number for traffic levels greater than 30 million ESALs).

5. The 7.5% binder content samples experienced some moisture infiltration in the rainfall simulator, however did not become fully saturated within the five-day analysis period. The 8.0% and 8.5% binder content samples saw no moisture infiltration within the five-day analysis period.

6. The combination of a fine aggregate gradation, high binder content (8.5%) and high binder stiffness (modified PG76-22 binder) can be used to produce asphalt pavements for bridge decks in Oregon which are both impermeable and have a strong resistance to rutting and cracking.

7. Sand patch testing found that impermeable asphalt mixture produced samples with a higher MTD than production mix samples, and suggested adequate texture for skid resistance on a roadway.

8. Tests conducted using the Oregon Field Torque Test (OFTT) indicated that there is no significant difference in interlayer shear strength between impermeable asphalt samples which had gone through freeze-thaw cycles as compared to samples which had not gone through freeze-thaw cycles.

Finite element modeling for bridge decks

9. FE modeling of an asphalt roadway in a critical scenario (soft asphalt layer with 2inch thickness, 30mph speed level at 30^{o}C temperature) resulted in vertical displacements within the asphalt layer of 0.03mm. This 0.03mm critical surface deformation was incorporated into laboratory beam sample tests.

Evaluation of waterproofing membrane strategies to protect and seal concrete bridge decks

10. Samples which incorporated a roll-on waterproofing membrane experienced some moisture infiltration through the membrane during a simulated extended rainfall event. Samples which has a mastic asphalt layer over the roll-on membrane experienced moisture infiltration at a much slower rate. Overall, the roll-on membrane systems did not provide adequate impermeability. However, it should be noted that only two replicate samples were tested for moisture infiltration in this study. Additional laboratory and/or field testing are required to validate the results.

11. Installation of roll-on membrane systems requires less effort during construction when compared to poured and sprayed membrane strategies due to easier surface preparation. Shot blasting and hand tooling are generally required to prepare the bridge deck surface before the installation of poured and sprayed membranes. These surface preparation steps require a substantial amount of time and effort. Achieving a clean surface before the application of poured and sprayed membranes is also critical.

12. Spray-on and poured waterproofing membranes both exhibited impermeability during moisture testing through a simulated extended rainfall event.

13. Samples subjected to freeze-thaw cycles generally had a lower rutting resistance and interlayer shear strength as compared to sample not subjected to temperature cycling.

14. Membrane surface texture has a significant impact on interlayer shear strength at the membrane-asphalt interface. High surface textures on the spray-on and poured membranes produced a much stronger bond with the asphalt overlay as compared to the smooth-textured roll-on membrane.

15. Samples with a mastic asphalt layer produced flow number values significantly lower than those without a mastic asphalt layer. The high binder content in the mastic layer is likely responsible for increased flow and deformation.

16. Beam samples with a mastic asphalt layer saw higher deformation following flexural fatigue tests as compared to samples without a mastic asphalt layer.

17. HWT test results showed that the samples with a mastic asphalt layer were not affected by freeze-thaw cycles since water could not reach the mastic-impermeable membrane interface due to the low air void content of the mastic layer. However, the samples with mastic layers had significantly higher surface deformation than all other strategies due to the high binder content and low stiffness of the mastic layer.

18. HWT test results also showed that the impact of freeze-thaw cycles on surface deformation for the samples with poured membranes was significantly less than the sprayed membrane samples.

Cost Comparison of waterproofing membrane strategies

19. Material costs for the roll-on and poured membrane systems (per square foot of bridge deck) are significantly less than that of the sprayed membrane system. The sprayed membrane, however, comes with a warranty to reassure DOTs of a proper membrane installation.

20. The installation equipment cost for the sprayed membrane system are typically much higher than those for the roll-on and poured membrane systems (excluding large scale applications for the poured membrane).

Test results for the designed impermeable asphalt layer indicated that it could potentially be used in place of a waterproofing membrane system to protect and seal concrete bridge decks in Oregon. The 8.0% binder content impermeable mixture achieved both impermeability and possessed high cracking and rutting resistance and is recommended for further testing. A pilot section should be constructed with this mix design to identify possible issues with constructability and further analyze surface texture and skid resistance of the pavement. Both the sprayed and poured membrane systems were found to be impermeable and have similar cracking and rutting resistance, as well as high interlayer bond strengths in laboratory tests. The poured membrane, however, is much faster and more cost effective to install as compared to the sprayed membrane system, indicating that is may be a more optimal waterproofing membrane strategy. In addition, the impact of freeze-thaw cycles on surface deformation for the samples with poured membranes was significantly less than the sprayed membrane samples. However, it should be noted that installation of roll-on membrane systems requires less effort during construction when compared to poured and sprayed membrane strategies due to easier surface preparation. Shot blasting and hand tooling are generally required to prepare the bridge deck surface before the installation of poured and sprayed membranes. These surface preparation steps require a substantial amount of time and effort. Achieving a clean surface before the application of poured and sprayed membranes is also critical. For these reasons, roll-on membrane systems maybe more ideal for rapid construction.

While the sprayed and poured membranes performed well in laboratory testing, their performance should be further quantified through field implementation and testing. Additional field testing is also required to validate the moisture infiltration of roll-on membranes. To conduct a field evaluation, pilot sections can be constructed on a bridge using each of the waterproofing membranes. Automated Pavement Condition Surveys (APCS) can be performed to monitor the rutting and cracking performance over the life of the bridge section. Chain dragging and thermal imaging can be used to check for delamination between the waterproofing membrane and the asphalt overlay. Finally, moisture sensors can be installed in the membrane-concrete interface of the pavement prior to installation of the membrane in order to validate the impermeability of the membrane over the course of its service life.

It should be noted that PS-Slab structures have a potential for differential movements. The impact of those differential movements on membrane performance was assumed to be minimal in this study and not included in the experimental plan. For this reason, additional laboratory and/or field testing are required to evaluate the performance of membrane strategies under these differential slab movements.

8.0 REFERENCES

Association of Asphalt Paving Technologists (U.S.). (2011). *Asphalt Paving Technology 2011: Journal of the Association of Asphalt Paving Technologist: Tampa, Florida, March 27-30, 2011*. Lancaster, Penn: DEStech Publications.

American Association of State Highway Transportation Officials. (2010). *Determining the Asphalt Binder Content of Hot Mix Asphalt (HMA) by the Ignition Method* (Standard No. T 308-10). Washington, DC

American Association of State Highway Transportation Officials. (2010). *Standard Method of Test for Mechanical Analysis of Extracted Aggregate* (Standard No. T 30-10). Washington, DC

American Association of State Highway Transportation Officials. (2010). *Standard Practice for Mixture Conditioning of Hot Mix Asphalt (HMA)* (Standard No. R 30-10). Washington, DC

American Association of State Highway Transportation Officials. (2011). *Standard Method of Test for Sieve Analysis of Fine and Coarse Aggregates* (Standard No. T 27-11). Washington, DC.

American Association of State Highway Transportation Officials. (2012). T 312-12. *Preparing and Determining the Density of Hot Mix Asphalt (HMA) Specimens by Means of the Superpave Gyratory Compactor* (Standard No. T 312-12). Washington, DC.

American Association of State Highway Transportation Officials. (2012). *Theoretical Maximum Specific Gravity (Gmm) and Density of Hot Mix Asphalt* (Standard No. T 209-12). Washington, DC.

American Association of State Highway Transportation Officials. (2012). *Viscosity Determination of Asphalt Binder Using Rotational Viscometer*. (Standard No. T 316-11) Washington, DC.

American Association of State Highway Transportation Officials. (2013). *Standard Method for Determining the Dynamic Modulus and Flow Number for Hot Mix Asphalt (HMA) Using the Asphalt Mixture Performance Tester (AMPT)* (Standard No. TP 79-13, A. T.). Washington, DC.

American Association of State Highway Transportation Officials. (2013). TP 105-13.*Standard Method for Determining the Fracture Energy of Asphalt Mixtures Using the Semi Circular Bend Geometry (SCB)* (Standard No. TP 105-13). Washington, DC.

American Association of State Highway Transportation Officials. (2014). *Standard Method of Test for Determining the Fatigue Life of Compacted Hot-Mix Asphalt (HMA) Subjected to Repeated Flexural Bending* (Standard No. T 321-14). Washington, DC.

American Association of State Highway Transportation Officials. (2015) *Standard Method of Test for Determining the Interlayer Shear Strength (ISS) of Asphalt Pavement Layers* (Standard No. TP 114-15). Washington, DC.

American Association of State Highway and Transportation Officials. (2015). *Standard practice for developing dynamic modulus master curves for Asphalt Mixtures using the Asphalt Mixture Performance Tester (AMPT): AASHTO designation, PP 61-13 (2015)[1] [2].*

Asphalt Institute. (2016, December 7). Determining Lab Mixing and Compaction Temperatures for Binders. Retrieved from http://www.asphaltinstitute.org/engineering/determining-lab-mixing-compaction-temperatures-binders/

American Society for Testing and Materials (2012), *Standard Practice for Measuring Delaminations in Concrete Bridge Decks by Sounding*, (Standard No. D4580/D4580M-12). West Conshohocken, PA. https://doi.org/10.1520/D4580_D4580M-12.

American Society for Testing and Materials. (2013). *Standard Test Method for Detecting Delaminations in Bridge Decks Using Infrared Thermography* (Standard No. D4788-03). West Conshohocken, PA. https://doi.org/10.1520/D4788-03.

American Society for Testing and Materials. (2015). *Standard Test Method for Measuring Pavement Microtexture Depth Using a Volumetric Technique* (Standard No. E965-15). West Conshohocken, PA.

American Society for Testing and Materials. (2017). *Standard Test Method for Infiltration Rate of In-Place Previous Concrete* (Standard No. C1701-17) West Conshohocken, PA.

American Society for Testing and Materials. (2017) *Standard Test Method for Pull-Off Strength of Coatings Using Portable Adhesion Testers.* (Standard No. D4541-17). West Conshohocken, PA. https://doi.org/10.1520/D4541-17

Applied Research Associates Inc. (2004). *Guide for Mechanistic-Empirical Design of New and Rehabilitated Pavement Structures*. Champaign, Il: National Cooperative Highway Research Program. Retrieved from http://onlinepubs.trb.org/onlinepubs/archive/mepdg/2appendices_RR.

Bennert, T., Fee, F., Sheehy, E., Blight, R., & Sauber, R. (January 01, 2011). Implementation of Performance-Based HMA Specialty Mixtures in New Jersey. *Asphalt Paving Technology, 80,* 719-758.

Biligiri, K. P., Kaloush, K. E., Mamlouk, M. S., & Witczak, M. W. (2007). Rational Modeling of Tertiary Flow for Asphalt Mixtures. *Transportation Research Record: Journal of the Transportation Research Board*, *2001*(1), 63–72. doi: 10.3141/2001-08

Bonaquist, R. F., Christensen, D. W., & Stump III, W. (2003). *Simple performance tester for Superpave mix design: first-article development and evaluation* (513th ed.). Washington D.C.: Transportation Research Board.

Campbell Scientific, INC. (n.d.). CS650 and CS655 Water Content Reflectometers. Retrieved from https://www.campbellsci.eu/

Clark, M., Mccann, D., & Forde, M. (2003). Application of infrared thermography to the non-destructive testing of concrete and masonry bridges. *NDT & E International*, *36*(4), 265–275. doi: 10.1016/s0963-8695(02)00060-9

Coleri, E., Harvey, J. T., Yang, K., & Boone, J. M. (2012). A micromechanical approach to investigate asphalt concrete rutting mechanisms. *Construction and Building Materials*, *30*, 36–49. doi: 10.1016/j.conbuildmat.2011.11.041

Coleri, E., Covey, D., Mahmoud, A., Batti, J., & Anisimova, N. (2017). *Hmac Layer Adhesion through Tack Coat*. Salem, OR: Oregon Department of Transportation. Retrieved from https://www.oregon.gov/ODOT/Programs/ResearchDocuments/SPR782_HMAC_Layer_Adhesion_Tack_Coat_Final.pdf

Coleri, E., Sreedhar, S., Haddadi, S., & Wruck, B. (2018). *Adjusting Asphalt Mixes for Increased Durability and Implementation of a Performance Tester to Evaluate Fatigue Cracking of Asphalt*. Salem, OR: Oregon Department of Transportation.

Concrete Reinforcing Steel Institute. (2019). Retrieved from http://www.crsi.org/

Covey, D., Coleri, E., & Mahmoud, A. (2017). Tack Coat Rheological Properties and the Effects on Interlayer Shear Strength. *Journal of Materials in Civil Engineering*, *29*(11), 1–11. doi: 10.1061/(asce)mt.1943-5533.0002054

Darnell, J., & Bell, C. (2015). *Performance Based Selection of Rap/Ras in Asphalt Mixtures*. Salem, OR: Oregon Department of Transportation. Retrieved from https://www.oregon.gov/odot/Programs/ResearchDocuments/SPR755_RAP-RAS_final.pdf

Dodge, E. C., & Lewis, A. R. (2013). Waterproofing and elevation profiling of a sub-surface drainage layer. *Construction and Building Materials*, *38*, 1270–1275. doi: 10.1016/j.conbuildmat.2010.03.004

Dong, Z., Ye, S., Gao, Y., Fang, G., Zhang, X., Xue, Z., & Zhang, T. (2016). Rapid Detection Methods for Asphalt Pavement Thicknesses and Defects by a Vehicle-Mounted Ground Penetrating Radar (GPR) System. *Sensors*, *16*(12). doi: 10.3390/s16122067

European Asphalt Pavement Association (EAPA). (2013). *Asphalt Pavements on Bridge Decks*. Rue du Commerce 77, Brussels, Belgium, pp. 14-19.

Federal Highway Administration Research & Technology. (2016). *Thermal Coefficient of Portland Cement Concrete*. Washington D.C. Retrieved from

https://www.fhwa.dot.gov/publications/research/infrastructure/pavements/pccp/thermal.cfm

Francken, L., & University of Michigan, Ann Arbor. (1977). Volume 1. In *Pavement Deformation Law of Bituminous Road Mixes in Repeated Load Triaxial Compression*. Retrieved from https://trid.trb.org/view/60959

Frosch, R., Kreger, M., & Strandquist, B. (2013). *Implementation of Performance-Based Bridge Deck Protective Systems*. Indianapolis, IN: Indiana Department of Transportation.

Gucunski, N., Imani, A., Romero, F., Nazarian, S., Yuan, D., Wiggenhauser, H., Shokouhi, P., Taffe, A., and Kutrubes, D. (2013). *Nondestructive Testing to Identify Concrete Bridge Deck Deterioration.* Washington D.C.: Transportation Research Board.

Hartman, A. M., & Gilchrist, M. D. (2004). Evaluating Four-Point Bend Fatigue of Asphalt Mix Using Image Analysis. *Journal of Materials in Civil Engineering*, *16*(1), 60–68. doi: 10.1061/(asce)0899-1561(2004)16:1(60)

Hawk, H. (2003). *Bridge Life-Cycle Cost Analysis*. Washington D.C.: Transportation Research Board. Retrieved from http://onlinepubs.trb.org/onlinepubs/nchrp/nchrp_rpt_483.pdf

Haynes, M. A., Coleri, E., & Sreedhar, S. (June 01, 2019). Impermeable Asphalt Concrete Layer to Protect and Seal Concrete Bridge Decks. *Transportation Research Record, 2673,* 6, 355-367.

Lee, C.M. (2017). *Maintenance Operations Manual: Bridge Deck Protection Systems*. Texas Department of Transportation. Accessed October 16, 2017.

Liu, J. (2017). *SDI-12 USB Adapter User Manual*. Saint Cloud, MN.

Liu, Y., Wu, J., & Chen, J. (2014). Mechanical properties of a waterproofing adhesive layer used on concrete bridges under heavy traffic and temperature loading. *International Journal of Adhesion and Adhesives*, *48*, 102–109. doi: 10.1016/j.ijadhadh.2013.09.015

Mahmoud, A., Coleri, E., Batti, J., & Covey, D. (2017). Development of a field torque test to evaluate in-situ tack coat performance. *Construction and Building Materials*, *135*, 377–385. doi: 10.1016/j.conbuildmat.2017.01.013

Mamlouk, M., Witczak, M., Kaloush, K., & Hasan, N. (2005). Determination of Thermal Properties of Asphalt Mixtures. *Journal of Testing and Evaluation*, *33*(2), 118–126. doi: 10.1520/jte12592.

Manning, D. G., National Research Council (U.S.), American Association of State Highway and Transportation Officials, & United States. (1995). *Waterproofing membranes for concrete bridge decks*. Washington, D.C: National Academy Press.

The MathWorks, Inc. (2016). Retrieved from https://www.mathworks.com/products/statistics.html

McCarthy, L. (2017). *Trb Webinar*. *TRB Webinar*. Pennsylvania. Retrieved from http://onlinepubs.trb.org/onlinepubs/webinars/170330.pdf

McDaniel, R., Soleymani, H., Anderson, R. M., Turner, P., & Peterson, R. (2000). *Recommended Use of Reclaimed Asphalt Pavement in the Superpave Mix Design Method*. Washington D.C.: Transportation Research Board. Retrieved from http://onlinepubs.trb.org/onlinepubs/nchrp/nchrp_w30-a.pdf

Moser, P., & Doelp, G. (2017). Membrane-Level Drainage on Highway Bridge Decks. *Civil and Structural Engineer*, *4*(3), 40–43. Retrieved from https://www.sgh.com/sites/default/files/downloads/Knowledge-Sharing/cs-membrane-drainage.pdf

Muslich, S. (2010). Retrieved from http://eprints.nottingham.ac.uk/id/eprint/11115.

NEXCO-West USA. (2014). *Comparison of Infrared Cameras for Concrete Bridge Deck Scanning: - Vol.2 Field Test at Haymarket Bridge*. Washington D.C.: NEXCO-West USA. Retrieved from https://w-nexco-usa.com/assets/documents/Vol.2 On-Site Test.pdf

Newberry, Jr., D. C. (1973). *Vibratory Roller Evaluation*. Lexington, KY: Kentucky Department of Highways

Newcomb, D., Martin, A., Yin, F., Arambula, E., Park, E., Chowdhury, A., … Signore, J. (2015). *Short-Term Laboratory Conditioning of Asphalt Mixtures*. Washington D.C.: Transportation Research Board. https://dx.doi.org/10.17226/22077.

Oregon Department of Transportation. (2015). *Self-Issue Permit Program.* Salem, OR: Oregon Department of Transportation. Retrieved from https://www.oregon.gov/ODOT/MCT/Pages/SelfIssuePermit.aspx

Oregon Department of Transportation. (2015). *Oregon Standard Specifications for Construction 2015*. Salem, OR: Oregon Department of Transportation. Retrieved from https://www.oregon.gov/ODOT/Business/Documents/2015_STANDARD_SPECIFICATIONS.pdf

Ozer, H., Al-Qadi, I. L., Lambros, J., El-Khatib, A., Singhvi, P., & Doll, B. (2016). Development of the fracture-based flexibility index for asphalt concrete cracking potential using modified semi-circle bending test parameters. *Construction and Building Materials*, *115*, 390–401. doi: 10.1016/j.conbuildmat.2016.03.144

Özgan, E., & Serin, S. (2013). Investigation of certain engineering characteristics of asphalt concrete exposed to freeze–thaw cycles. *Cold Regions Science and Technology*, *85*, 131–136. doi: 10.1016/j.coldregions.2012.09.003.

Rantala, T. (2010). *Life Cycle Analysis of Three Finnish Standard Bridges*. Helsinki, Finland: Finnish Transport Agency. Retrieved from https://julkaisut.vayla.fi/pdf3/life_cycle_analysis_of_three_finnish_standard_bridges_web.pdf

Rodezno, M. C., West, R., & Taylor, A. (2015). Flow Number Test and Assessment of AASHTO TP 79-13 Rutting Criteria. *Transportation Research Record: Journal of the Transportation Research Board*, *2507*(1), 100–107. doi: 10.3141/2507-11

Russell, H. (2012). *Waterproofing Membranes for Concrete Bridge Decks*. Washington D.C.: Transportation Research Board, https://dx.doi.org/10.17226/14654.

Sakulich, A. R., & Bentz, D. P. (2012). Increasing the Service Life of Bridge Decks by Incorporating Phase-Change Materials to Reduce Freeze-Thaw Cycles. *Journal of Materials in Civil Engineering*, *24*(8), 1034–1042. doi: 10.1061/(asce)mt.1943-5533.0000381

Sherman, M., Carrasquillo, R. L., & Fowler, D. W. (1993). *Field Evaluation of Bridge Corrosion Protection Measures* (pp. 21–24). Austin, TX: Texas Department of Transportation. Retrieved from https://library.ctr.utexas.edu/digitized/texasarchive/phase1/1300-1.pdf

Sholar, G., Page, G., Musselman, J., Upshaw, P., & Moseley, H. (2004). Preliminary Investigation of a Test Method to Evaluate Bond Strength of Bituminous Tack Coats. *Association of Asphalt Paving Technologies*, *73*, 771–806.

Sreedhar, S., Coleri, E., & Haddadi, S. S. (2018). Selection of a performance test to assess the cracking resistance of asphalt concrete materials. *Construction and Building Materials*, *179*, 285–293. doi: 10.1016/j.conbuildmat.2018.05.258

Tarefder, R., & Yousefi, S. (2012). Laboratory Evaluation of Moisture Damage in Asphalt. *Canadian Journal of Civil Engineering*, *39*, 104–115.

Tsai, B.-W., Coleri, E., Harvey, J. T., & Monismith, C. L. (2016). Evaluation of AASHTO T 324 Hamburg-Wheel Track Device test. *Construction and Building Materials*, *114*, 248–260. doi: 10.1016/j.conbuildmat.2016.03.171

Washington State Department of Transportation. (2016). HMA Paving on Bridge Decks: HMA Compaction. *HMA Paving on Bridge Decks: HMA Compaction*. Olympia, WA: Washington State Department of Transportation.

Wenzlick, J. (2007). *Bridge Deck Concrete Sealers*. Jefferson City, MO: Missouri Department of Transportation. Retrieved from https://spexternal.modot.mo.gov/sites/cm/CORDT/or07009.pdf

West, R., Zhang, J., & Moore, J. (2005). *Evaluation of Bond Strength between Pavement Layers*. Auburn, AL: National Center for Asphalt Technology. Retrieved from https://www.eng.auburn.edu/research/centers/ncat/files/technical-reports/rep05-08.pdf.

Wu, Z., Mohammad, L., Wang, L., & Mull, M. (2004). Fracture Resistance Characterization of Superpave Mixtures Using the Semi-Circular Bending Test. *Journal of ASTM International*, *2*(3). doi: https://doi.org/10.1520/JAI12264

Yildirim, Y., & Stokoe III, K. (2006). *Analysis of Hamburg Wheel Tracking Device Results in Relation to Field Performance*. Austin, TX: Texas Department of Transportation. Retrieved from https://ctr.utexas.edu/wp-content/uploads/pubs/0_4185_5.pdf

Yildirim, Y., Jayawickrama, P., Hossain, M., Alhabshi, A., Yildirim, C., Smit, A., & Little, D. (2007). *Hamburg Wheel-Tracking Database Analysis*. Austin, TX: Texas Department of Transportation. Retrieved from https://static.tti.tamu.edu/tti.tamu.edu/documents/0-1707-7.pdf

Zhou, Q., & Xu, Q. (2009). Experimental study of waterproof membranes on concrete deck: Interface adhesion under influences of critical factors. *Materials & Design*, *30*(4), 1161–1168. doi: 10.1016/j.matdes.2008.06.023.